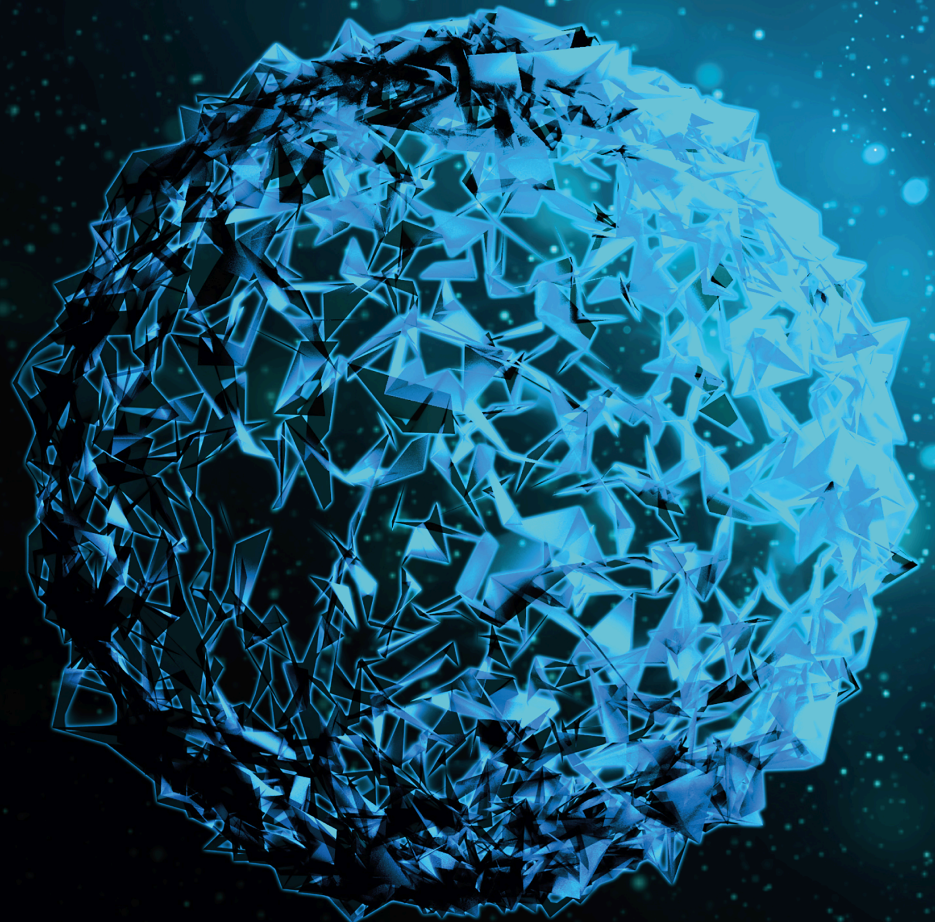


# Tumor Cell Plasticity: From Tumorigenesis to Metastasis

Lead Guest Editor: Simona Gurzu

Guest Editors: Zoltán Szentirmay and Ioan Jung



---



# **Tumor Cell Plasticity: From Tumorigenesis to Metastasis**

BioMed Research International

---

# **Tumor Cell Plasticity: From Tumorigenesis to Metastasis**

Lead Guest Editor: Simona Gurzu

Guest Editors: Zoltán Szentirmay and Ioan Jung



---

Copyright © 2020 Hindawi Limited. All rights reserved.

This is a special issue published in "BioMed Research International." All articles are open access articles distributed under the Creative Commons Attribution License, which permits unrestricted use, distribution, and reproduction in any medium, provided the original work is properly cited.






## Section Editors

Penny A. Asbell, USA  
David Bernardo , Spain  
Gerald Brandacher, USA  
Kim Bridle , Australia  
Laura Chronopoulou , Italy  
Gerald A. Colvin , USA  
Aaron S. Dumont, USA  
Pierfrancesco Franco , Italy  
Raj P. Kandpal , USA  
Fabrizio Montecucco , Italy  
Mangesh S. Pednekar , India  
Letterio S. Politi , USA  
Jinsong Ren , China  
William B. Rodgers, USA  
Harry W. Schroeder , USA  
Andrea Scribante , Italy  
Germán Vicente-Rodriguez , Spain  
Momiao Xiong , USA  
Hui Zhang , China

## Academic Editors

### Oncology

Fawzy A.S., Australia  
Gitana Maria Aceto , Italy  
Amedeo Amedei, Italy  
Aziz ur Rehman Aziz , China  
Riadh Badraoui , Tunisia  
Stergios Boussios , Greece  
Alberto Briganti, Italy  
Franco M. Buonaguro , Italy  
Xianbin Cai , Japan  
Melchiorre Cervello , Italy  
Winson Cheung, Canada  
Somchai Chutipongtanate , Thailand  
Kate Cooper, USA  
Enoc Mariano Cortes-Malagon , Mexico  
Alessandro De Vita , Italy  
Hassan, El-Abid, Morocco  
Yujiang Fang , USA

Zhien Feng , China  
Stefano Gambardella , Italy  
Dian Gao , China  
Piotr Gas , Poland  
Nebu Abraham George, India  
Xin-yuan Guan, Hong Kong  
Hirotaka Iwase, Japan  
Arumugam R. Jayakumar , USA  
Mitomu Kioi , Japan  
Krzysztof Ksiazek , Poland  
Yuan Li , China  
Anna Licata , Italy  
Wey-Ran Lin , Taiwan  
César López-Camarillo, Mexico  
João F Mota , Brazil  
Rakesh Sathish Nair , USA  
Peter J. Oefner, Germany  
Mana Oloomi , Iran  
Vera Panzarella , Italy  
Pierpaolo Pastina , Italy  
Georgios G. Pissas, Greece  
Kyoung-Ho Pyo , Republic of Korea  
Giandomenico Roviello , Italy  
Daniele Santini, Italy  
Wen Shi , USA  
Krzysztof Siemianowicz , Poland  
Henrique César Santejo Silveira , Brazil  
Himangshu Sonowal, USA  
Maurizio Soresi, Italy  
Kenichi Suda , Japan  
Farzad Taghizadeh-Hesary, Iran  
Seyithan Taysi , Turkey  
Fernando Toshio Ogata , Sweden  
Abhishek Tyagi , USA  
Marco A. Velasco-Velázquez , Mexico  
Thirunavukkarasu Velusamy , India  
Navin Viswakarma , USA  
Ya-Wen Wang , China  
Hushan Yang , USA  
Zongguo Yang , China  
Hui Yu, USA  
Baotong Zhang , USA  
Yi Zhang , China







---

Eugenio Zoni , Switzerland




## Contents

---

**Establishment of a Human Gastric Cancer Xenograft Model in Immunocompetent Mice Using the Microcarrier-6**

Yanzhen Bi , Quanyi Wang, Yonghong Yang, Quanquan Wang, Kai Zhang, Xiaobei Zhang, William C. Cho , Zhenfeng Shu, Jiannan Li, Lili Liu, Chuanping Si , and Feng Hong   
Research Article (7 pages), Article ID 1893434, Volume 2020 (2020)


**Analysis of the Expression of *Cell Division Cycle-Associated* Genes and Its Prognostic Significance in Human Lung Carcinoma: A Review of the Literature Databases**

Chongxiang Chen, Siliang Chen, Lanlan Pang, Honghong Yan, Ma Luo, Qingyu Zhao , Jielan Lai , and Huan Li   
Research Article (14 pages), Article ID 6412593, Volume 2020 (2020)

**TRIM32 Promotes the Growth of Gastric Cancer Cells through Enhancing AKT Activity and Glucose Transportation**

Jianjun Wang , Yuejun Fang, and Tao Liu  
Research Article (10 pages), Article ID 4027627, Volume 2020 (2020)

**Epithelial Mesenchymal and Endothelial Mesenchymal Transitions in Hepatocellular Carcinoma: A Review**

Simona Gurzu , Laszlo Kobori, Decebal Fodor, and Ioan Jung  
Review Article (12 pages), Article ID 2962580, Volume 2019 (2019)

## Research Article

# Establishment of a Human Gastric Cancer Xenograft Model in Immunocompetent Mice Using the Microcarrier-6

Yanzhen Bi <sup>1</sup>, Quanyi Wang,<sup>2</sup> Yonghong Yang,<sup>3</sup> Quanquan Wang,<sup>4</sup> Kai Zhang,<sup>5</sup> Xiaobei Zhang,<sup>3</sup> William C. Cho <sup>6</sup>, Zhenfeng Shu,<sup>7</sup> Jiannan Li,<sup>5</sup> Lili Liu,<sup>8</sup> Chuanping Si <sup>9</sup>, and Feng Hong <sup>3</sup>

<sup>1</sup>Difficult and Complicated Liver Diseases and Artificial Liver Center, Beijing Youan Hospital, Capital Medical University, Beijing, China

<sup>2</sup>Department of Pathology, Affiliated Hospital of Jining Medical University, Jining, China

<sup>3</sup>Institute of Liver Diseases, Affiliated Hospital of Jining Medical University, Jining, China

<sup>4</sup>Department of Neuromuscular Disease, The Third Hospital of Hebei Medical University, Shijiazhuang, China

<sup>5</sup>Department of General Surgery, The Second Hospital of Jilin University, Changchun, China

<sup>6</sup>Department of Clinical Oncology, Queen Elizabeth Hospital, Hong Kong, China

<sup>7</sup>Shanghai Meifeng Biotechnology Co., Ltd, Shanghai, China

<sup>8</sup>Department of Anorectal Surgery, Affiliated Hospital of Jining Medical University, Jining, China

<sup>9</sup>Institute of Immunology and Molecular Medicine, Jining Medical University, Jining, China

Correspondence should be addressed to Chuanping Si; [chpsi@163.com](mailto:chpsi@163.com) and Feng Hong; [fenghong9508@163.com](mailto:fenghong9508@163.com)

Received 22 October 2019; Revised 2 March 2020; Accepted 4 March 2020; Published 6 April 2020

Guest Editor: Simona Gurzu

Copyright © 2020 Yanzhen Bi et al. This is an open access article distributed under the Creative Commons Attribution License, which permits unrestricted use, distribution, and reproduction in any medium, provided the original work is properly cited.

Gastric cancer is among the most common malignant tumors of the digestive tract. Establishing a robust and reliable animal model is the foundation for studying the pathogenesis of cancer. The present study established a mouse model of gastric carcinoma by inoculating immunocompetent mice with MKN45 cells using microcarrier. Sixty male C57BL/6 mice were randomly divided into three groups: a 2D group, an empty carrier group, and a 3D group, according to the coculture system of MKN45 and the microcarrier. The mouse models were established by hypodermic injection. Time to develop tumor, rate of tumor formation, and pathological features were observed in each group. In the 3D group, the tumorigenesis time was short, while the rate of tumor formation was high (75%). There was no detectable tumor formation in either the 2D or the empty carrier group. Both H&E and immunohistochemical staining of the tumor xenograft showed characteristic evidence of human gastric neoplasms. The present study successfully established a human gastric carcinoma model in immunocompetent mice, which provides a novel and valuable animal model for the cancer research and development of anticancer drugs.

## 1. Introduction

With approximately one million newly diagnosed cases annually, gastric cancer poses a serious threat to the health and lives of people worldwide [1, 2]. However, the pathogenesis and mechanisms of metastasis of gastric cancer have yet to be completely clarified. *In vivo* models of gastric cancer are essential tools for exploration of the biological characteristics of this cancer and potential novel treatment options [3, 4]. Human-derived gastric cancer xenograft models have been

established in immunodeficient mice, such as nude mice and mice with severe combined immunodeficiency. However, immunodeficient mice are not easily reared and are costly. Importantly, immunodeficient mice do not reflect the important roles of the immune system in tumor development and progression. Thus, the establishment of a novel human gastric cancer xenograft model in mice with a normal immune system is of great significance [5, 6]. In the present study, MKN45, human gastric cancer cells and the microcarrier were cocultured, and immunocompetent mice were subsequently

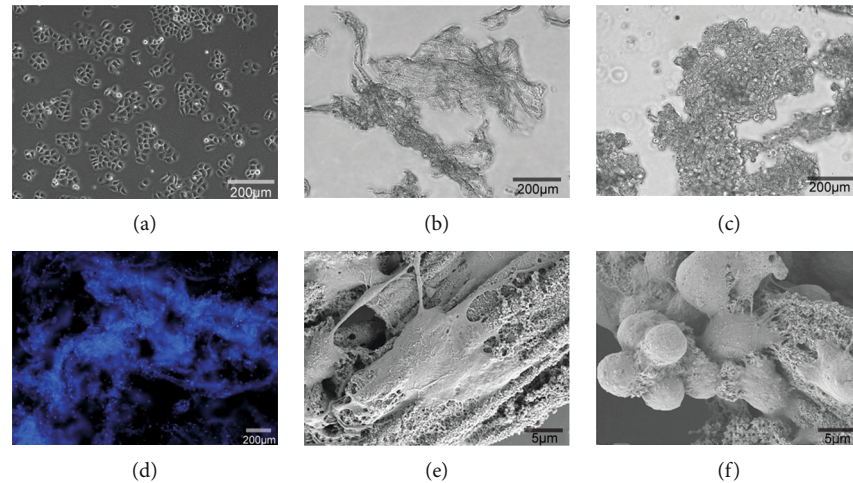


FIGURE 1: 3D coculture system of MKN45 cells under the microscope and the electron microscope. (a) In the 2D culture environment, the MKN45 cells exhibited an irregular polygon shape. (b) The microcarrier-6 type C; irregular “maze”-like structure. (c) Following a 24 h coculture, MKN45 cells adhered well to the microcarrier-6, as observed by microscopy. Irregular cell clusters were observed surrounding the MKN45 cells adhered to the microcarrier-6. (d) Following a 24 h coculture, DAPI staining showed a large number of MKN45 cells adhered to the microcarrier-6 scaffold. (e) Multilayer porous structure of microcarriers can be observed under the scanning electron microscope. (f) MKN45 cells adhered to the microcarriers, and the cells adhered to the surface formed cell clusters.

inoculated with the suspension, successfully establishing a novel human-derived gastric cancer xenograft.

## 2. Materials and Methods

**2.1. Materials.** Roswell Park Memorial Institute- (RPMI-) 1640 culture medium, trypsin, fetal bovine serum, and penicillin were purchased from Gibco (Thermo Fisher Scientific, Waltham, MA, USA). Rabbit anti-human carbohydrate antigen 199 (CA199), cytokeratin 7 (CK-7), and caudal type homeobox 2 (CDX-2) monoclonal antibodies were purchased from Abcam (Cambridge, UK). The microcarrier-6 was purchased from Elyon Biotechnologies LLC (Gaithersburg, MD, USA).

**2.2. Experimental Animals.** Sixty 6–8-week-old male C57BL/6 mice weighing 22–25 g were purchased from Jinan Pengyue Experimental Animal Breeding Co., Ltd. (license number: SCXK 20140007, Shandong Province, China) and housed in a specific pathogen-free animal center at the Affiliated Hospital of Jining Medical College (Shandong Province, China). All animal experiments were performed with the approval of the Institutional Animal Care and Use Committee of the Affiliated Hospital of Jining Medical University and carried out in accordance with the approved guidelines.

**2.3. Cell Lines.** The MKN45 human gastric cancer cell line was purchased from Cell Bank of the Chinese Academy of Science (Shanghai, China) and cultured in RPMI-1640 medium containing 10% fetal bovine serum and 100 U/mL penicillin at 37°C with 5% CO<sub>2</sub>. The culture medium was changed every 24 h, and the cells harvested by digestion with 0.25% trypsin.

**2.4. Establishment of a Three-Dimensional (3D) Tumor Cell Culture Model.** The microcarrier-6 was soaked in 75% ethanol for 24 h, washed three times with 1x phosphate-buffered saline, and incubated in RPMI-1640 medium for 24 h. Subsequently, the microcarrier-6 was modified via a 3 h incubation with stromal cell-derived factor-1 alpha (SDF-1 $\alpha$ ) and vascular endothelial growth factor (VEGF), both at a concentration of 100 ng/mL. Cells in the logarithmic growth phase were counted following trypan blue staining and adjusted to a concentration of  $2 \times 10^7$ /mL when the viability was >95%. The MKN45 cell suspension was mixed with the modified microcarrier-6 and incubated at 37°C with 5% CO<sub>2</sub> for a further 24 h to saturate the cells with the microcarrier, as observed by microscopy (Figures 1(c) and 1(d)).

**2.5. Animal Grouping.** The 60 C57BL/6 mice were randomly divided into three groups (20 mice per group): the two-dimensional (2D) group (animals inoculated with  $1 \times$  PBS containing  $2 \times 10^6$  MKN45 cells), the empty carrier group (animals inoculated with  $1 \times$  PBS containing 30  $\mu$ g microcarrier-6), and the 3D group (animals inoculated with  $1 \times$  PBS containing  $2 \times 10^6$  MKN45 cells and 30  $\mu$ g microcarrier-6).

**2.6. Animal Model Generation.** The 3D tumor cell culture model was established on the first day of the experiment and incubated for 24 h. On the second day, the cultured cell-microcarrier complexes were washed three times in  $1 \times$  PBS and gently mixed with  $1 \times$  PBS to adjust the concentration to  $2 \times 10^7$  cells and 300  $\mu$ g microcarrier-6 per 1 mL of suspension, and placed on ice for later use. MKN45 cells in the logarithmic growth phase were harvested, trypsinized, washed three times with  $1 \times$  PBS, and resuspended in  $1 \times$  PBS at a concentration of  $2 \times 10^7$  cells/mL, which was placed on ice for later use. The modified microcarrier-6 was washed three times with  $1 \times$  PBS, resuspended in  $1 \times$  PBS at a



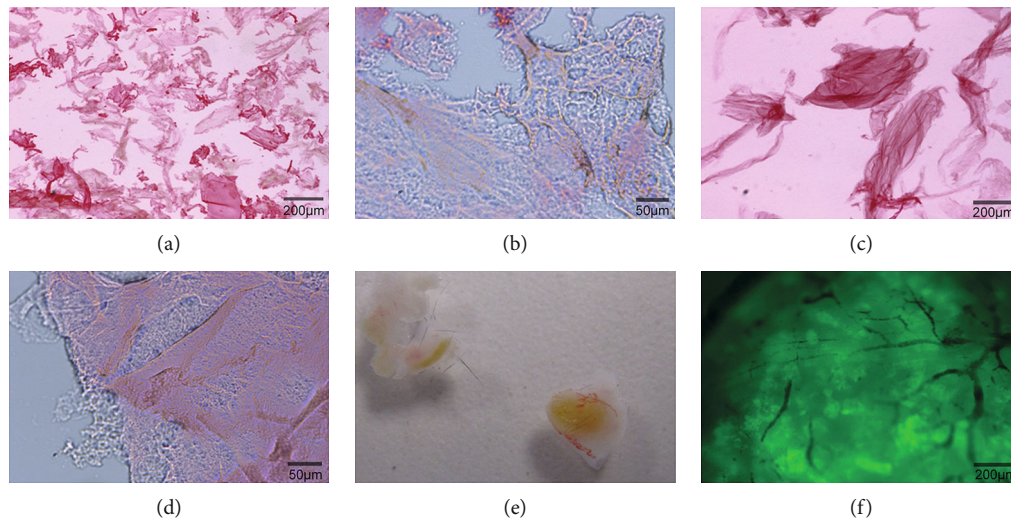


FIGURE 2: The characteristics of the microcarrier-6 by microscopy. (a, b) Type C microcarrier-6, small volume, large aperture. (c, d) Type M microcarrier-6, large volume, small aperture. The pore size, the positive surface charge density, and the size of the microcarrier-6 can be adjusted by chemical synthesis. The microcarrier-6 is multilayered and cross-linked to form an irregular “maze”-like structure with sufficient space (b, d). The microcarrier-6 is directly embedded in the skin of C57BL/6 mice for 5 weeks, inducing blood vessel ingrowth (e, f). (e) Visually, the red surfaces are blood vessels. (f) Under the microscope, the dendritic shadows are blood vessels.

concentration of 300  $\mu\text{g/mL}$ , and placed on ice for later use. Each mouse in all three experimental groups was inoculated with 100  $\mu\text{L}$  of the corresponding solution under the right axillary crest.

**2.7. Indicator Detection and Pathological Examination.** Following inoculation, the mice were housed separately by group, and daily appetite, activities, and weight were monitored. The time for local tumor formation and tumor volume in each mouse was recorded. Once tumors were visible, the long diameter (a) and short diameter (b) of each tumor were measured daily, and the tumor volume was calculated according to the tumor volume formula [7]:  $V = \frac{1}{2} \times a \times b^2$ . Tumor-bearing mice were sacrificed in three batches: 10, 20, and 30 days postinoculation. Tumor tissues were completely removed from each mouse, and tumor quality, texture, and degree of infiltration and necrosis were recorded. Tumor tissues were subsequently fixed in 4% neutral buffered formaldehyde and stained with hematoxylin and eosin (H&E). The EnVision two-step staining technique was used for immunohistochemistry. The staining results were determined based on the positive granular cytoplasmic staining of the tumor. Negative (–ve) staining was defined as <5% positively stained cells, and positive (+ve) staining was defined as  $\geq 5\%$  positively stained cells.

**2.8. Statistical Analysis.** The SPSS 13.0 software (IBM SPSS, Chicago, IL, USA) was used for statistical analysis. Measurement data are presented as means  $\pm$  standard error of the mean (SEM). The differences between the mean values of each group were compared using one-way analysis of variance (ANOVA) or the Kruskal–Wallis test as appropriate.  $P < 0.05$  is considered a statistically significant difference.

### 3. Results

**3.1. Establishment of the In Vitro MKN45 3D Tumor Culture System Using the Microcarrier-6.** The microcarrier-6 is a novel microcarrier composed of positively electrifiable organic polymers with a multilayered porous structure. The pore size, the positive surface charge density, and the size of the microcarrier-6 can be adjusted by chemical synthesis. Type C microcarrier-6, small volume, large pore size, and many times of space folding, is mainly used for 3D cell culture and drug sensitivity experiments (Figures 2(a) and 2(b)). Type M microcarrier-6, large volume, small pore size, and low internal folding times, is mainly used for tissue engineering research (Figures 2(c) and 2(d)). Type C microcarrier-6 was used in our study. The microcarrier-6 is a pure organic compound that is not prone to contamination, has no impurities, is low in immunogenicity and metabolism, and is highly biocompatible, providing a stable microenvironment for cell growth (Figures 2(a)–2(d)). In addition, the microcarrier-6 is directly embedded in the skin of mice, inducing blood vessel ingrowth (Figures 2(e) and 2(f)), which can provide sufficient blood supply for tumor cell growth. MKN45 cells adhered rapidly in the 2D environment, and the cell morphology observed by microscopy following 24 h of culture exhibited an irregular polygon shape (Figure 1(a)). The microcarrier-6 exhibited an irregular or long spindle shape and a loose texture (Figure 1(b)). Following a 24 h coculture of MKN45 and the modified microcarrier-6, MKN45 cells adhered well to the microcarrier and reached confluence. In addition, irregular cell clusters were observed surrounding the MKN45 cells adhered to the microcarrier-6 (Figure 1(c)). The MKN45 cell-microcarrier complexes were stained with 4',6-diamidino-2-phenylindole (DAPI) solution, revealing a large number of MKN45 cells adhered to the microcarrier-6 scaffold (Figure 1(d)).

TABLE 1: Body weight and tumor volume of mice at different time points.

Time (day)	Empty carrier group		2D group		3D group	
	Body weight (g)	Volume (mm <sup>3</sup> )	Body weight (g)	Volume (mm <sup>3</sup> )	Body weight (g)	Volume (mm <sup>3</sup> )
1	24.15 ± 1.01	0	24.53 ± 1.06	0	24.44 ± 1.23	0
3	24.32 ± 1.21	0	24.71 ± 1.11	0	24.56 ± 1.39	0
5	24.87 ± 1.12	0	24.74 ± 1.27	0	24.73 ± 1.23	7.36 ± 3.15 (n = 8)
7	25.12 ± 1.37	0	24.91 ± 1.43	0	24.87 ± 0.85	35.18 ± 6.24 (n = 13)
10	25.67 ± 1.51	0	25.34 ± 1.27	0	25.13 ± 1.31	95.76 ± 10.27 (n = 15)
14	25.93 ± 0.96	0	25.96 ± 1.08	0	25.56 ± 1.19	415.35 ± 30.71 (n = 15)
21	26.65 ± 1.02	0	26.37 ± 1.07	0	26.14 ± 1.28	534.27 ± 45.18 (n = 15)
30	27.31 ± 1.35	0	26.85 ± 1.37	0	26.37 ± 1.05	527.16 ± 50.62 (n = 15)

Data are shown as the mean ± SEM.

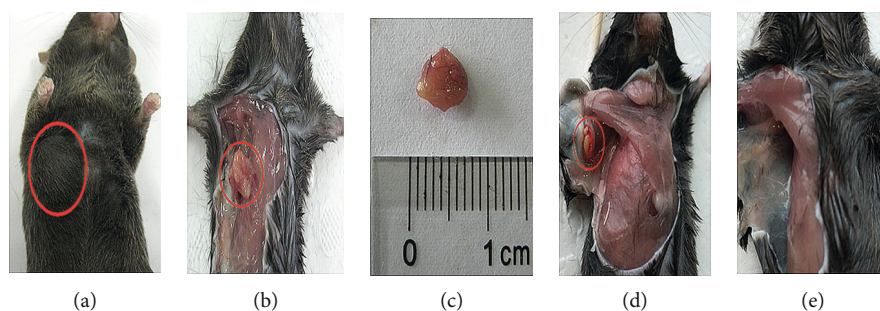


FIGURE 3: Histological changes in the injection sites of the different groups. (a, b, c) Large subcutaneous masses were observed 10 days following inoculation in the 3D group. (b, c) The xenograft tissues were easily separated from the adjacent tissues and presented as relatively regular shapes, mostly round or oval, and grayish white or grayish red in color. (d) Small subcutaneous masses were observed with a yellow color in the empty carrier group. (e) No subcutaneous mass was observed in the 2D group.

Multilayer porous structure of microcarriers can be observed under scanning electron microscope (Figure 1(e)). MKN45 cells adhered to the microcarriers, and the cells adhered to the surface formed cell clusters (Figure 1(f)).

**3.2. Mouse Survival and Tumor Formation.** No significant change in appetite, coat, or body weight was noted among the groups during the experiment (Table 1). Mice in the 3D group showed a slight decrease in activity one week postinoculation. No animals died in any group, and no tumor formation was found in the empty carrier or 2D groups during the 30-day experiment. Subcutaneous masses in 15 of the 20 mice in the 3D group were identified via palpation 7–10 days following inoculation, suggesting a tumor formation rate of 75% (Table 1). Tumor xenografts grew rapidly and were observed as subcutaneous masses approximately 10 days following inoculation (Figure 3(a), Supplementary Figure 3). Tumor xenografts grew to 0.5–1.0 cm<sup>3</sup> in size from 2 to 3 weeks postinoculation. The tumor xenograft tissues were easily separated from the adjacent tissues and presented as relatively regular shapes, mostly round or oval, grayish white or grayish red in color, and with an abundant peripheral blood supply (Figures 3(b) and 3(c) and Supplementary Figure 3). There were histological changes of the injection site in the empty carrier group, but no

changes in the 2D group (Figures 3(d) and 3(e)). Small subcutaneous masses were observed with a yellow color in the empty carrier group (Figure 3(d)).

**3.3. H&E Staining.** Histomorphology, as seen by light microscopy, showed a large number of disordered and atypical cells in the tumor xenografts from mice in the 3D group (Figures 4(a)–4(c)). A large number of heterotypic cells, residual microcarriers, and abundant blood vessels were observed, 10 days postinoculation (Figure 4(a)). A small number of residual microcarriers (Figure 4(b)) and a large number of necrotic lesions (Figure 4(d)) were observed, 20 days postinoculation. However, the microcarriers were substantially eliminated 30 days postinoculation (Figure 4(c)). A large number of microcarriers and a small number of inflammatory cells were observed in the empty carrier group, but no tumor cells were found (Figure 4(e)).

**3.4. Immunohistochemistry.** Immunohistochemistry was carried out in animals euthanized 20 days following tumor xenograft. The tumor xenograft tissues showed positive CA199, CK-7, and CDX-2 staining (Figures 4(f)–4(h)), further confirming that the atypical cells were human-derived tumor cells.



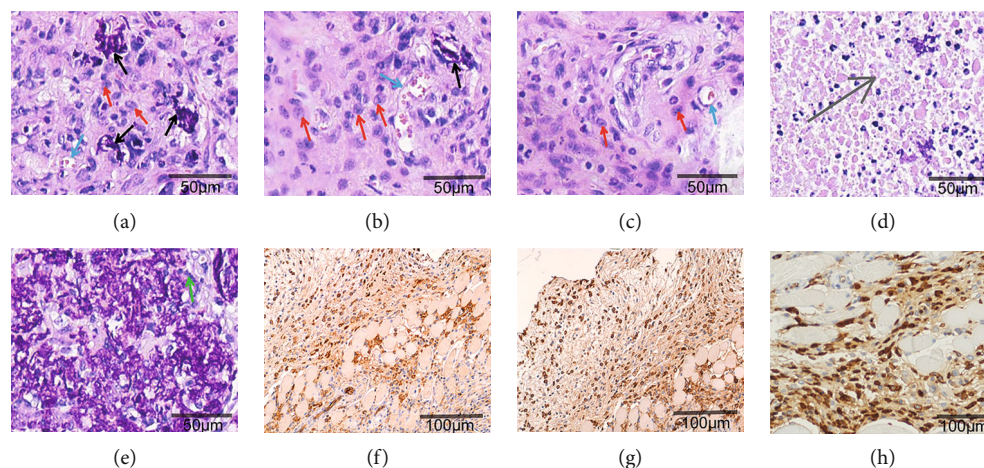


FIGURE 4: H&E and immunohistochemical staining of a human gastric cancer xenograft (200x). (a) A large number of heterotypic cells, residual microcarriers, and abundant blood vessels were observed, 10 days postinoculation. (b, d) A small number of residual microcarriers (b) and a large number of necrotic lesions (d), 20 days postinoculation. (c) Almost no residual microcarriers can be found, 30 days postinoculation. (e) A large number of microcarriers and a small number of inflammatory cells were seen in the empty carrier group. Blue arrows refer to blood vessels, red arrows indicate heterotypic cells, and black arrows show residual microcarriers (a, b, c). Gray arrows refer to necrotic lesions (d), and green arrows refer to inflammatory cells (e). The human gastric cancer xenograft displayed diffuse and strong immunoreactivity in the cytoplasm or nuclei of the cancer cells. (f) CA199, (g) CK-7, and (h) CDX-2.

#### 4. Discussion

Animal models have been extensively used to study the pathogenesis and metastatic mechanisms of gastric cancer and play an extremely important role in the evaluation of the efficacy and toxicity of therapeutic drugs [8–10]. At present, gastric cancer animal models mainly include the following: the induction model, the transplantation model, and the genetic engineering model [11]. Among the three types of models, the transplantation model is easily operated and thus widely used. The type of experimental animals, tumor xenografts, and the site and route of transplantation have been considered factors that affect the success of xenograft models [11]. Mice with defects in immune function, such as nude mice and mice with severe combined immunodeficiency (SCID), are commonly used for xenograft models [11, 12]. However, due to the comparatively expensive cost, short life span, and the lack of immune response to tumors in immunodeficiency mice, we selected immunocompetent C57BL/6 mice for the xenograft model to avoid the shortcomings of immunodeficiency mice. It is generally believed that the occurrence of gastric cancer is not related to the level of estrogen, and the incidence of gastric cancer in males is higher than that in females. Thus, we used male mice as models. In addition, the present study used MKN45 human gastric cancer cells to establish the *in vitro* model mainly because of the strong invasive and metastatic characteristics of the cell line [13]. Moreover, the underarm subcutaneous region and ectopic transplantation were selected as the site and route of tumor cell transplantation, respectively, as a result of the abundant blood supply and loose tissue structure of this area, which facilitates tumor growth in mice [14].

As a bridge between the 2D cell culture system and the animal model, 3D cell culture system better simulates the

microenvironment of tumor cell growth and has become an attractive topic in current research [15–17]. 3D culture of cancer cells will form tumor organoids, and mouse tumor xenograft models based on tumor organoids have begun to be applied to the screening of anticancer drugs [18, 19]. The present study used the novel microcarrier-6 and MKN45 cells for the coculture experiments to successfully establish a 3D growth model. We directly embedded the microcarrier-6 into the subcutaneous tissue of mice to allow blood vessels to enter the microcarriers, presenting a specific advantage that is not achieved with other microcarriers. Studies have reported mild immunosuppression of immunocompetent mice to achieve resistance to human tumor cells, successfully establishing a tumor-bearing mouse model [20]; however, to date, there are no reports of successful ectopic transplantation of a human tumor in normal mice under non-immunosuppressive conditions. In addition, when we adjusted the concentration of MKN45 cells to  $2 \times 10^8$  cells/mL and immediately injected  $100 \mu\text{L}$  MKN45 cell suspension subcutaneously to each mouse, stable tumor formation was not achieved due to the strong immune clearance of the ectopically transplanted human tumor cells. The microcarrier-6 used in the present study exhibited low immunogenicity and a loose texture with numerous pores in the center, facilitating tumor cell growth. The microcarrier-6 also acted as a barrier to block the immune cells from directly killing the tumor cells. The modified microcarrier-6 allowed blood vessels to easily grow inside the tumor, providing suitable conditions for the rapid growth of tumor cells.

Cellular immunity is the main army against tumor growth; the cells involved mainly include T cells, natural killer cells, macrophages, and dendritic cells [6, 12]. Due to the irregular “maze”-like structure of the microcarrier-6, it can act as a short-term barrier and block the direct killing of tumor cells

by immune cells to some extent. In addition, three hours prior to the experiment, the microcarrier-6 was further modified with SDF-1 $\alpha$  and VEGF to accelerate blood vessel formation and provide a blood supply for rapid tumor growth, which surpassed the antitumor immune effect of the mice. Simultaneously, we found that macrophages in peripheral blood and splenic tissues of the mice were significantly decreased during the early stage of transplanted tumor formation, as compared with the normal control group (Supplementary Figure 1). The number of bone marrow macrophages gradually decreased between the empty carrier group, the 2D group, and the 3D group, but there was no statistical significance (Supplementary Figure 2A, 2B). Compared with the empty carrier group, the number of spleen T lymphocytes in the 2D group was reduced, but there was no statistical significance (Supplementary Figure 2C). The number of spleen T lymphocytes in the 3D group was significantly less than that in the 2D group (Supplementary Figure 2C). This suggests that the growth of the tumor inhibited the immune system, allowing the tumor to grow rapidly.

The present study established a MKN45 cell 3D growth model, successfully establishing a human gastric cancer xenograft model in immunocompetent mice in the 3D group, whereas the mice in the 2D and empty carrier groups did not form any tumors. This xenograft model was characterized by the rapid growth of tumors, which could be palpated by hand 7–10 days postinoculation and reached optimal growth by 10–15 days postinoculation; the tumor volume was 0.5–1.0 cm<sup>3</sup> approximately 20 days following inoculation. A large number of cells with nuclear atypia that had infiltrated muscle and fat tissues were detected by H&E staining. Residual microcarrier-6 was surrounded by inflammatory cells and formed granulomas with a large area of necrosis in the center, which was likely caused by an insufficient blood supply due to rapid tumor growth. These phenomena are consistent with tumor development in humans. Moreover, the abundant capillaries were mainly located in the periphery of the tumors. At present, there is no specific tumor marker for gastric cancer; however, CA199, CK-7, and CDX-2 are commonly used as markers of gastrointestinal tumors [21–23]. Thus, we chose these three markers for the labeling and identification of human-derived gastric cancer cells. Immunohistochemical staining of CA199, CK-7, and CDX-2 was positive, further confirming that heteromorphic cells were human gastric cancer cells.

## 5. Conclusions

We successfully established a human gastric cancer xenograft model in immunocompetent mice. This model can reflect the interaction between the body's immune system and tumors and has broad application prospects in the future research on tumor immunity as well as new drug research and development [24].

## Data Availability

The data used to support the findings of this study are available from the corresponding author upon request.

## Conflicts of Interest

The authors declare that they have no conflicts of interest.

## Authors' Contributions

Yanzhen Bi, Quanyi Wang, and Yonghong Yang contributed equally to this work.

## Acknowledgments

This study was supported by grants from the National Natural Science Foundation of China (81170395 and 81570556), the Natural Science Foundation of Jilin Province (20180101137JC and 20180101130JC), and Research Fund for Lin He's Academician Workstation of New Medicine and Clinical Translation in Jining Medical University (JYHL2019FMS21).

## Supplementary Materials

The changes of inflammatory cells and other tumorigenic data. Supplementary Figure 1: the changes of inflammatory cells in tumor-bearing mice during the early stage of transplanted tumor formation. Supplementary Figure 2: the changes of inflammatory cells in different groups during the early stage of transplanted tumor formation. Supplementary Figure 3: tumor-bearing mice and transplanted tumor tissues. (*Supplementary Materials*)

## References

- [1] F. Bray, J. Ferlay, I. Soerjomataram, R. L. Siegel, L. A. Torre, and A. Jemal, "Global cancer statistics 2018: GLOBOCAN estimates of incidence and mortality worldwide for 36 cancers in 185 countries," *CA: A Cancer Journal for Clinicians*, vol. 68, no. 6, pp. 394–424, 2018.
- [2] Global Burden of Disease Cancer Collaboration, C. Fitzmaurice, C. Allen et al., "Global, regional, and national cancer incidence, mortality, years of life lost, years lived with disability, and disability-adjusted life-years for 32 cancer groups, 1990 to 2015: a systematic analysis for the global burden of disease study," *JAMA Oncology*, vol. 3, no. 4, pp. 524–548, 2017.
- [3] T. Kuwata, K. Yanagihara, Y. Iino et al., "Establishment of Novel Gastric Cancer Patient-Derived Xenografts and Cell Lines: Pathological Comparison between Primary Tumor, Patient-Derived, and Cell-Line Derived Xenografts," *Cells*, vol. 8, no. 6, p. 585, 2019.
- [4] M. Tellez-Gabriel, D. Cochonneau, M. Cadé, C. Jubelin, M. F. Heymann, and D. Heymann, "Circulating tumor cell-derived pre-clinical models for personalized medicine," *Cancers*, vol. 11, no. 1, p. 19, 2019.
- [5] M. T. Basel, S. Narayanan, C. Ganta et al., "Developing a xenograft human tumor model in immunocompetent mice," *Cancer Letters*, vol. 412, pp. 256–263, 2018.
- [6] M. Wang, R. A. Busuttill, S. Pattison, P. J. Neeson, and A. Boussioutas, "Immunological battlefield in gastric cancer and role of immunotherapies," *World Journal of Gastroenterology*, vol. 22, no. 28, pp. 6373–6384, 2016.
- [7] K. Ogawa, T. Mukai, D. Asano et al., "Therapeutic effects of a 186Re-complex-conjugated bisphosphonate for the palliation of metastatic bone pain in an animal model," *Journal of*

- nuclear medicine : official publication, Society of Nuclear Medicine*, vol. 48, no. 1, pp. 122–127, 2007.
- [8] L. Ding, M. El Zaatari, and J. L. Merchant, “Recapitulating human gastric cancer pathogenesis: experimental models of gastric cancer,” *Advances in experimental medicine and biology*, vol. 908, pp. 441–478, 2016.
- [9] X. Liu and S. J. Meltzer, “Gastric cancer in the era of precision medicine,” *Cellular and Molecular Gastroenterology and Hepatology*, vol. 3, no. 3, pp. 348–358, 2017.
- [10] Y. Song, C. Tong, Y. Wang et al., “Effective and persistent anti-tumor activity of HER2-directed CAR-T cells against gastric cancer cells in vitro and xenotransplanted tumors in vivo,” *Protein & Cell*, vol. 9, no. 10, pp. 867–878, 2018.
- [11] A. R. Poh, R. J. O’Donoghue, M. Ernst, and T. L. Putoczki, “Mouse models for gastric cancer: matching models to biological questions,” *Journal of Gastroenterology and Hepatology*, vol. 31, no. 7, pp. 1257–1272, 2016.
- [12] L. Zitvogel, J. M. Pitt, R. Daillère, M. J. Smyth, and G. Kroemer, “Mouse models in oncoimmunology,” *Nature Reviews Cancer*, vol. 16, no. 12, pp. 759–773, 2016.
- [13] R. A. Busuttill, D. S. Liu, N. di Costanzo, J. Schröder, C. Mitchell, and A. Boussioutas, “An orthotopic mouse model of gastric cancer invasion and metastasis,” *Scientific Reports*, vol. 8, no. 1, p. 825, 2018.
- [14] M. J. Zheng, J. Wang, Y. W. Chen et al., “A novel mouse model of gastric cancer with human gastric microenvironment,” *Cancer Letters*, vol. 325, no. 1, pp. 108–115, 2012.
- [15] S. Jaeger, M. Duran-Frigola, and P. Aloy, “Drug sensitivity in cancer cell lines is not tissue-specific,” *Molecular Cancer*, vol. 14, no. 1, p. 40, 2015.
- [16] A. Mitra, L. Mishra, and S. Li, “Technologies for deriving primary tumor cells for use in personalized cancer therapy,” *Trends in Biotechnology*, vol. 31, no. 6, pp. 347–354, 2013.
- [17] M. Rimann and U. Graf-Hausner, “Synthetic 3D multicellular systems for drug development,” *Current Opinion in Biotechnology*, vol. 23, no. 5, pp. 803–809, 2012.
- [18] G. Vlachogiannis, S. Hedayat, A. Vatsiou et al., “Patient-derived organoids model treatment response of metastatic gastrointestinal cancers,” *Science*, vol. 359, no. 6378, pp. 920–926, 2018.
- [19] F. Weeber, S. N. Ooft, K. K. Dijkstra, and E. E. Voest, “Tumor organoids as a pre-clinical cancer model for drug discovery,” *Cell Chemical Biology*, vol. 24, no. 9, pp. 1092–1100, 2017.
- [20] J. A. Bennett, V. A. Pilon, and R. MacDowell, “Evaluation of growth and histology of human tumor xenografts implanted under the renal capsule of immunocompetent and immunodeficient mice,” *Cancer Research*, vol. 45, no. 10, pp. 4963–4969, 1985.
- [21] M. K. Heatley, “Immunohistochemical biomarkers of value in distinguishing primary ovarian carcinoma from gastric carcinoma: a systematic review with statistical meta-analysis,” *Histopathology*, vol. 52, no. 3, pp. 267–276, 2008.
- [22] L. Hui, L. Rixv, and Z. Xiuying, “A system for tumor heterogeneity evaluation and diagnosis based on tumor markers measured routinely in the laboratory,” *Clinical Biochemistry*, vol. 48, no. 18, pp. 1241–1245, 2015.
- [23] H. S. Kim, J. S. Lee, J. N. Freund et al., “CDX-2 homeobox gene expression in human gastric carcinoma and precursor lesions,” *Journal of Gastroenterology and Hepatology*, vol. 21, no. 2, pp. 438–442, 2006.
- [24] R. S. Choi, W. Y. X. Lai, L. T. C. Lee et al., “Current and future molecular diagnostics of gastric cancer,” *Expert Review of Molecular Diagnostics*, vol. 19, no. 10, pp. 863–874, 2019.

## Research Article

# Analysis of the Expression of Cell Division Cycle-Associated Genes and Its Prognostic Significance in Human Lung Carcinoma: A Review of the Literature Databases

Chongxiang Chen,<sup>1,2</sup> Siliang Chen,<sup>3</sup> Lanlan Pang,<sup>4</sup> Honghong Yan,<sup>2</sup> Ma Luo,<sup>5</sup> Qingyu Zhao ,<sup>2</sup> Jielan Lai ,<sup>6</sup> and Huan Li <sup>2</sup>

<sup>1</sup>Guangzhou Institute of Respiratory Diseases, State Key Laboratory of Respiratory Disease, The First Affiliated Hospital of Guangzhou Medical University, Guangzhou 510120, China

<sup>2</sup>Department of Intensive Care Unit, Sun Yat-sen University Cancer Center, State Key Laboratory of Oncology in South China, Collaborative Innovation Center for Cancer Medicine, Guangzhou 510060, China

<sup>3</sup>Department of Hematology, Sun Yat-sen University Cancer Center, State Key Laboratory of Oncology in South China, Collaborative Innovation Center for Cancer Medicine, Guangzhou 510060, China

<sup>4</sup>Zhongshan School of Medicine, Sun Yat-sen University, Guangzhou, Guangdong Province, China

<sup>5</sup>Department of Interventional Radiology, Sun Yat-Sen University Cancer Center, State Key Laboratory of Oncology in South China, Collaborative Innovation Center for Cancer Medicine, Guangzhou 510060, China

<sup>6</sup>Department of Anesthesiology, Sun Yat-sen University Cancer Center, State Key Laboratory of Oncology in South China, Collaborative Innovation Center for Cancer Medicine, Guangzhou, Guangdong 510060, China

Correspondence should be addressed to Jielan Lai; laiyl@sysucc.org.cn and Huan Li; lihuan@sysucc.org.cn

Received 9 October 2019; Accepted 30 December 2019; Published 12 February 2020

Guest Editor: Simona Gurzu

Copyright © 2020 Chongxiang Chen et al. This is an open access article distributed under the Creative Commons Attribution License, which permits unrestricted use, distribution, and reproduction in any medium, provided the original work is properly cited.

**Background.** Lung cancer (LC) has become the top cause responsible for cancer-related deaths. *Cell division cycle-associated (CDCA)* genes exert an important role in the life process. Dysregulation in the process of cell division may lead to malignancy. **Methods.** Transcriptional data on CDCA gene family and patient survival data were examined for lung cancer (LC) patients from the GEPIA, OncoPrint, cBioPortal, and Kaplan–Meier Plotter databases. **Results.** CDCA1/2/3/4/5/7/8 expression levels were higher in lung adenocarcinoma tissues, and the CDCA1/2/3/4/5/6/7/8 expression levels were increased in squamous cell LC tissues compared with those in noncarcinoma lung tissues. The expression levels of CDCA1/2/3/4/5/8 showed correlation with tumor classification. The Kaplan–Meier Plotter database was employed to carry out survival analysis, indicating that increased CDCA1/2/3/4/5/6/7/8 expression levels were obviously related to poor overall survival (OS) and progression-free survival (PFS) ( $P < 0.05$ ). Only LC patients with increased CDCA3/4/5/8 expression were significantly related to lower post-progression survival (PPS) ( $P < 0.05$ ). The following processes were affected by CDCA genes' alteration: R-HAS-2500257: resolution of sister chromatid cohesion; GO:0051301: cell division; CORUM: 1118: chromosomal passenger complex (CPC), including CDCA8, INCENP, AURKB, and BIRC5; CORUM: 127: NDC80 kinetochore complex; M129: the PID PLK1 pathway; and GO: 0007080: mitotic metaphase plate congression, all of which were remarkably modulated since the alterations affected CDCA genes. **Conclusions.** Upregulated CDCA genes' expression levels in LC tissues probably play a crucial part in LC oncogenesis. The upregulated CDCA genes' expression levels are used as the potential prognostic markers to improve patient survival and the LC prognostic accuracy. CDCA genes probably exert their functions in tumorigenesis through the PLK1 pathway.



## 1. Introduction

In the United States, lung cancer (LC) has turned into the top cause responsible for cancer-related deaths. According to estimation, there are over 200 thousand new LC cases and over 100 thousand deaths in 2019 [1]. LC can be classified as small-cell lung cancer (SCLC) as well as non-small-cell lung cancer (NSCLC). Among them, squamous cell carcinoma (SCC) and adenocarcinoma represent the two major NSCLC types. Nowadays, some studies have found that the platinum-based chemotherapy regimens generate a plateau, and the median overall survival (OS) is 8–14 months [2, 3]. Great progress has been made in gene-targeted therapies and immunotherapies in treating NSCLC patients, and metastatic LC patients treated with these therapies can survive for a longer period than before (over 2 years) [2, 3]. Mutations in *epidermal growth factor receptor* (EGFR), as well as rearrangement of *ROS1* and *anaplastic lymphoma kinase* (ALK), are suggested as the first-line treatment for metastatic LC, which contribute a lot to cancer patient OS. [2, 3]. Besides, remarkable progress has been made in a new gene study, which has been recommended in the clinical guidelines, like *neurotrophic tyrosine kinase receptor* (*NTRK*) gene fusion. Larotrectinib has been added as the treatment option for metastatic NSCLC patients, which is sensitive to the *NTRK* gene fusion [4].

There are 8 respective members in the *cell division cycle-associated* (*CDCA*) gene and protein families, namely, *CDCA1-8*. Cell division takes an important role in the life process. It has been suggested in numerous reports that any dysregulation in the process of cell division may lead to malignancy [5–7]. *CDCA2* plays a role in modulating the response of DNA injury in the cell cycle, which is achieved through binding onto protein phosphatase 1  $\gamma$  (PP1 $\gamma$ ) [8, 9]. *CDCA3* functions modulate the progression of the cell cycle, and the expression level is regulated via protein degradation and transcription at the G1 phase in the cell cycle [10]. Moreover, *CDCA4* can regulate the cell cycle, which is associated with the transition of the G1/S phase [11] and regulates the expression of p53 [12]. *CDCA5* serves as a primary regulatory factor for the sister chromatid separation and cohesion [13]. In the undifferentiated hematopoietic populations, *CDCA7* can be triggered in the precursors of hematopoietic stem cells in the murine embryo and is maintained afterwards. Additionally, *CDCA8* plays an essential role in regulating mitosis [14].

This study aimed to evaluate systematically the association of *CDCAs* mRNA expression with LC patient survival. The *CDCAs* mRNA expression was detected in both normal and LC tissues. Then, the significance of all *CDCA* family members in predicting the prognosis for LC was analyzed based on the Kaplan–Meier Plotter database, and later the gene–gene interaction network of *CDCAs* was established to examine the underlying mechanisms of action. This study explored the *CDCAs* clinical value, so as to provide a certain theoretical foundation for making an early diagnosis, prognosis evaluation, and specific treatment for LC.

## 2. Materials and Methods

Each dataset used in the current work was searched based on the published literature. Gene Expression Omnibus (GEO) datasets and The Cancer Genome Atlas (TCGA) dataset were used for the analysis in the OncoPrint dataset, the Gene Expression Profiling Interactive Analysis (GEPIA) dataset, and the Kaplan–Meier Plotter dataset. Additionally, the informed consent of participated subjects has been submitted by the researchers, which could be searched in the TCGA database and GEO datasets.

**2.1. OncoPrint Analyses.** The transcription levels of *CDCAs* among various cancer types were examined based on the online cancer microarray database, namely, the OncoPrint gene expression array dataset ([www.oncoPrint.org](http://www.oncoPrint.org)). Moreover, *CDCAs* mRNA expression was compared between the clinical tumor samples and normal specimens. The *P* value was generated by Student's *t*-test. The threshold fold change and *P* value were set at 2 and 0.01, respectively.

**2.2. The Gene Expression Profiling Interactive Analysis (GEPIA) Dataset.** As the latest designed interactive web server, GEPIA was used to analyze RNA sequencing materials based on the GTEx and TCGA projects with the normalized processing pipeline. GEPIA allows us to offer the differential expression analyses on normal and tumor tissues, as well as the access to the profiling of cancer type and pathologic stage, analysis of patient survival, detection of a similar gene, and dimensionality reduction and correlation analyses.

**2.3. The Kaplan–Meier Plotter.** Kaplan–Meier Plotter (<http://www.kmplot.com>), the online database, was used to evaluate the prognostic significance of *CDCAs* mRNA expression, which offered the data on LC patient survival and gene expression. To examine the postprogression survival (PPS), progression-free survival (PFS), and overall survival (OS) of LC cases, all patient specimens were divided into two groups (namely, high and low expression groups) according to the median expression. Afterwards, the Kaplan–Meier survival plot was used for the evaluation on the basis of hazard ratio (HR) and the corresponding 95% confidence intervals (CI), as well as the log-rank *P* value. The Kaplan–Meier plots were obtained through the *CDCAs* Jetset best probe set alone, where the number at risk was suggested under the major plot.

**2.4. Bioinformatic Analysis and Functional Enrichment.** The online database Metascape (<http://metascape.org>) has integrated more than 40 bioinformatic knowledge bases, which enables us to extract rich annotations, identify the enriched pathways, and construct the protein-protein interaction (PPI) network based on the lists of protein and gene identifiers. The *CDCA* genes were analyzed using the Kyoto Encyclopedia of Genes and Genomes (KEGG) and

Gene Ontology (GO) approaches of Metascape, so as to search for linked genes with the highest alteration frequency.

### 3. Results

Eight *CDCA* factors are recognized in mammalian cells. In the present study, the OncoPrint databases were used to compare *CDCA*s transcriptional levels between cancer tissues and normal specimens (Figure 1). According to our results, the mRNA expression of *CDCA*s was remarkably upregulated in LC patients of many databases. In terms of the Garber dataset, *CDCA1* overexpression was detected in SCLC and SCC tissues, with the fold changes of 13.086 and 9.240, respectively [15]. In Hou et al.'s dataset, *CDCA1* was overexpressed in SCC, large-cell LC, and adenocarcinoma, and the fold changes were 10.202, 13.352, and 5.248, respectively [16]. According to Okayama's dataset, *CDCA1* overexpression was detected in lung adenocarcinoma, and the fold change was 3.267 [17]. For *CDCA2*, Hou et al.'s dataset showed that the fold changes in lung adenocarcinoma, SCC, and large-cell LC were 2.752, 4.844, and 5.076, separately [16]. Okayama et al.'s dataset also indicated *CDCA2* overexpression in lung adenocarcinoma, and the fold change was 2.511 [17]. *CDCA3* overexpression was found in lung adenocarcinoma, and the fold change was suggested to be 4.143 by Su et al.'s dataset [18], 2.828 by Okayama et al.'s dataset [17], and 3.551 by Hou's dataset. In Hou's dataset, *CDCA3* was also expressed, and the fold change in SCC was 7.717 and that in large-cell LC was 4.431 [16]. *CDCA4* was found to be overexpressed in Hou's dataset, and the fold change in SCC was 3.354 [16]. For *CDCA5*, the fold changes in Garber Lung's dataset were shown to be 7.928, 5.343, and 3.557 in large-cell LC, SCC, and lung adenocarcinoma in comparison with the common tissues, respectively [15]. Hou's dataset demonstrated the fold changes of 5.533, 6.249, and 2.853 in SCC, large-cell LC, and lung adenocarcinoma, respectively [16]. In addition, the *CDCA5* fold changes in lung adenocarcinoma were 3.324 and 2.291 in Selamat et al.'s [19] and Okayama et al.'s datasets [17], respectively. For *CDCA6*, the fold changes presented in Hou's dataset were 5.371, 3.744, and 2.267 in large-cell LC, SCC, and lung adenocarcinoma compared with common tissues, respectively [16]. For *CDCA7*, the fold changes displayed in Hou's dataset were 5.997, 9.075, and 7.392 in lung adenocarcinoma, SCC, and large-cell LC, respectively [16]. Okayama's dataset showed that the fold change was 6.000 in lung adenocarcinoma [17]. Besides, Selamat's dataset indicated that the fold change was 2.935 in lung adenocarcinoma. For *CDCA8*, in Hou's dataset, the fold changes in lung adenocarcinoma, SCC, and large-cell LC were 2.935, 3.743, and 4.913, respectively, compared with normal tissues [16]. Selamat et al.'s dataset showed a fold change of 2.000 in lung adenocarcinoma [19], while Okayama et al.'s dataset presented a fold change of 5.763 in lung adenocarcinoma [17] (Table 1).

**3.1. Associations of *CDCA*s mRNA Expression with Clinicopathological Variables in LC Patients.** The GEPIA dataset

(<http://gepia.cancer-pku.cn/>) was performed to compare the mRNA expression of *CDCA*s in LC tissues with that in normal lung tissues. According to our findings, the *CDCA1/2/3/4/5/6/7/8* expression levels were upregulated in LC tissues relative to that in noncarcinoma ones (Figures 2 and 3). Additionally, the association of the expression of *CDCA* genes with the LC stage was analyzed. There were significant differences in *CDCA1/2/3/4/5/8* expression (Figure 4).

**3.2. Relationship between Elevated *CDCA 2/3/4/5/7/8* mRNA Expression and Dismal Prognosis for LC Cases.** The crucial *CDCA*s efficiency in LC patient survival was also found. The Kaplan–Meier Plotter approach was utilized to examine the relationship of mRNA expression of *CDCA*s with LC patient survival based on the public datasets. Our results suggested that increased *CDCA 1–8* showed a significant relationship with poorer OS and PFS ( $P < 0.05$ ). Only LC patients with upregulated *CDCA3/4/5/8* expression were significantly correlated with the lower PPS ( $P < 0.05$ ) (Figure 5).

### 3.3. Genetic Alteration and Correlation

**3.3.1. Pathway Enrichment Analyses and Predicted Functions of *CDCA* Genes among LC Cases.** Genes showing co-expression with *CDCA* genes would be examined using the String and Functional protein association networks. *NUF2*, *CDCA2*, *CDCA3*, *CDCA4*, *CDCA5*, *CDCA6*, *CDCA7*, *CDCA8*, *CDC20*, *AURKB*, *CBX2*, *CDK1*, *ZWINT*, *BUB1*, *NDC80*, *SPC24*, *SPC25*, *BIRC5*, and *INCENP* were discovered in our results (Figure 6). Then, the lists of all the *CDCA* genes expressed, together with linked genes displaying the highest alteration frequency, were compiled before they were analyzed by the KEGG and GO approaches in Metascape (Figure 7). According to our results, the processes below were subjected to the influence of *CDCA* gene alteration: R-HAS-2500257: resolution of sister chromatid cohesion; GO:0051301: cell division; CORUM: 1118: Chromosomal passenger complex (CPC, including *CDCA8*, *INCENP*, *AURKB*, and *BIRC5*); CORUM: 127: NDC80 kinetochore complex; M129: PID PLK1 pathway; and GO: 0007080: mitotic metaphase plate congression.

## 4. Discussion

*CDCA1*, one of the Ndc80 complex members, plays a role in regulating mitosis [20], which is coexpressed with the known cell cycle genes [21] (such as cyclin and topoisomerase II). Some studies demonstrate that *CDCA1* overexpression is related to the dismal prognosis for patients with colorectal cancer (CRC) [22, 23]. Moreover, the study conducted by Hayama, et al. [21] showed that *CDCA1* knockdown using small interfering RNA remarkably suppressed the growth of NSCLC cells. Furthermore, *CDCA1* has been used as the vaccination for patients with advanced biliary tract cancer and prostate cancer, and well toleration is achieved in these phase I clinical trials [24, 25]. The current study suggested that The Cancer Genome Atlas and the OncoPrint datasets

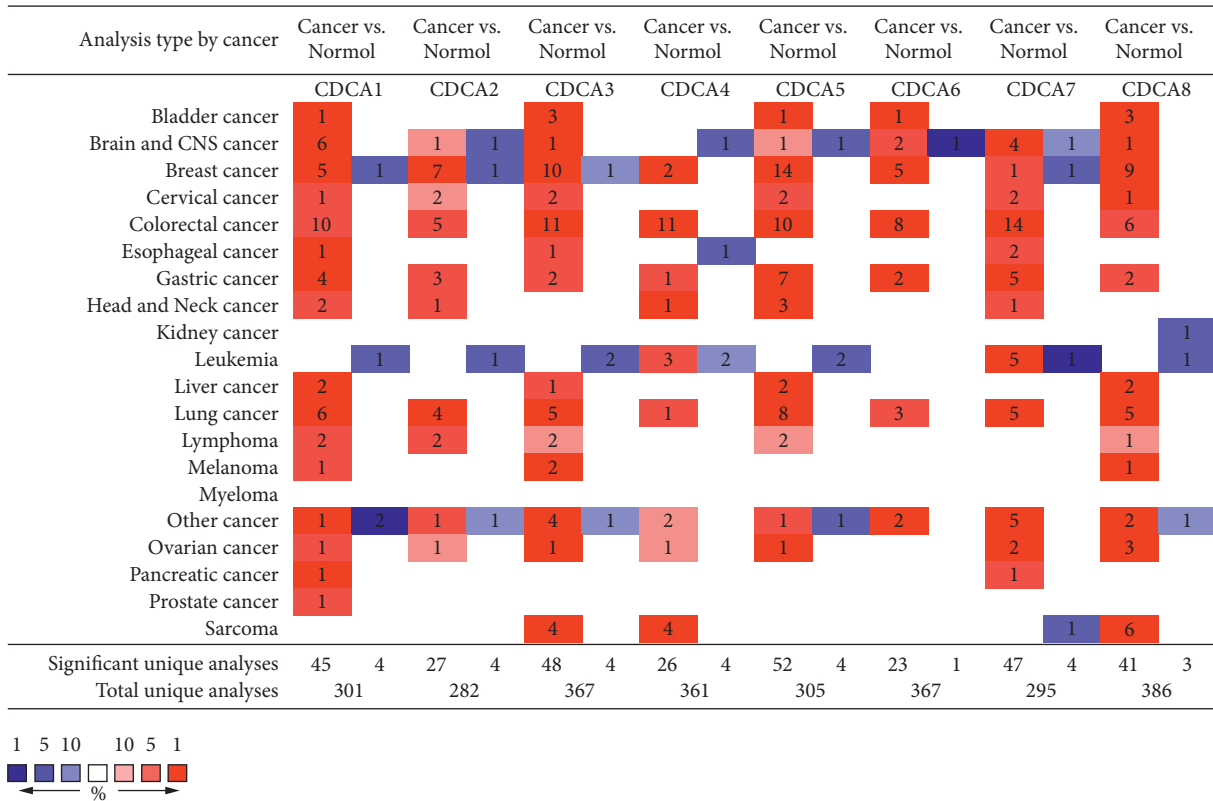


FIGURE 1: CDCA expression at transcription level among various cancer types (the ONCOMINE).

TABLE 1: The significant changes of CDCA expression in transcription level between types of lung cancer and normal lung tissues (Oncomine Database).

	Type of lung cancer versus normal lung tissue	Fold change	P value	t-test	Source and/or reference
CDCA1	Small cell lung carcinoma	13.086	1.21E-5	8.683	Garber et al. [15]
	Squamous cell lung carcinoma	9.240	4.71E-6	6.905	Garber et al. [15]
	Squamous cell lung carcinoma	10.202	1.55E-19	18.306	Hou et al. [16]
	Lung adenocarcinoma	5.248	7.31E-15	10.550	Hou et al. [16]
	Large-cell lung carcinoma	13.352	2.73E-8	8.647	Hou et al. [16]
	Lung adenocarcinoma	3.267	2.26E-12	10.264	Okayama et al. [17]
CDCA2	Lung adenocarcinoma	2.752	3.07E-15	10.285	Hou et al. [16]
	Squamous cell lung carcinoma	4.844	1.20E-13	12.093	Hou et al. [16]
	Large-cell lung carcinoma	5.076	1.34E-6	6.586	Hou et al. [16]
	Lung adenocarcinoma	2.511	1.03E-12	10.242	Okayama et al. [17]
CDCA3	Lung adenocarcinoma	4.143	2.60E-11	8.366	Su et al. [18]
	Squamous cell lung carcinoma	7.717	5.79E-26	21.275	Hou et al. [16]
	Lung adenocarcinoma	3.551	9.34E-16	10.511	Hou et al. [16]
	Large-cell lung carcinoma	4.431	1.08E-8	9.131	Hou et al. [16]
Lung adenocarcinoma	2.828	3.60E-12	10.001	Okayama et al. [17]	
CDCA4	Squamous cell lung carcinoma	3.354	1.66E-13	12.179	Hou et al. [16]
CDCA5	Large-cell lung carcinoma	7.928	2.49E-6	10.744	Garber et al. [15]
	Squamous cell lung carcinoma	5.343	8.05E-7	8.173	Garber et al. [15]
	Lung adenocarcinoma	3.557	3.03E-5	7.382	Garber et al. [15]
	Squamous cell lung carcinoma	5.533	1.77E-23	21.214	Hou et al. [16]
	Large-cell lung carcinoma	6.249	1.74E-8	8.843	Hou et al. [16]
	Lung adenocarcinoma	2.853	8.10E-14	9.704	Hou et al. [16]
	Lung adenocarcinoma	3.324	9.19E-20	13.055	Selamat et al. [19]
	Lung adenocarcinoma	2.291	2.02E-9	8.518	Okayama et al. [17]



TABLE 1: Continued.

	Type of lung cancer versus normal lung tissue	Fold change	P value	t-test	Source and/or reference
CDCA6	Large-cell lung carcinoma	5.371	$7.64E-7$	6.902	Hou et al. [16]
	Squamous cell lung carcinoma	3.744	$5.28E-10$	8.850	Hou et al. [16]
	Lung adenocarcinoma	2.267	$1.35E-8$	6.564	Hou et al. [16]
CDCA7	Lung adenocarcinoma	5.997	$9.23E-17$	6.009	Hou et al. [16]
	Squamous cell lung carcinoma	9.075	$1.91E-19$	15.046	Hou et al. [16]
	Large-cell lung carcinoma	7.392	$6.18E-6$	5.779	Hou et al. [16]
	Lung adenocarcinoma	6.000	$1.26E-16$	15.108	Okayama et al. [17]
	Lung adenocarcinoma	2.935	$2.00E-14$	9.214	Selamat et al. [19]
CDCA8	Lung adenocarcinoma	2.935	$3.18E-15$	10.818	Hou et al. [16]
	Squamous cell lung carcinoma	3.743	$3.32E-17$	15.713	Hou et al. [16]
	Large-cell lung carcinoma	4.913	$1.07E-8$	9.151	Hou et al. [16]
	Lung adenocarcinoma	2.000	$4.40E-17$	11.529	Selamat et al. [19]
	Lung adenocarcinoma	5.763	$5.05E-10$	9.625	Okayama et al. [17]

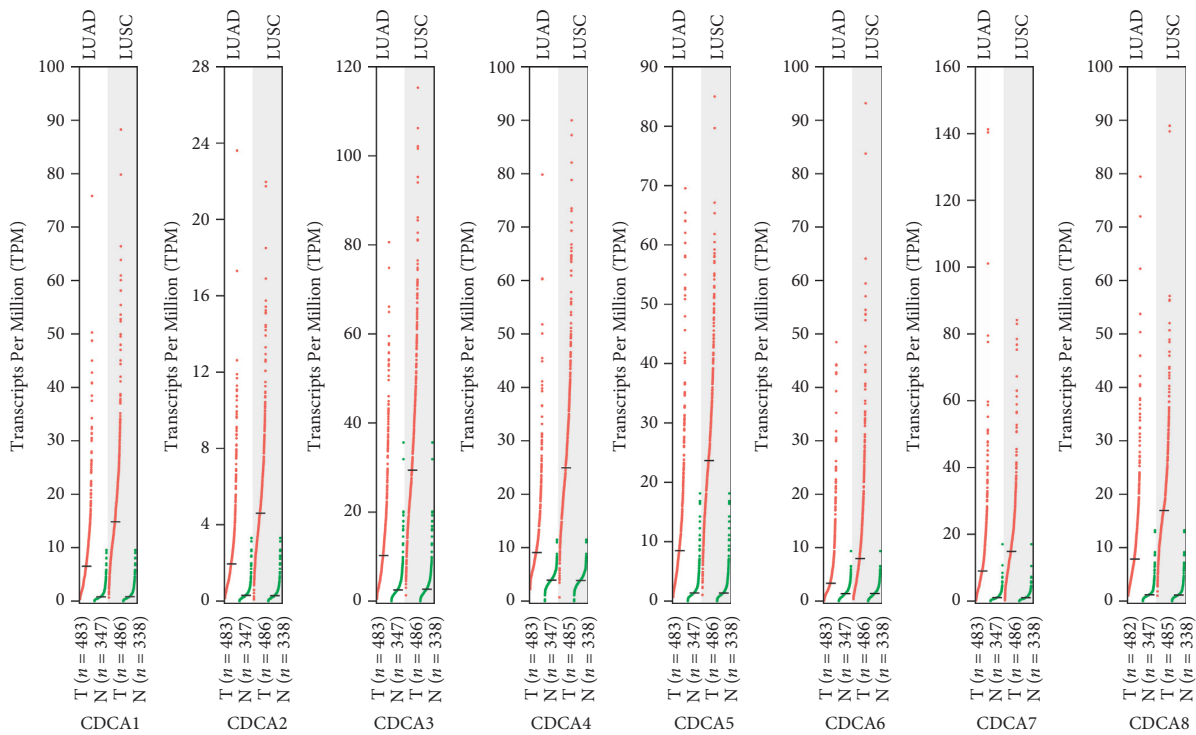


FIGURE 2: CDCA expression in LC (GEPIA).

revealed higher *CDCA1* expression in LC tissues than in noncarcinoma tissues. A high *CDCA1* level revealed a significant correlation with worse OS in all LC patients.

*CDCA2* acts as the PP1 $\gamma$  expression regulator, which inhibits the activation of DNA damage response [8, 9]. Recent research results demonstrate that *CDCA2* methylation in HeLa cells promotes cell proliferation and suppresses apoptosis [26]. Additionally, *CDCA2* overexpression promotes the proliferation of CRC cells and oral squamous cell carcinoma (OSCC) cells [27, 28]. Furthermore, a study on lung adenocarcinoma suggests that *CDCA2* proliferates lung adenocarcinoma cells and predicts the poor prognosis for these patients [29]. Our results indicated that *CDCA2* expression level in LC tissues was upregulated relative to that

in noncarcinoma tissues. The expression of *CDCA2* showed a correlation with the LC stage. High *CDCA2* expression level displayed a significant correlation with the improved OS for all LC patients.

*CDCA3* controls the G1 phase [30], which acts as one of the prognostic genes for hepatocellular carcinoma (HCC) [31] and is also involved in LC cell proliferation, migration, invasion, and apoptosis [30], as well as CRC cell proliferation [32]. Moreover, it has been reported that *CDCA3* expression is related to prognosis for bladder cancer cases [33] and luminal A breast cancer [34]. Current studies show that overexpression of *CDCA3* frequently occurs in the process of oral carcinogenesis [35]. It was discovered that *CDCA3* expression was upregulated among LC tissues

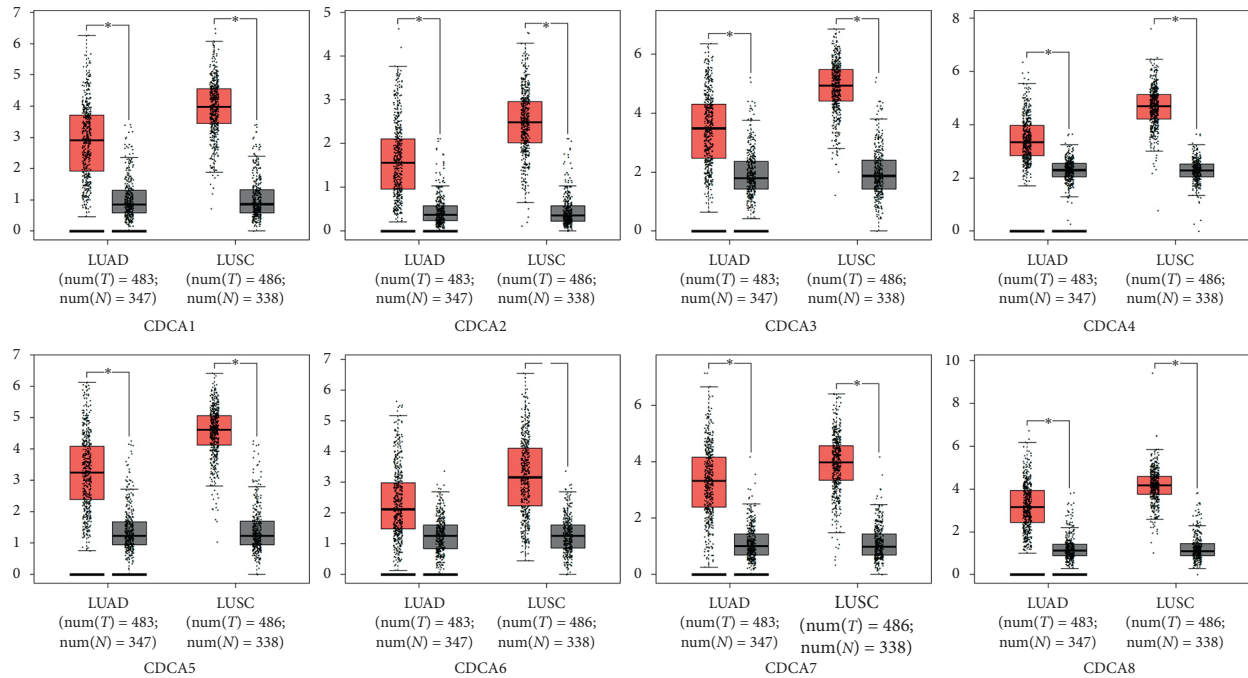


FIGURE 3: CDCA expression in LC presented in the form of a boxplot (GEPIA).

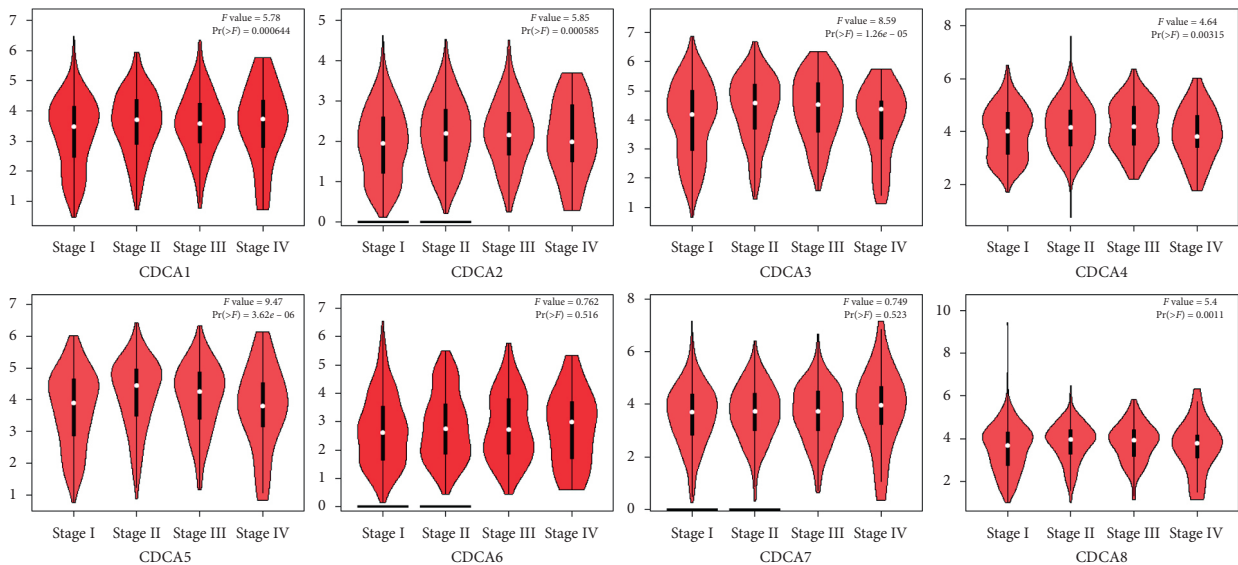


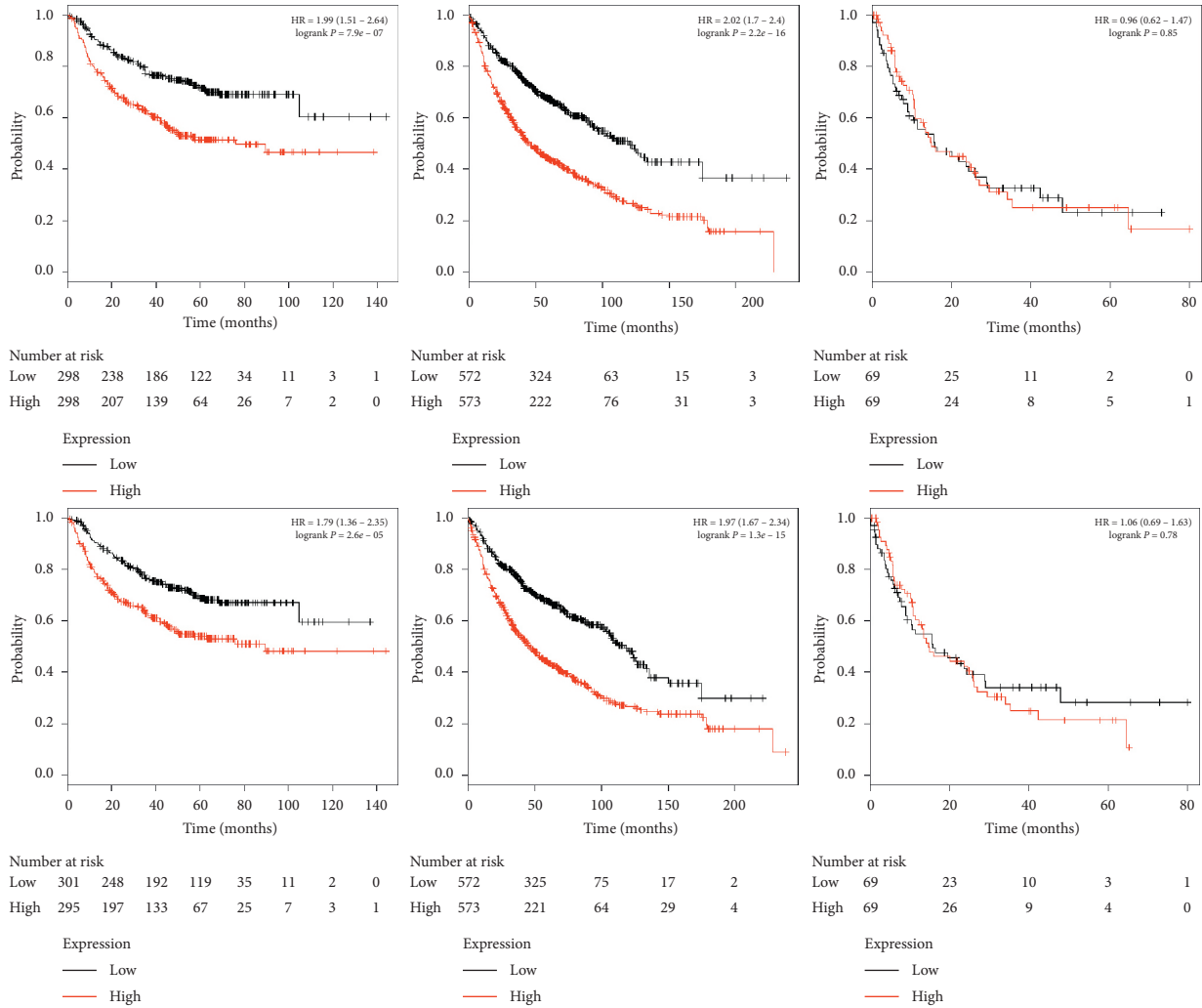
FIGURE 4: Correlation of the CDCA expression with tumor stage among LC cases (GEPIA).

compared with that in noncarcinoma counterparts, but not with the LC stage. Additionally, the upregulated *CDCA3* expression showed a significant correlation with the improved PFS, OS, and PPS among all LC patients.

*CDCA4* protein expression is found in some human cells, which can be induced when cells enter the  $G_1/S$  phase in the cell cycle [11]. In a previous study, Hayashi et al. showed that *CDCA4* participated in cell proliferation [11]. Moreover, *CDCA4* is involved in the triple-negative breast cancer (TNBC) cells [36], and it is shown that RNA interference of *CDCA4* markedly increases cell apoptotic rate. In addition, one recent study suggests that *CDCA4* enhances

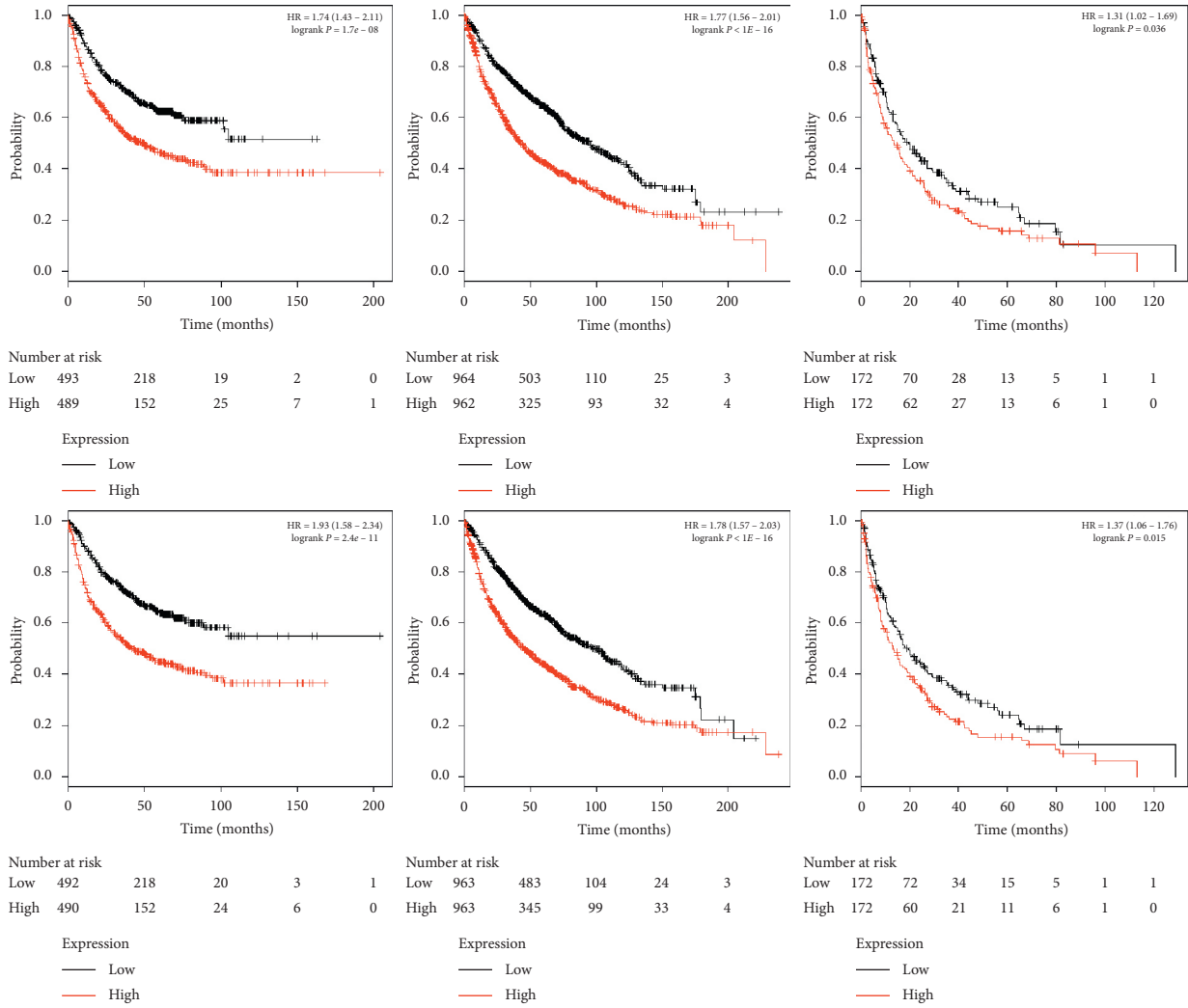
human BC cell proliferation and reduces their apoptosis [37]. In this study, we found that *CDCA4* expression was increased in human LC tissues relative to that in noncarcinoma tissues, and such expression showed a correlation with the LC stage. The upregulated *CDCA4* expression showed a marked correlation with the improved PFS and OS of all LC patients.

A recent study shows that *CDCA5* probably serves as a biomarker for the prognosis, treatment, and diagnosis for HCC [38–40]. It also exerts a vital part in the proliferation of HCC cells [41, 42], OSCC [41, 42], and bladder cancer [43]. For digestive system cancer, *CDCA5* is found to play crucial



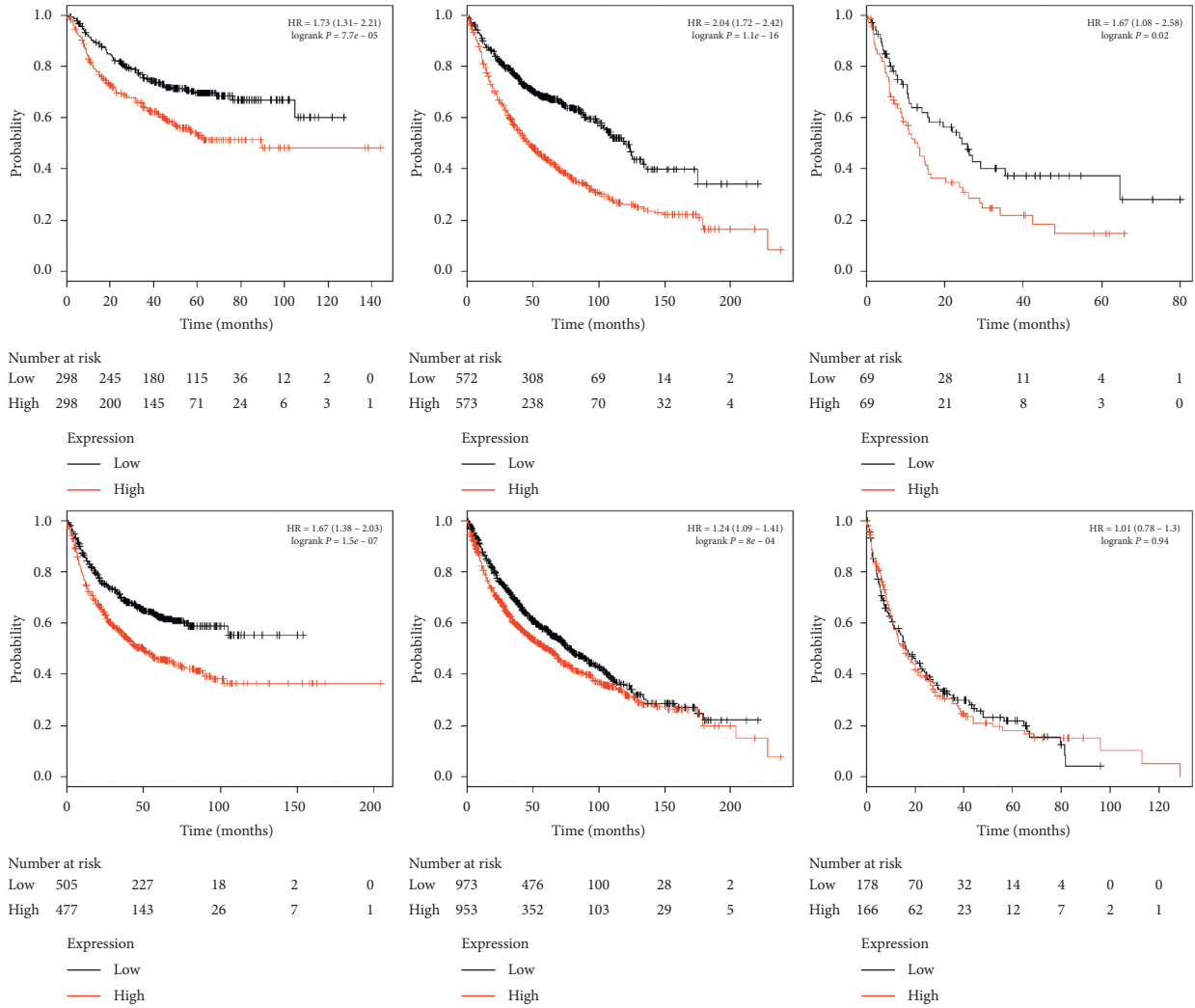
(a)

FIGURE 5: Continued.



(b)

FIGURE 5: Continued.



(c)

FIGURE 5: Continued.

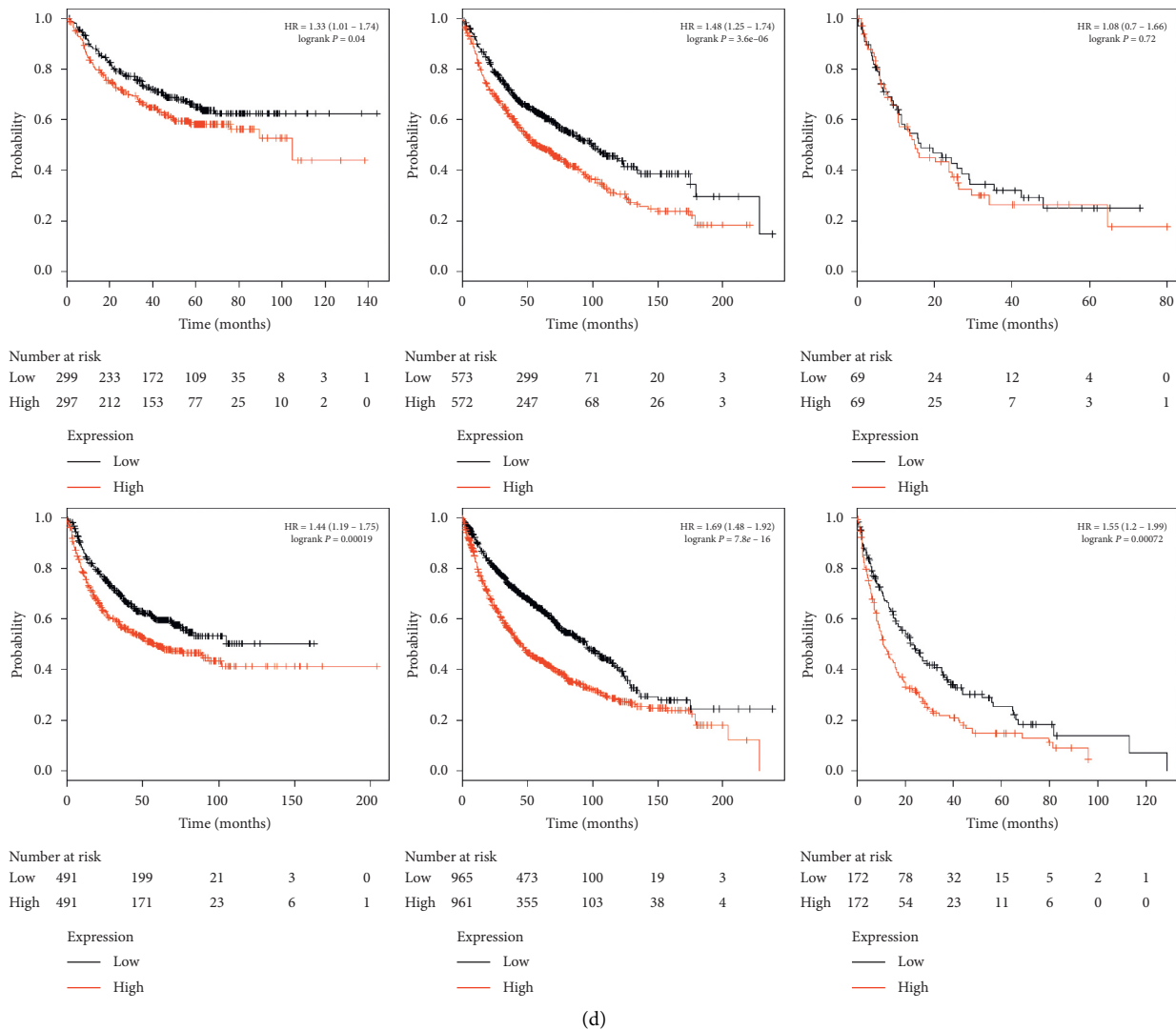


FIGURE 5 Significance of the CDCA mRNA expression in predicting the prognosis for LC cases (Kaplan-Meier plotter).

roles in the proliferation of gastric cancer cells [44]. Moreover, *CDCA5* is also differentially expressed in patients with localized and locally advanced prostate cancer [45]. Regarding LC, the transactivation of *CDCA5* and its phosphorylation exert vital parts in the proliferation of LC cells [13]. Wu et al. [46] also indicated that *CDCA5* acted as a novel promising target for NSCLC diagnosis and treatment. In this study, the *CDCA5* expression level was down-regulated in LC tissues compared with that in noncarcinoma counterparts. Besides, such expression showed an association with the LC stage. Obviously, the high *CDCA5* expression displayed a significant correlation with the improved OS for all LC patients.

*CDCA7* has been recognized as an MYC-target gene [47]. A recent study shows that *CDCA7* is overexpressed in lymphoid tumors, and *CDCA7* knockdown decreases the growth rate of the lymphoid tumor, without inhibiting the proliferation of normal cells [48]. In this study, the *CDCA7* expression level was upregulated in human LC tissues compared with that in noncarcinoma counterparts, and such expression showed no correlation with the LC stage.

Obviously, the high *CDCA7* expression displayed a remarkable correlation with the improved PFS and OS in all LC patients.

*CDCA8* protein has been identified as an integral part of the vertebrate chromosomal passenger complex (cPc) [49]. The expression of *CDCA8* is closely associated with tumor progression, N stage, T stage, and grade of bladder cancer [50]. *CDCA8* is related to the distant metastasis risk of breast cancer [51, 52]. With regard to renal cancer, *CDCA8* has also certain prognostic value [53]. *CDCA8* promotes the malignant progression of cutaneous melanoma [54]. Furthermore, *CDCA8* also exerts a vital part during lung carcinogenesis [55]. In this study, the *CDCA8* expression level was upregulated in LC tissues relative to that in noncarcinoma counterparts, and such expression exerted no correlation with the LC stage. Obviously, the high *CDCA8* expression showed a close association with the improved PFS and OS of all LC patients.

Besides, KEGG and GO analyses were also carried out to find the correlations between *CDCA* genes' expression and linked genes of the highest alteration frequency and

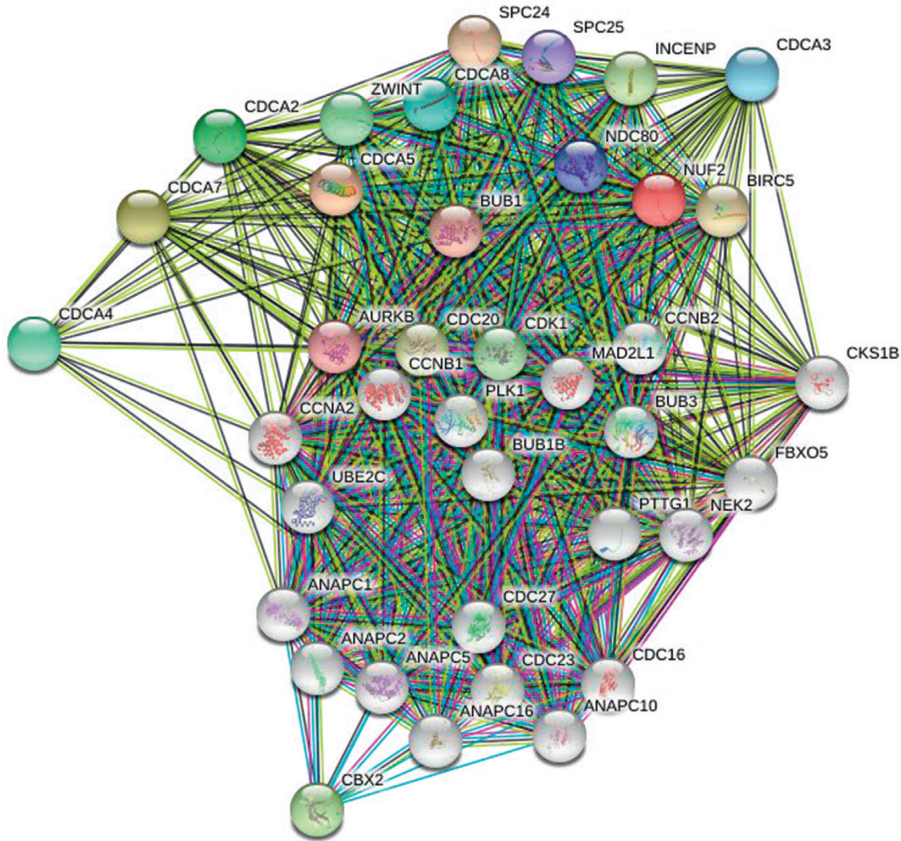
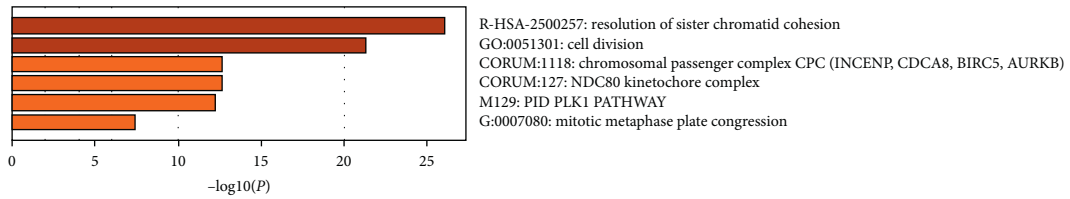
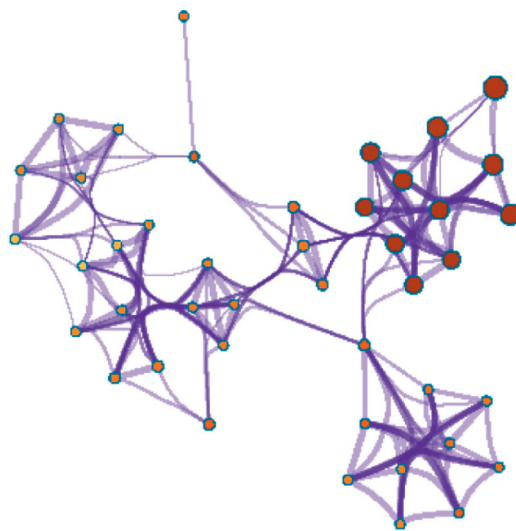


FIGURE 6: Gene coexpression among LC cases (STRING).



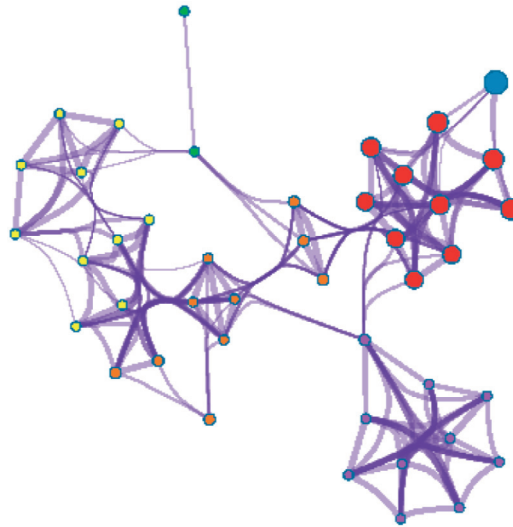
(a)



(b)

FIGURE 7: Continued.





(c)

FIGURE 7 Functions of CDCA genes as well as those showing significant correlation with CDCA gene alterations.

the prognosis for LC. According to our results, attention should be paid to some pathways including R-HAS-2500257: resolution of sister chromatid cohesion; GO: 0051301: cell division; CORUM: 1118: chromosomal passenger complex (CPC, including *CDCA8*, *INCENP*, *AURKB*, and *BIRC5*); CORUM: 127: NDC80 kinetochore complex; M129: PID PLK1 pathway; and GO: 0007080: mitotic metaphase plate congression. Previous studies show that the Polo-like kinase 1 (PLK1) is highly expressed in LC, which predicts the poor survival in metastatic LC patients [56, 57]. In addition, the PLK1 pathway plays a certain role in the progression of HCC [58], glioma [59], and lung adenocarcinoma [60].

The current research systemically examines the expression of *CDCA* genes and its prognostic significance in LC, which sheds more light on the complexity and heterogeneity of LC biological properties at the molecular level. Based on our results, *CDCAs* upregulation in LC tissues probably exerts a crucial part during LC oncogenesis. Besides, *CDCAs* upregulation can serve as a potential prognostic marker to improve the survival and prognostic accuracy for LC. Moreover, *CDCA* genes probably exert their functions in tumorigenesis through the PLK1 pathway.

### Data Availability

The data used to support the findings of this study are available from the corresponding author upon request.

### Conflicts of Interest

All authors declare no conflicts of interest.

### Authors' Contributions

HL and LJJ designed the research protocol, analyzed data, and revised the manuscript. CXC and SLC searched and

analyzed the data. CXC and LLP wrote the manuscript and participated in analyzing data. HHY and ML participated in searching the data. QYZ made a lot of work in reviewing and revising the manuscript. All authors read and approved the final manuscript. Chongxiang Chen and Siliang Chen contributed equally to this work.

### Acknowledgments

This work was supported by the grant from the Medical Research Fund of Guangdong Province (no. A2018237).

### References

- [1] R. L. Siegel, K. D. Miller, and A. Jemal, "Cancer statistics, 2019," *CA: A Cancer Journal for Clinicians*, vol. 69, no. 1, pp. 7–34, 2019.
- [2] M. Reck, D. Rodriguez-Abreu, A. G. Robinson et al., "Updated analysis of KEYNOTE-024: pembrolizumab versus platinum-based chemotherapy for advanced non-small-cell lung cancer with PD-L1 tumor proportion score of 50% or greater," *Journal of Clinical Oncology*, vol. 37, no. 7, pp. 537–546, 2019.
- [3] D. Zhao, X. Chen, N. Qin et al., "The prognostic role of EGFR-TKIs for patients with advanced non-small cell lung cancer," *Scientific Reports*, vol. 7, Article ID 40374, 2017.
- [4] A. Drilon, T. W. Laetsch, S. Kummar et al., "Efficacy of larotrectinib in TRK fusion-positive cancers in adults and children," *New England Journal of Medicine*, vol. 378, no. 8, pp. 731–739, 2018.
- [5] S. Preston-Martin, M. C. Pike, R. K. Ross, P. A. Jones, and B. E. Henderson, "Increased cell division as a cause of human cancer," *Cancer Research*, vol. 50, no. 23, pp. 7415–7421, 1990.
- [6] G. Vader and S. M. Lens, "The Aurora kinase family in cell division and cancer," *Biochim Biophys Acta*, vol. 1786, no. 1, pp. 60–72, 2008.
- [7] I. Collins and M. Garrett, "Targeting the cell division cycle in cancer: CDK and cell cycle checkpoint kinase inhibitors," *Current Opinion In Pharmacology*, vol. 5, no. 4, pp. 366–373, 2005.

- [8] A. Peng, A. L. Lewellyn, W. P. Schieman, and J. L. Maller, "Repo-man controls a protein phosphatase 1-dependent threshold for DNA damage checkpoint activation," *Current Biology*, vol. 20, no. 5, pp. 387–396, 2010.
- [9] P. Vagnarelli, "Repo-man at the intersection of chromatin remodelling, DNA repair, nuclear envelope organization, and cancer progression," *Cancer Biology and the Nuclear Envelope*, vol. 773, pp. 401–414, 2014.
- [10] K. Yoshida, "Cell-cycle-dependent regulation of the human and mouse Tome-1 promoters," *FEBS Letters*, vol. 579, no. 6, pp. 1488–1492, 2005.
- [11] R. Hayashi, Y. Goto, R. Ikeda, K. K. Yokoyama, and K. Yoshida, "CDCA4 is an E2F transcription factor family-induced nuclear factor that regulates E2F-dependent transcriptional activation and cell proliferation," *Journal of Biological Chemistry*, vol. 281, no. 47, pp. 35633–35648, 2006.
- [12] M. Tategu, H. Nakagawa, R. Hayashi, and K. Yoshida, "Transcriptional co-factor CDCA4 participates in the regulation of JUN oncogene expression," *Biochimie*, vol. 90, no. 10, pp. 1515–1522, 2008.
- [13] M.-H. Nguyen, J. Koinuma, K. Ueda et al., "Phosphorylation and activation of cell division cycle associated 5 by mitogen-activated protein kinase play a crucial role in human lung carcinogenesis," *Cancer Research*, vol. 70, no. 13, pp. 5337–5347, 2010.
- [14] T. Higuchi and F. Uhlmann, "Passenger acrobatics," *Nature*, vol. 426, no. 6968, pp. 780–781, 2003.
- [15] M. E. Garber, O. G. Troyanskaya, K. Schluens et al., "Diversity of gene expression in adenocarcinoma of the lung," *Proceedings of the National Academy of Sciences*, vol. 98, no. 24, pp. 13784–13789, 2001.
- [16] J. Hou, J. Aerts, B. den Hamer et al., "Gene expression-based classification of non-small cell lung carcinomas and survival prediction," *PLoS One*, vol. 5, no. 4, Article ID e10312, 2010.
- [17] H. Okayama, T. Kohno, Y. Ishii et al., "Identification of genes upregulated in ALK-positive and EGFR/KRAS/ALK-negative lung adenocarcinomas," *Cancer Research*, vol. 72, no. 1, pp. 100–111, 2012.
- [18] L.-J. Su, C.-W. Chang, Y.-C. Wu et al., "Selection of DDX5 as a novel internal control for Q-RT-PCR from microarray data using a block bootstrap re-sampling scheme," *BMC Genomics*, vol. 8, no. 1, p. 140, 2007.
- [19] S. A. Selamat, B. S. Chung, L. Girard et al., "Genome-scale analysis of DNA methylation in lung adenocarcinoma and integration with mRNA expression," *Genome Research*, vol. 22, no. 7, pp. 1197–1211, 2012.
- [20] J. G. DeLuca, B. J. Howell, J. C. Canman, J. M. Hickey, G. Fang, and E. D. Salmon, "Nuf2 and Hec1 are required for retention of the checkpoint proteins Mad1 and Mad2 to kinetochores," *Current Biology*, vol. 13, no. 23, pp. 2103–2109, 2003.
- [21] S. Hayama, Y. Daigo, T. Kato et al., "Activation of CDCA1-KNTC2, members of centromere protein complex, involved in pulmonary carcinogenesis," *Cancer Research*, vol. 66, no. 21, pp. 10339–10348, 2006.
- [22] Y. Kobayashi, A. Takano, Y. Miyagi et al., "Cell division cycle-associated protein 1 overexpression is essential for the malignant potential of colorectal cancers," *International Journal of Oncology*, vol. 44, no. 1, pp. 69–77, 2014.
- [23] Y. Miyata, K. Kumagai, T. Nagaoka et al., "Clinicopathological significance and prognostic value of Wilms' tumor gene expression in colorectal cancer," *Cancer Biomarkers*, vol. 15, no. 6, pp. 789–797, 2015.
- [24] A. Aruga, N. Takeshita, Y. Kotera et al., "Phase I clinical trial of multiple-peptide vaccination for patients with advanced biliary tract cancer," *Journal of Translational Medicine*, vol. 12, no. 1, p. 61, 2014.
- [25] W. Obara, F. Sato, K. Takeda et al., "Phase I clinical trial of cell division associated 1 (CDCA1) peptide vaccination for castration resistant prostate cancer," *Cancer Science*, vol. 108, no. 7, pp. 1452–1457, 2017.
- [26] C.-W. Li and B.-S. Chen, "Investigating core genetic-and-epigenetic cell cycle networks for stemness and carcinogenic mechanisms, and cancer drug design using big database mining and genome-wide next-generation sequencing data," *Cell Cycle*, vol. 15, no. 19, pp. 2593–2607, 2016.
- [27] Y. Feng, W. Qian, Y. Zhang et al., "CDCA2 promotes the proliferation of colorectal cancer cells by activating the AKT/CCND1 pathway in vitro and in vivo," *BMC Cancer*, vol. 19, no. 1, p. 576, 2019.
- [28] F. Uchida, K. Uzawa, A. Kasamatsu et al., "Overexpression of CDCA2 in human squamous cell carcinoma: correlation with prevention of G1 phase arrest and apoptosis," *PLoS One*, vol. 8, no. 2, Article ID e56381, 2013.
- [29] R. Shi, C. Zhang, Y. Wu et al., "CDCA2 promotes lung adenocarcinoma cell proliferation and predicts poor survival in lung adenocarcinoma patients," *Oncotarget*, vol. 8, no. 12, pp. 19768–19779, 2017.
- [30] Q. Hu, J. Fu, B. Luo et al., "OY-TE5-1 may regulate the malignant behavior of liver cancer via NANOG, CD9, CCND2 and CDCA3: a bioinformatic analysis combine with RNAi and oligonucleotide microarray," *Oncology Reports*, vol. 33, no. 4, pp. 1965–1975, 2015.
- [31] L. Guan, Q. Luo, N. Liang, and H. Liu, "A prognostic prediction system for hepatocellular carcinoma based on gene co-expression network," *Experimental and Therapeutic Medicine*, vol. 17, no. 6, pp. 4506–4516, 2019.
- [32] W. Qian, Z. Zhang, W. Peng et al., "CDCA3 mediates p21-dependent proliferation by regulating E2F1 expression in colorectal cancer," *International Journal of Oncology*, vol. 53, no. 5, pp. 2021–2033, 2018.
- [33] S. Li, X. Liu, T. Liu et al., "Identification of biomarkers correlated with the TNM staging and overall survival of patients with bladder cancer," *Frontiers in Physiology*, vol. 8, p. 947, 2017.
- [34] J. Perez-Pena, A. Alcaraz-Sanabria, C. Nieto-Jimenez et al., "Mitotic read-out genes confer poor outcome in luminal A breast cancer tumors," *Oncotarget*, vol. 8, no. 13, pp. 21733–21740, 2017.
- [35] F. Uchida, K. Uzawa, A. Kasamatsu et al., "Overexpression of cell cycle regulator CDCA3 promotes oral cancer progression by enhancing cell proliferation with prevention of G1 phase arrest," *BMC Cancer*, vol. 12, p. 321, 2012.
- [36] S. Pang, Y. Xu, J. Chen, G. Li, J. Huang, and X. Wu, "Knockdown of cell division cycle-associated protein 4 expression inhibits proliferation of triple negative breast cancer MDA-MB-231 cells in vitro and in vivo," *Oncology Letters*, vol. 17, no. 5, pp. 4393–4400, 2019.
- [37] Y. Xu, X. Wu, F. Li, D. Huang, and W. Zhu, "CDCA4, a downstream gene of the Nrf2 signaling pathway, regulates cell proliferation and apoptosis in the MCF7/ADM human breast cancer cell line," *Molecular Medicine Reports*, vol. 17, no. 1, pp. 1507–1512, 2017.
- [38] C. Cai, W. Wang, and Z. Tu, "Aberrantly DNA methylated-differentially expressed genes and pathways in hepatocellular carcinoma," *Journal of Cancer*, vol. 10, no. 2, pp. 355–366, 2019.

- [39] Y. Tian, J. Wu, C. Chagas et al., "CDCA5 overexpression is an Indicator of poor prognosis in patients with hepatocellular carcinoma (HCC)," *BMC Cancer*, vol. 18, no. 1, p. 1187, 2018.
- [40] J. Wang, C. Xia, M. Pu et al., "Silencing of CDCA5 inhibits cancer progression and serves as a prognostic biomarker for hepatocellular carcinoma," *Oncology Reports*, vol. 40, no. 4, pp. 1875–1884, 2018.
- [41] H. Chen, J. Chen, L. Zhao et al., "CDCA5, transcribed by E2F1, promotes oncogenesis by enhancing cell proliferation and inhibiting apoptosis via the AKT pathway in hepatocellular carcinoma," *Journal of Cancer*, vol. 10, no. 8, pp. 1846–1854, 2019.
- [42] N. Tokuzen, K. Nakashiro, H. Tanaka, K. Iwamoto, and H. Hamakawa, "Therapeutic potential of targeting cell division cycle associated 5 for oral squamous cell carcinoma," *Oncotarget*, vol. 7, no. 3, pp. 2343–2353, 2016.
- [43] S. Pan, Y. Zhan, X. Chen, B. Wu, and B. Liu, "Identification of biomarkers for controlling cancer stem cell characteristics in bladder cancer by network analysis of transcriptome data stemness indices," *Frontiers in Oncology*, vol. 9, p. 613, 2019.
- [44] T. Chen, Z. Huang, Y. Tian et al., "Role of triosephosphate isomerase and downstream functional genes on gastric cancer," *Oncology Reports*, vol. 38, no. 3, pp. 1822–1832, 2017.
- [45] Y. Tolkach, A. Merseburger, T. Herrmann, M. Kuczyk, J. Serth, and F. Imkamp, "Signatures of adverse pathological features, androgen insensitivity and metastatic potential in prostate cancer," *Anticancer Research*, vol. 35, no. 10, pp. 5443–5451, 2015.
- [46] Q. Wu, B. Zhang, Y. Sun et al., "Identification of novel biomarkers and candidate small molecule drugs in non-small-cell lung cancer by integrated microarray analysis," *Onco-Targets and Therapy*, vol. 12, pp. 3545–3563, 2019.
- [47] J. E. Prescott, R. C. Osthus, L. A. Lee et al., "A novel c-Myc-responsive Gene, JPO1, participates in neoplastic transformation," *Journal Of Biological Chemistry*, vol. 276, no. 51, pp. 48276–48284, 2001.
- [48] C. Martin-Cortazar, Y. Chiodo, R. P. Jimenez et al., "CDCA7 finely tunes cytoskeleton dynamics to promote lymphoma migration and invasion," *Haematologica*, vol. 105, no. 1, 2019.
- [49] N. N. Phan, C. Y. Wang, K. L. Li et al., "Distinct expression of CDCA3, CDCA5, and CDCA8 leads to shorter relapse free survival in breast cancer patient," *Oncotarget*, vol. 9, no. 6, pp. 6977–6992, 2018.
- [50] Y. Bi, S. Chen, J. Jiang et al., "CDCA8 expression and its clinical relevance in patients with bladder cancer," *Medicine*, vol. 97, no. 34, Article ID e11899, 2018.
- [51] Y. Cai, J. Mei, Z. Xiao et al., "Identification of five hub genes as monitoring biomarkers for breast cancer metastasis in silico," *Hereditas*, vol. 156, p. 20, 2019.
- [52] M. Kabisch, B. J. Lorenzo, T. Dunnebie et al., "Inherited variants in the inner centromere protein (INCENP) gene of the chromosomal passenger complex contribute to the susceptibility of ER-negative breast cancer," *Carcinogenesis*, vol. 36, no. 2, pp. 256–271, 2015.
- [53] Y. Gu, L. Lu, L. Wu, H. Chen, W. Zhu, and Y. He, "Identification of prognostic genes in kidney renal clear cell carcinoma by RNA-seq data analysis," *Molecular Medicine Reports*, vol. 15, no. 4, pp. 1661–1667, 2017.
- [54] C. Ci, B. Tang, D. Lyu et al., "Overexpression of CDCA8 promotes the malignant progression of cutaneous melanoma and leads to poor prognosis," *International Journal of Molecular Medicine*, vol. 43, no. 1, pp. 404–412, 2018.
- [55] S. Hayama, Y. Daigo, T. Yamabuki et al., "Phosphorylation and activation of cell division cycle associated 8 by aurora kinase B plays a significant role in human lung carcinogenesis," *Cancer Research*, vol. 67, no. 9, pp. 4113–4122, 2007.
- [56] S. B. Shin, H. R. Jang, R. Xu, J. Y. Won, and H. Yim, "Active PLK1-driven metastasis is amplified by TGF-beta signaling that forms a positive feedback loop in non-small cell lung cancer," *Oncogene*, vol. 39, no. 4, pp. 767–785, 2019.
- [57] Y. Liao, G. Yin, X. Wang, P. Zhong, X. Fan, and C. Huang, "Identification of candidate genes associated with the pathogenesis of small cell lung cancer via integrated bioinformatics analysis," *Oncology Letters*, vol. 18, no. 4, pp. 3723–3733, 2019.
- [58] R. Li, X. Jiang, Y. Zhang et al., "Cyclin B2 overexpression in human hepatocellular carcinoma is associated with poor prognosis," *Archives Of Medical Research*, vol. 50, no. 1, pp. 10–17, 2019.
- [59] R. Zhang, R. L. Wei, W. Du et al., "Long noncoding RNA ENST00000413528 sponges microRNA-593-5p to modulate human glioma growth via polo-like kinase 1," *CNS Neuroscience & Therapeutics*, vol. 25, no. 8, pp. 842–854, 2019.
- [60] P. S. Dalvi, I. F. Macheleidt, S.-Y. Lim et al., "LSD1 inhibition attenuates tumor growth by disrupting PLK1 mitotic pathway," *Molecular Cancer Research*, vol. 17, no. 6, pp. 1326–1337, 2019.

## Research Article

# TRIM32 Promotes the Growth of Gastric Cancer Cells through Enhancing AKT Activity and Glucose Transportation

Jianjun Wang , Yuejun Fang, and Tao Liu

Department of Gastroenterological Surgery, Jinhua Guangfu Oncology Hospital, Huancheng North Road No. 1296, Jinhua, Zhejiang, China

Correspondence should be addressed to Jianjun Wang; gfywjj@163.com

Received 22 August 2019; Revised 15 November 2019; Accepted 20 December 2019; Published 21 January 2020

Academic Editor: Pierfrancesco Franco

Copyright © 2020 Jianjun Wang et al. This is an open access article distributed under the Creative Commons Attribution License, which permits unrestricted use, distribution, and reproduction in any medium, provided the original work is properly cited.

Tripartite motif protein 32 (TRIM32), an E3 ubiquitin ligase, is a member of the TRIM protein family. However, the underlying function of TRIM32 in gastric cancer (GC) remains unclear. Here, we aimed to explore the function of TRIM32 in GC cells. TRIM32 was induced silencing and overexpression using RNA interference (RNAi) and lentiviral-mediate vector in GC cells, respectively. Moreover, the PI3K/AKT inhibitor LY294002 was used to examine the relationship between TRIM32 and AKT. Quantitative reverse-transcription PCR (qRT-PCR) and western blot were used to determine the mRNA and protein contents. The glucose analog 2-NBDG was used as a fluorescent probe for determining the activity of glucose transport. An annexin V-fluorescein isothiocyanate apoptosis detection kit was used to stain NCI-N87, MKN74, and MKN45 cells. Cell counting kit-8 (CCK-8) assay was used to examine cell proliferation. Our results indicated that TRIM32 was associated with poor overall survival of patients with GC. Moreover, TRIM32 was a proliferation and antiapoptosis factor and involved in the AKT pathway in GC cells. Furthermore, TRIM32 possibly mediated the metabolism of glycolysis through targeting GLUT1 and HKII in GC cells. Importantly, TRIM32 silencing deeply suppressed the tumorigenicity of GC cells *in vivo*. Our findings not only enhanced the understanding of the function of TRIM32 but also indicated its potential value as a target in GC treatment.

## 1. Introduction

Gastric cancer (GC) is one of the most common tumors, which is the third leading cause of death-related cancer all over the world [1]. Although the surgical operation and chemotherapy contribute to GC patients, the outcome is far from being fully satisfied. Due to the high morbidity and mortality rates of GC, the novel effective therapies for GC are urgently needed [2]. Therefore, gaining a deep insight into the molecule mechanism of GC is a critical step for developing novel therapeutic approaches.

Tripartite motif protein 32 (TRIM32) belongs to the TRIM protein family, which is identified as an E3 ubiquitin ligase [3]. A previous report has demonstrated that TRIM32 is overexpressed in breast cancer and promotes the proliferation of breast cancer cells [4]. The similar results are also obtained in hepatocellular carcinoma cells [5]. Furthermore, TRIM32 inhibits the activity of PI3K/AKT/Foxo signaling in muscle atrophy through improving plakoglobin-PI3K

dissociation [6]. However, the detailed function of TRIM32 in GC cells is less investigated.

The AKT signaling pathway plays an essential role in various biological functions, which is commonly abnormal in certain human cancer [7]. The phosphorylation of AKT is critical for its function. The inactivation of the PI3K/AKT pathway has induced G2/M arrest and apoptosis in lung cancer cells [8]. Previous evidence has demonstrated that enhancing the activity of AKT increases the chemoresistance for GC [9]. Moreover, PI3K/AKT also plays a key role in the apoptosis and proliferation of GC cells [10, 11]. However, the relationship between TRIM32 and AKT has not been confirmed yet in GC cells.

Glycolysis provides metabolic products and energy for cell survival. The activity of glycolysis is accelerated in certain human cancer cells [12]. A previous report has indicated that the glycolysis inhibitor not only prevents the tumor promoting effects but also shows the high value in cancer therapy treatment [13, 14]. Moreover, AKT has

enhanced the activity of glycolysis in human liver and cervical tumor cells [15]. Furthermore, the PI3K/AKT signaling pathway is essential for suppressing glycolysis in oral squamous cell carcinoma cells [16]. Furthermore, the combined inhibitors of AKT and glycolysis showed a stronger effect in lung cancer treatment [17]. However, the precise function of TRIM32 in the glycolysis process remains unclear in GC cells.

The aim of the present study is to examine the function of TRIM32 and potential target in GC cells. RNA interference (RNAi) and lentiviral vector were used to silencing and overexpression TRIM32 in GC cells. Our data not only obtain a deep insight of the molecular function of TRIM32 in GC cells but also provide evidences to indicate its potential value as a target for GC treatment.

## 2. Methods and Materials

**2.1. Cell Culture.** The GC cell lines used in this study (NCI-N87, MKN74, HGC27, AGS, MKN45, and GES-1) were purchased from the cell bank of the Shanghai Biology Institute (Shanghai, China). Fetal bovine serum (10%) (GIBCO, USA) was added to all culture media along with 2 mM L-glutamine and 1% penicillin/streptomycin (Solarbio, China). Cells were grown in DMEM (Trueline, USA) and maintained in a 5% CO<sub>2</sub> atmosphere at 37°C. The PI3K/AKT inhibitor LY294002 (Selleck, USA) was dissolved in DMSO. This study was approved by the ethics committee of Guangfu Hospital and followed the tenants of the Declaration of Helsinki. Moreover, there are no live subjects at the present study, so the informed consent is not necessary in this research.

**2.2. RNA Isolation and Real-Time PCR.** Total RNA from cell samples was extracted using TRIzol Reagent (Invitrogen, USA). Then, the cDNA synthesis kit (Fermentas, Canada) were used for the RNA reverse transcribed into complementary DNA (cDNA) according to the instructions of the manufacturer. The expression of GAPDH was used to normalize the gene expression and counted using the 2<sup>-ΔΔCt</sup> method. Three replicates are needed for each analysis. The primers used in this study are presented in Supplementary File 1.

**2.3. Lentiviral-Mediated RNA Interference and Overexpression of TRIM32.** Three plasmids containing siRNA targeting positions of human TRIM32 (NM\_012210.3) were synthesized (Major, China). The negative control (siNC) contained a nonspecific scrambled siRNA sequence. A lentiviral plasmid (pLVX-puro) containing the full-length human TRIM32 cDNA sequence and an empty plasmid acted as negative controls (oeNC). Lipofectamine 2000 (Invitrogen, USA) was used to transiently transfect plasmids into cells according to the instructions of the manufacturer. Experiments were performed 48 h after the transfection. Detailed information on the sequence of siTRIM32s is provided in Supplementary Table 1.

**2.4. Western Blot.** Whole protein lysates were extracted from the indicated cells (NCI-N87, MKN74, and MKN45) using RIPA lysis buffer (JRDUN, Shanghai, China) with an EDTA-free protease inhibitor cocktail (Roche, Germany). An enhanced BCA protein assay kit (Thermo Fisher, USA) was utilized to estimate the protein concentration. Equal amounts of total protein (25 μg) were fractionated using 10% SDS-PAGE and transferred to a nitrocellulose membrane (Millipore, USA) overnight. Then, after being blocked with 5% nonfat dry milk for 1 h at room temperature, the membranes were probed at 4°C overnight with the primary antibodies followed by incubation for 1 h at 37°C with the secondary antibody (anti-mouse IgG) (1:1000; Beyotime, China). An enhanced chemiluminescence system (Tanon, China) was used to detect the level of protein expression. Each sample was tested in triplicate, and GAPDH served as the internal reference. Detailed information on the primary antibodies is provided in Supplementary Table 2.

**2.5. Cell Proliferation Assay.** Cell counting kit-8 (CCK-8) assay (SAB, USA) was used to examine the cell proliferation according to the protocol of the manufacturer. Briefly, cells transfected as indicated were seeded in 96-well plates and cultured for 0, 24, 48, and 72 h, and then CCK-8 solution (1:10) was mixed into each well and incubated for 1 h. A microplate reader (Pulangxin, China) was used to measure the optical density values (OD) at a wavelength of 450 nm. Each time point was tested in triplicate.

**2.6. Cell Apoptosis Assay.** In brief, an annexin V-fluorescein isothiocyanate (FITC) apoptosis detection kit (Beyotime, China) was used to stain NCI-N87, MKN74, and MKN45 cells according to the instructions of the manufacturer at 48 h after viral infection. Then, a flow cytometer (BD, USA) was used to determine cells.

**2.7. Glucose Transport and Lactate Production Assay.** In brief, the glucose analog 2-NBDG (Molecular Probes, Eugene, OR) was used as a fluorescent probe for determining the activity of glucose transport. In order to examine the uptake of 2-NBDG, a total of 5 × 10<sup>5</sup> cells from different groups were seeded in 6-well plates. Then, all the cells were preincubated in Krebs-Ringer bicarbonate (KRB) buffer (glucose free) for 15 min after maintaining in a 5% CO<sub>2</sub> atmosphere at 37°C for 24 h. After that, cells incubated in fresh KRB buffer were supplemented with 2-NBDG for 45 min at 37°C, 5% CO<sub>2</sub>. Flow cytometry using a GloMax®-Multi + flow cytometer (Promega, USA) was used to quantitatively analyze the stained cells. Moreover, a Lactate Assay Kit (njcbio, China) was utilized to examine the production of lactate in different cells according to the protocol of the manufacturer.

**2.8. TUNEL Staining.** TUNEL staining assays were performed with sections using a Tunel kit (11684817910, Roche, Switzerland) principally according to the supplier's instruction. Three replicates were needed for each sample.



**2.9. Xenograft Model.** The assay was carried out according to the Institute's guidelines for animal experiments and was approved by the independent ethics committee of Jin hua Guangfu Oncology Hospital, Jinhua, zhejiang, P.R. China, and all animals were treated in accordance with the Institutional Animal Care and Use Committee (IACUC). An equal number of siNC- and siTRIM32-transfected NCI-N87 cells ( $n = 5 \times 10^6$ ) were subcutaneously injected into the right flank of 4- to 6-week-old nude mice ( $n = 6$  for each group; Shanghai Laboratory Animal Company, Shanghai). The length and width of the tumor were examined every 3 days for 33 days after being injected. The volume of the tumor was counted as length  $\times$  (width  $2/2$ ). Six weeks after injection, six mice from the siNC- and siTRIM32-injected groups were sacrificed by cervical dislocation, and tumor tissues were fixed in 4% formalin for further analysis.

**2.10. Statistical Analysis.** GraphPad Prism software Version 7.0 (CA, USA) was utilized for the statistical analyses. Data were displayed as the mean  $\pm$  SD of at least three samples. Statistical significance was determined by one-way analysis of variance (ANOVA) for multiple comparisons. Statistical significance was accepted by the  $P$  value  $< 0.05$ .

### 3. Results

**3.1. TRIM32 Upregulation was Associated with Poor Overall Survival of GC Patients.** To determine the function of TRIM32, one data set (ID: 203846\_at) collected from gastric cancer database (<http://kmplot.com>) was used to quantify the connection between TRIM32 and overall survival (OS) of patients with GC. As presented in Figure 1, the OS of GC patients with high level of TRIM32 ( $n = 534$ ) was much lower than that in GC patients with low-TRIM32 level (Figure 1). Thus, these results demonstrated that TRIM32 upregulation was associated with poor OS of GC patients.

**3.2. The mRNA and Protein Level of TRIM32 in GC Cell Lines.** In this study, a total of six GC cell lines were used to examine the mRNA and protein level of TRIM32, including NCI-N87, MKN74, HGC27, AGS, MKN45, and GES-1. As shown in Figures 2(a) and 2(b), both the mRNA and protein of TRIM32 were significantly upregulated in NCI-N87 and MKN74 cells compared with that of AGS cells. Moreover, the level of TRIM32 was obviously downregulated in MKN45 cells among the GC cell lines as indicated above. Therefore, NCI-N87, MKN74, and MKN45 were chosen for knockdown and overexpression (OE) analysis.

**3.3. Silencing and Overexpression of TRIM32 in GC Cells.** To silence the expression of TRIM32, three short interference RNAs (siRNAs) targeting human TRIM32 (siTRIM32-1, siTRIM32-2, and siTRIM32-3) and a nonspecific scrambled siRNA (siNC) were synthesized and transfected into NCI-N87 and MKN74 cell lines. The untreated cells acted as a blank control (BLANK). As shown in Figures 3(a)

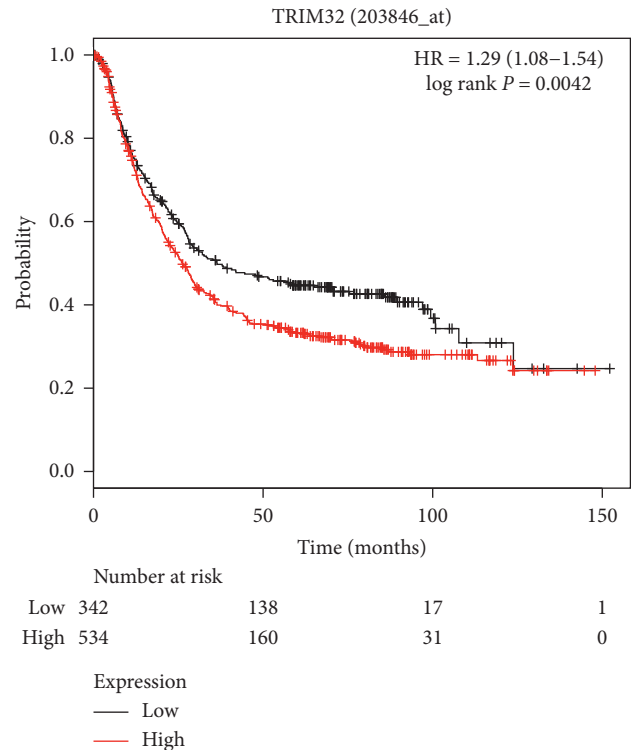


FIGURE 1: TRIM32 upregulation was associated with poor overall survival of GC patients.

and 3(b), all three TRIM32-siRNAs strongly reduced the level of endogenous TRIM32. Moreover, RNAi1-1 and RNAi1-2 showed a stronger effect in inhibiting the expression of TRIM32 than RNAi1-3. Therefore, RNAi1-1 and RNAi1-2 were chosen for further study.

Moreover, MKN45 cells were transfected with a plasmid-overexpressing TRIM32 (oeTRIM32) and a mock plasmid (oeNC). Clearly, both the relative mRNA and protein level of TRIM32 were significantly upregulated in oeTRIM32-transfected cells (Figures 3(c) and 3(d)). Hence, the oeTRIM32-transfected cells were chosen for the following overexpression analysis.

**3.4. TRIM32 siRNAs Inhibited the Proliferation and Induced the Apoptosis of GC Cells.** The Cell Counting Kit-8 (CCK-8) assay was performed to examine the function of siTRIM32s in the proliferation of GC cells. As shown in Figures 4(a) and 4(b), the cell proliferation rate was significantly suppressed in siTRIM32-transfected cells. Moreover, we also determined the function of siTRIM32s in the apoptosis of GC cells. Our results suggested that TRIM32 silencing remarkably improved the apoptosis of GC cells (Figure 4(c)). These results demonstrated that TRIM32 was a proliferation and antiapoptosis factor in GC cells.

**3.5. Glucose Transport Activity and Lactate Production was Decreased by siTRIM32s.** We also determined the glucose transport activity and lactate production in TRIM32 siRNA transfected cells. As shown in Figure 4(d), the glucose

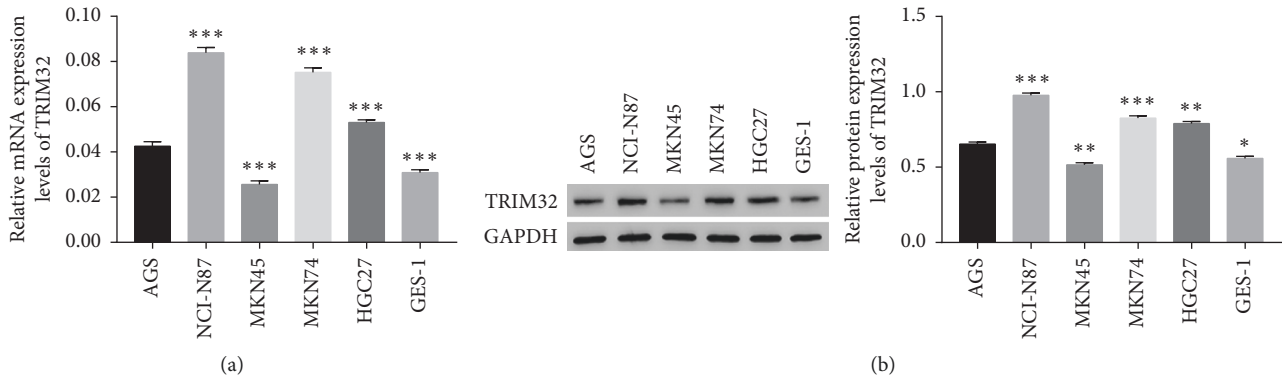


FIGURE 2: The relative mRNA and protein level of TRIM32 in different GC cells. (a) The relative mRNA level of TRIM32 in different GC cells. \*\*\* $P < 0.001$  vs. AGS. (b) The relative protein level of TRIM32 in different GC cells. \*\*\* $P < 0.001$  vs. AGS.

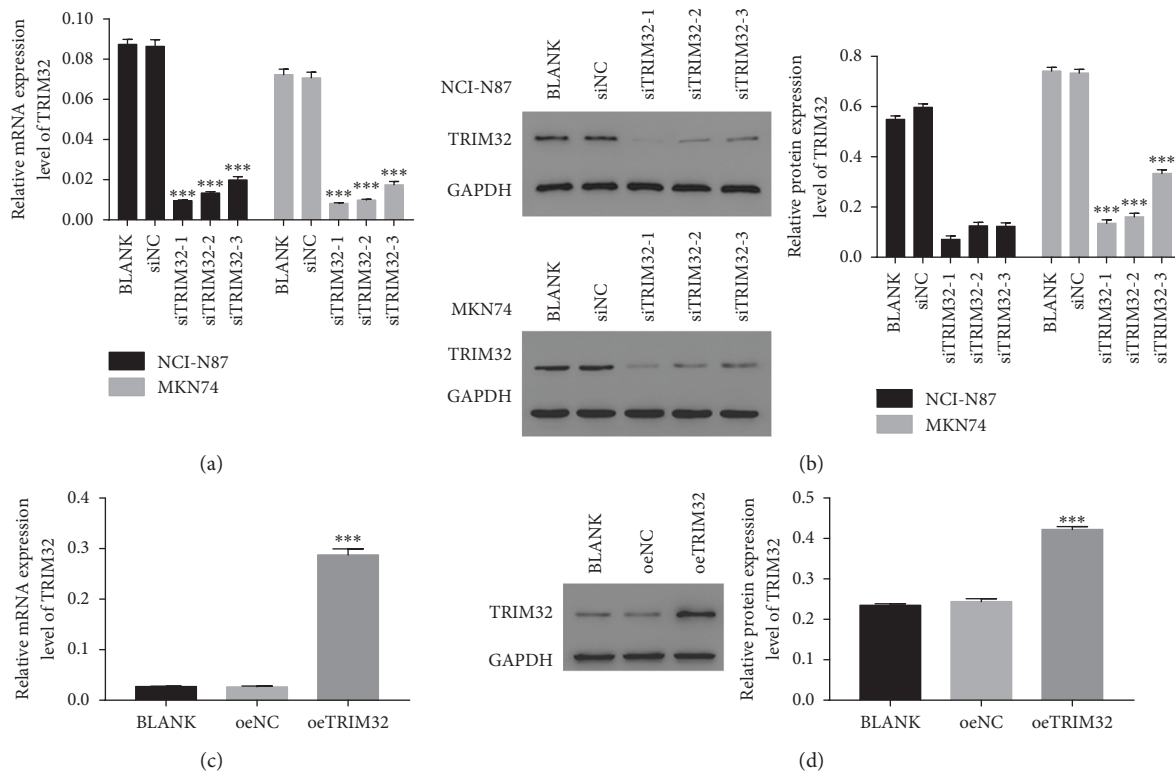


FIGURE 3: Knockdown and overexpression of TRIM32 in GC cells. (a) and (b) stand for the relative mRNA and protein level of NCI-N87 and MKN74 cells transfected with siNC, siTRIM32-1, siTRIM32-2, and siTRIM32-3, respectively. \*\*\* $P < 0.001$  vs. siNC. (c) and (d) stand for the mRNA and protein level of oeTRIM32 transfected into MKN45 cells. \*\*\* $P < 0.001$  vs. oeNC.

transport activity showed no difference between BLANK and siNC transfected cells. However, the glucose transport activity was deeply decreased in NCI-N87 and MKN74 cells transfected with siTRIM32, respectively. Additionally, the lactate production also presented no difference between BLANK and siNC transfected cells. However, a remarkable downregulation of the lactate production was appeared in siTRIM32 transfected cells (Figure 4(e)). Taken together, these results reflected the possible function of TRIM32 in the energy metabolism of GC cells.

**3.6. Silencing TRIM32 Suppressed the Glycolysis-Related Protein in GC Cells.** Glucose transporter 1 (GLUT1) is an important regulator in the process of glucose uptake. Previous report has demonstrated that GLUT1 promotes the proliferation and metastasis of breast cancer cells [18]. Moreover, it has been reported that GLUT1 is involved in the invasion and metastasis of lung cancer cells [19]. Furthermore, Glycolytic enzyme Hexokinase II (HKII) has played an important role in tumor glycolysis and the progression of cancers. HKII is necessary for tumor initiation and



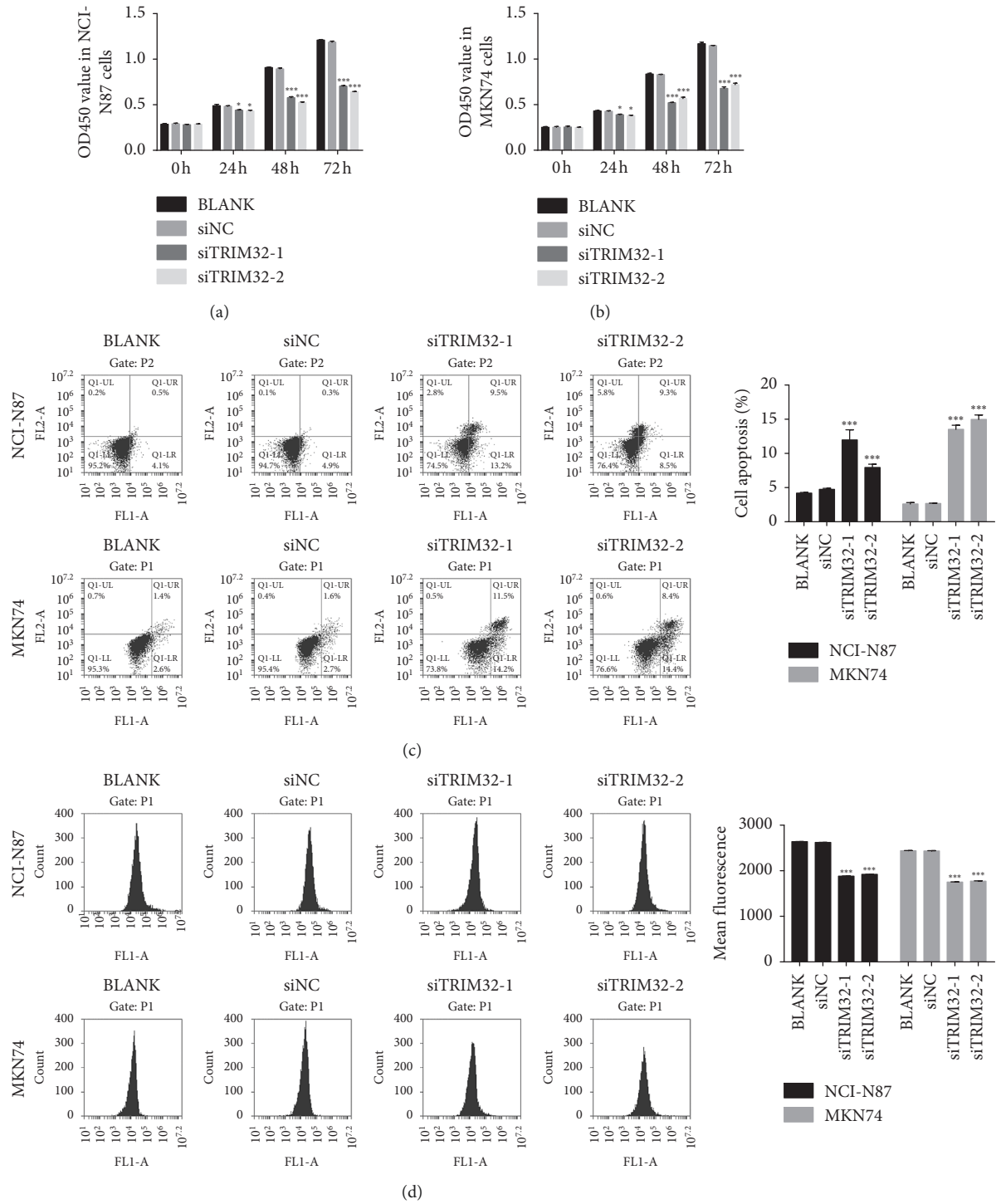


FIGURE 4: Continued.

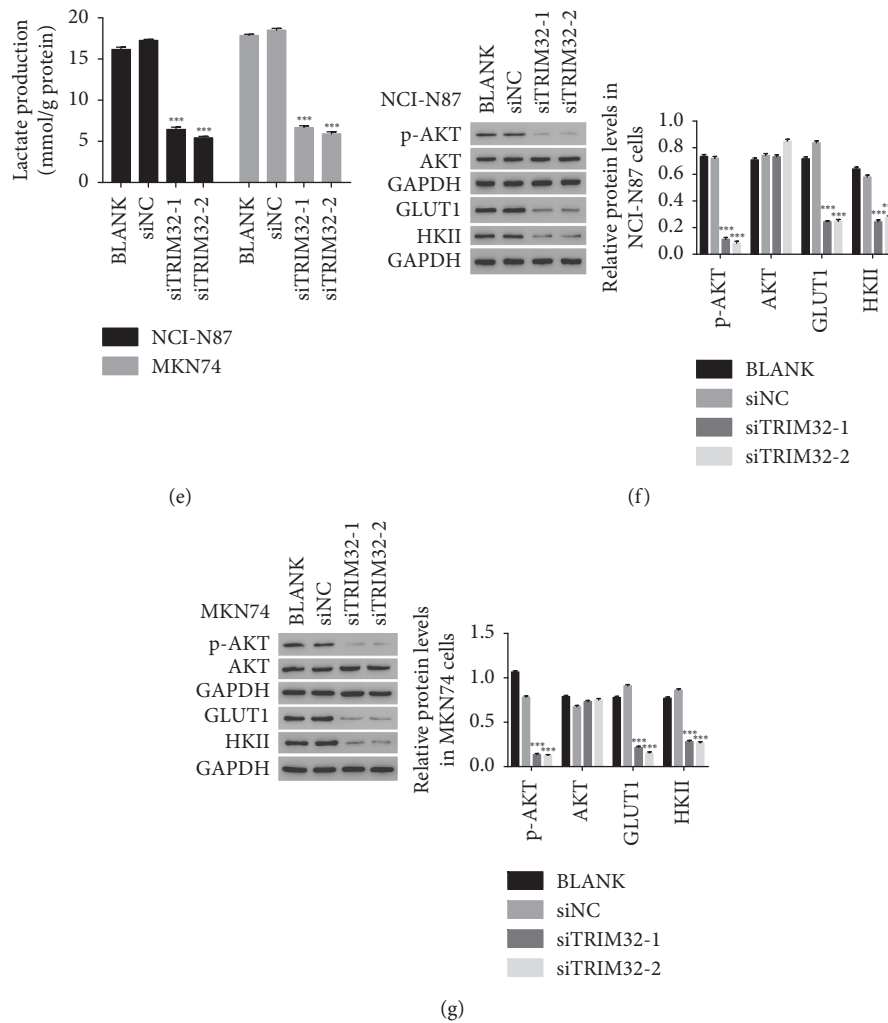


FIGURE 4: Knockdown of TRIM32 suppressed GC cells growth. (a) and (b) stand for cell proliferation that was detected 0, 24, 48, and 72 hours after transfection with siNC, siTRIM32-1, and siTRIM32-2 in NCI-N87 and MKN74 cells, respectively.  $*P < 0.05$  vs. siNC,  $***P < 0.001$  vs. siNC. (c) The apoptosis profile of siNC, siTRIM32-1, and siTRIM32-2 transfected into NCI-N87 and MKN74 cells, respectively.  $***P < 0.001$  vs. siNC. (d) Glucose transport activity measured using the fluorescent glucose analog 2-NBDG in NCI-N87 and MKN74 cells transfected with siNC, siTRIM32-1, and siTRIM32-2, respectively.  $***P < 0.001$  vs. siNC. (e) The production of lactate in NCI-N87 and MKN74 cells transfected with siNC, siTRIM32-1, and siTRIM32-2, respectively.  $***P < 0.001$  vs. siNC. (f) and (g) stand for the protein level of AKT, p-AKT, GLUT1, and HKII in NCI-N87 and MKN74 cells transfected with siNC, siTRIM32-1, and siTRIM32-2, respectively.  $***P < 0.001$  vs. siNC.

maintenance [20]. Moreover, downregulating the expression of HKII contributes to suppress tumor glycolysis metabolism and tumor growth and induce apoptosis in cervical cancer cells [21].

In this study, western blot was used to determine the protein level of GLUT1 and HKII in different NCI-N87 and MKN74 transfected cells as indicated. Our results indicated that the protein contents of GLUT1 and HKII were down-regulated in siTRIM32 transfected cells (Figures 4(f) and 4(g)). Therefore, TRIM32 might target GLUT1 and HKII in the regulation of glycolysis metabolism in GC cells. Interestingly, knockdown of TRIM32 significantly deeply inhibited the phosphorylation of AKT in a time-dependent manner in NCI-N87 and MKN74 (Figure S1).

**3.7. The Function of TRIM32 Was Inhibited by a Specific AKT Inhibitor LY294002.** In order to further examine the correlation between AKT and TRIM32, the oeNC and oeTRIM32 transfected cells were cultured in the presence of a specific AKT inhibitor LY294002. As shown in Figure 5(a), the cell proliferation rate was obviously increased in oeTRIM32 transfected cells compared with oeNC. After being cultured with the inhibitor LY29004, cell proliferation rate was deeply suppressed in oeNC or oeTRIM32 transfected cells. Meanwhile, a glycolysis inhibitor 2-deoxyglucose (2-DG) was used to further determine the function of TRIM32 in cell proliferation. As shown in Figure 5(b), the cell proliferation rate of oeNC or oeTRIM32 transfected cells was also significantly inhibited by 2-DG. Therefore, these

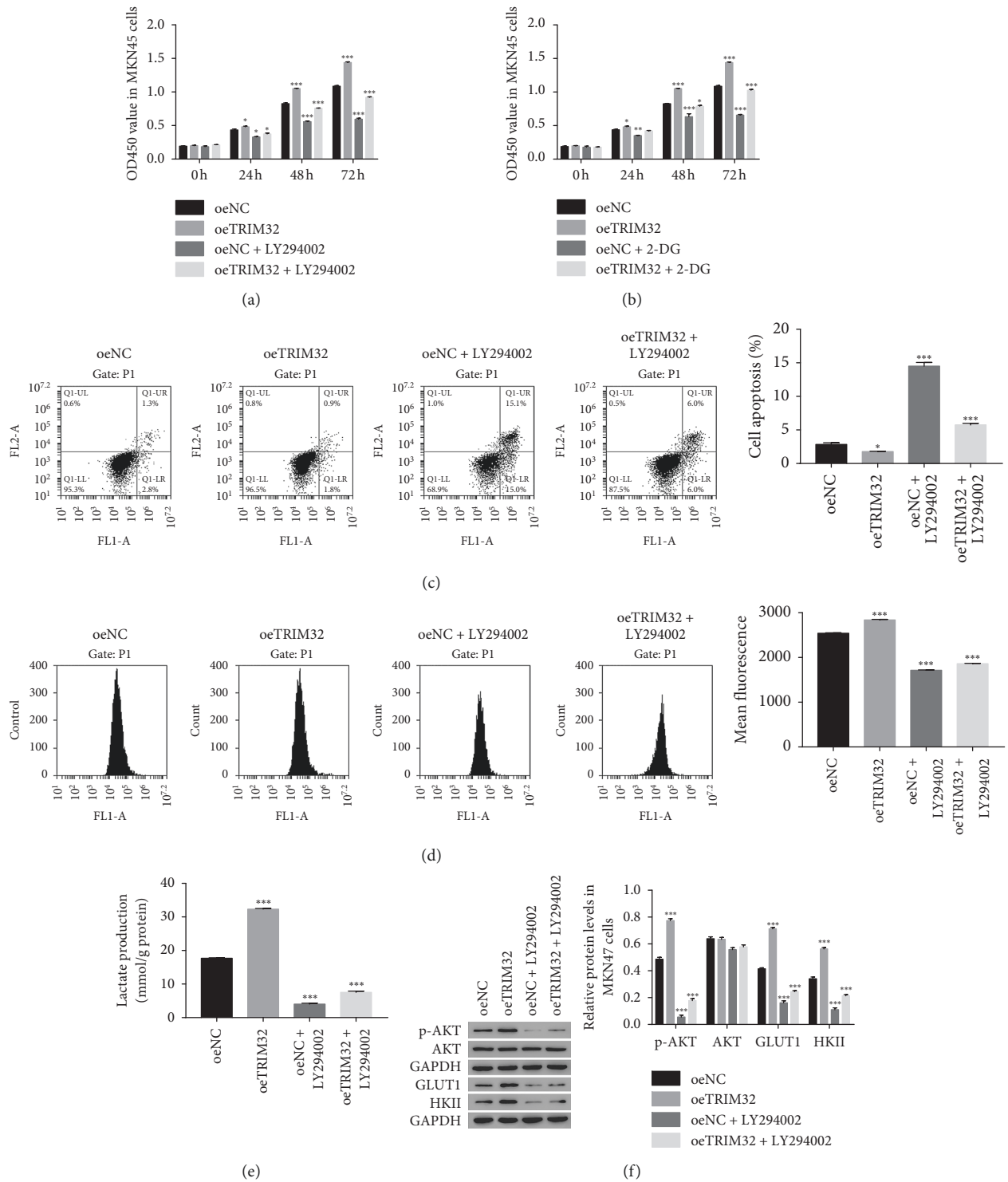


FIGURE 5: The function of TRIM32 was suppressed by the P13/AKT inhibitor LY294002. (a) Cell proliferation was detected 0, 24, 48, and 72 hours after transfection with oeNC, oeTRIM32, oeNC + LY294002, and oeTRIM32 + LY294002 in MKN45 cells, respectively. \* $P < 0.05$  vs. oeNC, \*\*\* $P < 0.001$  vs. oeNC. (b) Cell proliferation was detected 0, 24, 48 and 72 hours after transfection with oeNC, oeTRIM32, oeNC + 2-DG, and oeTRIM32 + 2-DG in MKN45 cells, respectively. \* $P < 0.05$  vs. oeNC, \*\* $P < 0.01$  vs. oeNC, \*\*\* $P < 0.001$  vs. oeNC. (c) The apoptosis profile of oeNC, oeTRIM32, oeNC + LY294002, and oeTRIM32 + LY294002 in MKN45 cells, respectively. \* $P < 0.05$  vs. oeNC, \*\*\* $P < 0.001$  vs. oeNC. (d) Glucose transport activity measured using the fluorescent glucose analog 2-NBDG in MKN45 cells transfected with oeNC, oeTRIM32, oeNC + LY294002, and oeTRIM32 + LY294002. \*\*\* $P < 0.001$  vs. oeNC. (e) The production of lactate in MKN45 cells transfected with oeNC, oeTRIM32, oeNC + LY294002, and oeTRIM32 + LY294002. \*\*\* $P < 0.001$  vs. oeNC. \*\*\* $P < 0.001$  vs. oeNC. (f). The protein level of AKT, p-AKT, GLUT1, and HKII in MKN45 cells transfected with oeNC, oeTRIM32, oeNC + LY294002, and oeTRIM32 + LY294002. \*\*\* $P < 0.001$  vs. oeNC.

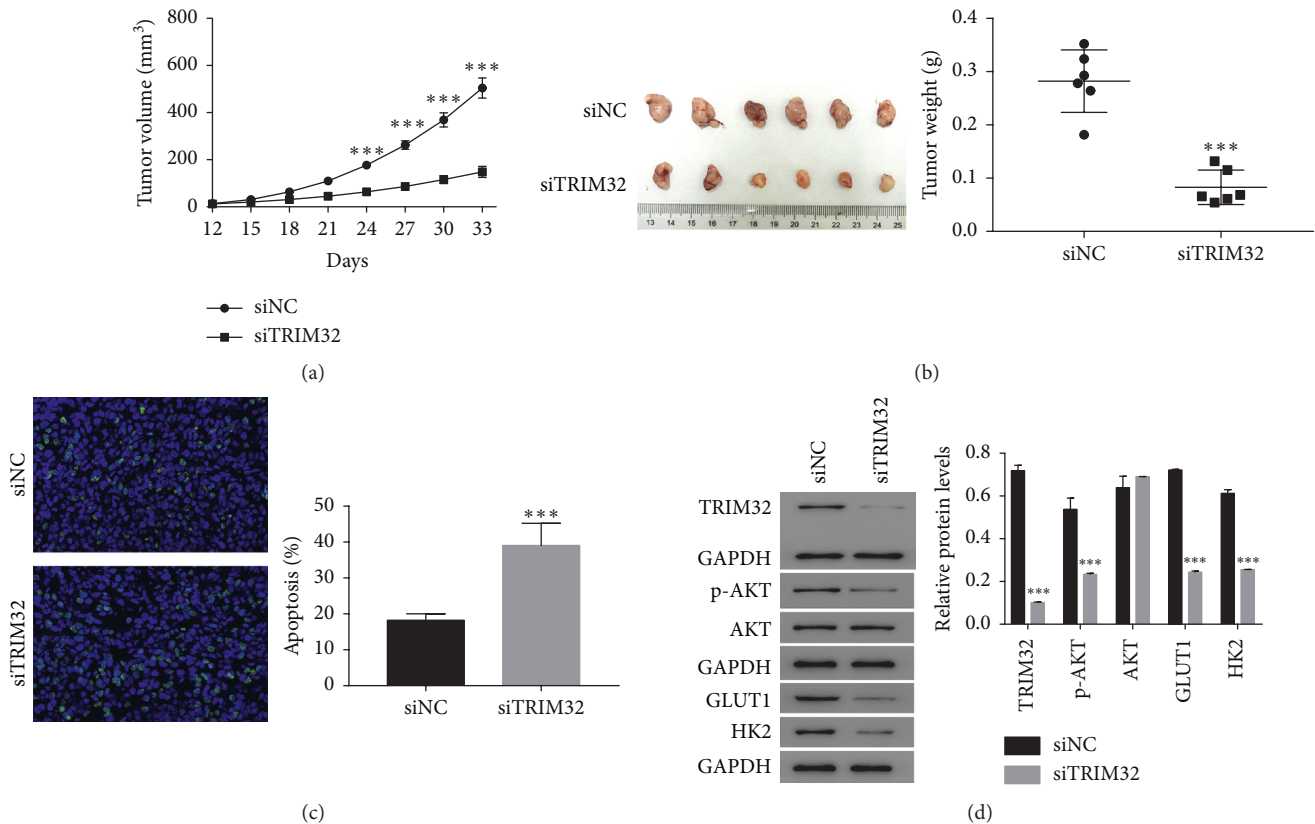


FIGURE 6: TRIM32 silencing suppressed the tumorigenicity of GC cells *in vivo*. (a) and (b) The tumor volume and weight were down-regulated in nude mice that were injected with siTRIM32-transfected NCI-N87 cells. \*\*\* $P < 0.001$  vs. siNC. (c) TUNEL staining assay was performed to examine the apoptosis ratio in siNC or siTRIM32 tumor, respectively. \*\*\* $P < 0.001$  vs. siNC. (d) Western blot was used to examine the protein contents of TRIM32, p-AKT, AKT, GLUT1, and HK2 in siNC or siTRIM32 tumor, respectively. \*\*\* $P < 0.001$  vs. siNC.

results indicated the similar function of the inhibitor LY294002 and 2-DG in the regulation of cell proliferation. Moreover, overexpression of TRIM32 significantly inhibited the apoptosis of GC cells, whereas this function was totally released by the AKT inhibitor LY29004 (Figure 5(c)). Furthermore, the AKT inhibitor LY294002 also significantly inhibited the production of glucose and lactate in oeTRIM32 transfected cells (Figures 5(d) and 5(e)). Additionally, the protein level of AKT, p-AKT, GLUT1, and HKII was also examined in different OE transfected cells. As shown in Figure 5(f), the phosphorylation of AKT was deeply suppressed by the inhibitor LY294002 in oeNC and oeTRIM32 transfected cells. Moreover, TRIM32 overexpression improved the phosphorylation of AKT in MKN45 cells in a time-dependent manner in the presence of the inhibitor LY294002 (Figure S2). Furthermore, the glycolysis-related protein GLUT1 and HKII were also significantly decreased by the inhibitor LY294002 in oeNC or oeTRIM32 transfected cells. Therefore, these results demonstrated that TRIM32 was involved in the AKT signaling pathway and regulated the glycolysis metabolism through targeting GLUT1 and HKII in GC cells.

**3.8. TRIM32 Silencing Suppressed the Tumorigenicity of GC Cells *In Vivo*.** To further assess the role of TRIM32 in tumorigenicity *in vivo*, a number of  $5 \times 10^6$  of NCI-N87 cells

that are transfected with siNC or siTRIM32 was hypodermically injected into nude mice ( $n = 6$  for each group) and tumor formation was determined every 3 days for 33 days (starting at day 12). In the current study, both siNC and siTRIM32 transfected cells were capable to develop tumor *in vivo*. However, siTRIM32 cells significantly reduced the tumor volume as that of siNC cells. Moreover, the tumor weight of siTRIM32-injected mice was much lower than that in siNC-injected mice (Figures 6(a) and 6(b)). Furthermore, results collected from TUNEL assay indicated that siTRIM32 transfected cells remarkably improved the apoptosis rate of GC cells *in vivo* (Figure 6(c)). Together, all these results demonstrated that TRIM32 silencing deeply reduced the tumorigenicity of GC cells *in vivo*. Furthermore, the protein contents of TRIM32, p-AKT, GLUT1, and HK2 was deeply reduced in siTRIM32 tumors (Figure 6(d)).

#### 4. Discussion

GC is one of the common death-related cancers all over the world. Although more and more attentions have been paid on improving its therapeutic strategies, the 5-year survival rate is still less than 30% [22]. Therefore, the novel effective treatment for GC is urgently needed. A previous report has indicated that TRIM32 overexpression correlates with poor prognosis in GC patients [23]. In the present research, we

investigated the biological function of TRIM32 in GC cells. Our results indicated that TRIM32 was a proliferation and antiapoptosis factor in GC cells. Therefore, these findings demonstrated that TRIM32 was an oncogene in the progression of human GC. More importantly, targeting TRIM32 might be a novel approach in the treatment for GC.

Previous report has reported that TRIM14 mediates cell proliferation in osteosarcoma through upregulating the AKT signaling pathway [24]. Moreover, the oncogene TRIM27 has activated the phosphorylation of AKT in colorectal cancer cells [25]. Recently, TRIM11 promotes proliferation and glycolysis of breast cancer cells via targeting the AKT/GLUT1 pathway [26]. Recently, TRIM32 is reported to promote cell proliferation and invasion in gastric cancer by activating  $\beta$ -catenin signalling [27]. Importantly, AKT-dependent regulation of  $\beta$ -catenin plays a critical role in tumor development [28]. In this study, we found TRIM32 was positively correlated with the phosphorylation of AKT in GC cells. Moreover, AKT inhibitor LY294002 blocked the function of TRIM32 in GC cells. To our knowledge, it was the first time to illustrate that the connection between TRIM32 and AKT in GC cells. Moreover, TRIM32 might promote the progression of human GC through regulating the phosphorylation of AKT.

Suppressing GLUT1 and HKII inhibits the activity of glycolysis and induces cell apoptosis [21, 29–31]. Moreover, the inactivation of the AKT-GLUT1/HKII signaling pathway suppressed the proliferation and glycolysis of lung cancer cells [32]. In the present research, our results firstly indicated the function of TRIM32 in the glycolysis metabolism in GC cells. Furthermore, TRIM32 might be a novel component in the AKT-GLUT1/HKII signaling pathway in GC cells. Furthermore, it has been confirmed that the combined inhibitors of AKT and glycolysis benefit lung cancer as indicated above [17]. Our results further provided evidences to indicate the potential value of the combination of the AKT inhibitor LY294002 and 2-DG in the treatment for GC.

## 5. Conclusion

In the present study, we systematically identified the function of TRIM32 in GC cells. Our findings not only indicated that the function of TRIM32 was achieved in GC cells might be via regulating the activity of AKT and glycolysis but also highlighted the potential value of TRIM32 for GC treatment.

## Data Availability

All data generated or analyzed during this study are included in this published article.

## Disclosure

Jianjun Wang, Jianjun Wang, and Yuejun Fang are co-first authors.

## Conflicts of Interest

All authors declare no conflicts of interest in this work.

## Authors' Contributions

Jianjun Wang designed this project and wrote the manuscript; Yuejun Fang performed the experiments; and Yuejun Fang and Tao Liu analyzed the data and edited the diagrams.

## Acknowledgments

The authors acknowledge the support given by the Guangfu Hospital. This research was supported by the Jin hua Science and Technology Plan Project (2018-3-3001C).

## Supplementary Materials

Supplementary Table 1: human gene TRIM32 (NM\_012210.3) RNAi targeting locus information. Supplementary Table 2: the primary antibodies information. Figure S1: TRIM32 siRNAs inhibited the phosphorylation of AKT in a time-dependent manner in GC cells. A. Western blot was used to examine the protein contents of p-AKT and AKT in NC1-N87 cells that were transfected with siTRIM32-1 and siTRIM32-2 at 12, 24, and 48 h, respectively. B. Western blot was used to examine the protein contents of p-AKT and AKT in MKN74 cells that were transfected with siTRIM32-1 and siTRIM32-2 at 12, 24, and 48 h, respectively. Figure S2: overexpression of TRIM32 improved the phosphorylation of AKT in MKN45 cells in the presence of the 8 inhibitor LY294002. (*Supplementary Materials*)

## References

- [1] Y. J. Choi and N. Kim, "Gastric cancer and family history," *The Korean Journal of Internal Medicine*, vol. 31, no. 6, pp. 1042–1053, 2016.
- [2] H. H. Wu, W. C. Lin, and K. W. Tsai, "Advances in molecular biomarkers for gastric cancer: miRNAs as emerging novel cancer markers," *Expert Reviews in Molecular Medicine*, vol. 16, p. e1, 2014.
- [3] M. Locke, C. L. Tinsley, M. A. Benson, and D. J. Blake, "TRIM32 is an E3 ubiquitin ligase for dysbindin," *Human Molecular Genetics*, vol. 18, no. 13, pp. 2344–2358, 2009.
- [4] T. T. Zhao, F. Jin, J. G. Li et al., "TRIM32 promotes proliferation and confers chemoresistance to breast cancer cells through activation of the NF- $\kappa$ B pathway," *Journal of Cancer*, vol. 9, no. 8, pp. 1349–1356, 2018.
- [5] X. Cui, Z. Lin, Y. Chen et al., "Upregulated TRIM32 correlates with enhanced cell proliferation and poor prognosis in hepatocellular carcinoma," *Molecular and Cellular Biochemistry*, vol. 421, no. 1-2, pp. 127–137, 2016.
- [6] S. Cohen, D. Lee, B. Zhai, S. P. Gygi, and A. L. Goldberg, "Trim32 reduces PI3K-Akt-FoxO signaling in muscle atrophy by promoting plakoglobin-PI3K dissociation," *The Journal of Cell Biology*, vol. 204, no. 5, pp. 747–758, 2014.
- [7] A. Yoshizawa, J. Fukuoka, S. Shimizu et al., "Overexpression of phospho-eIF4E is associated with survival through AKT pathway in non-small cell lung cancer," *Clinical Cancer Research: An Official Journal of the American Association for Cancer Research*, vol. 16, no. 1, pp. 240–248, 2010.
- [8] X. Xu, Y. Zhang, D. Qu, T. Jiang, and S. Li, "Osthole induces G2/M arrest and apoptosis in lung cancer A549 cells by modulating PI3K/Akt pathway," *Journal of Experimental & Clinical Cancer Research*, vol. 30, no. 1, p. 33, 2011.



- [9] E. Oki, H. Baba, E. Tokunaga et al., "Akt phosphorylation associates with LOH of PTEN and leads to chemoresistance for gastric cancer," *International Journal of Cancer*, vol. 117, no. 3, pp. 376–380, 2005.
- [10] D. Li, X. Qu, K. Hou et al., "PI3K/Akt is involved in bufalin-induced apoptosis in gastric cancer cells," *Anti-cancer Drugs*, vol. 20, no. 1, pp. 59–64, 2009.
- [11] L. Wang, F. Ouyang, J. Zhu et al., "Overexpressed CISD2 has prognostic value in human gastric cancer and promotes gastric cancer cell proliferation and tumorigenesis via AKT signaling pathway," *Oncotarget*, vol. 7, no. 4, 2016.
- [12] S. O. Lim, C. W. Li, W. Xia et al., "EGFR signaling enhances aerobic glycolysis in triple-negative breast cancer cells to promote tumor growth and immune escape," *Cancer Research*, vol. 76, no. 5, pp. 1284–1296, 2016.
- [13] S. Ganapathy-Kanniappan and J.-F. H. Geschwind, "Tumor glycolysis as a target for cancer therapy progress and prospects," *Molecular Cancer*, vol. 12, no. 1, p. 152, 2013.
- [14] G. Bonuccelli, D. Whitaker-Menezes, R. Castello-Cros et al., "The reverse Warburg effect: glycolysis inhibitors prevent the tumor promoting effects of caveolin-1 deficient cancer associated fibroblasts," *Cell Cycle*, vol. 9, no. 10, pp. 1960–1971, 2010.
- [15] T. Shimura, N. Noma, Y. Sano et al., "AKT-mediated enhanced aerobic glycolysis causes acquired radioresistance by human tumor cells," *Radiotherapy and Oncology: Journal of the European Society for Therapeutic Radiology and Oncology*, vol. 112, no. 2, pp. 302–307, 2014.
- [16] J. Wei, J. Wu, W. Xu et al., "Salvianolic acid B inhibits glycolysis in oral squamous cell carcinoma via targeting PI3K/AKT/HIF-1 $\alpha$  signaling pathway," *Cell Death & Disease*, vol. 9, no. 6, p. 599, 2018.
- [17] M. Ye, S. Wang, T. Wan et al., "Combined inhibitions of glycolysis and AKT/autophagy can overcome resistance to EGFR-targeted therapy of lung cancer," *Journal of Cancer*, vol. 8, no. 18, pp. 3774–3784, 2017.
- [18] S. Oh, H. Kim, K. Nam, and I. Shin, "Glut1 promotes cell proliferation, migration and invasion by regulating epidermal growth factor receptor and integrin signaling in triple-negative breast cancer cells," *BMB Reports*, vol. 50, no. 3, pp. 132–137, 2017.
- [19] H. Liao, Z. Wang, Z. Deng, H. Ren, and X. Li, "Curcumin inhibits lung cancer invasion and metastasis by attenuating GLUT1-MT1-MMP-MMP2 pathway," *International Journal of Clinical and Experimental Medicine*, vol. 8, no. 6, pp. 8948–8957, 2015.
- [20] K. C. Patra, Q. Wang, P. T. Bhaskar et al., "Hexokinase 2 is required for tumor initiation and maintenance and its systemic deletion is therapeutic in mouse models of cancer," *Cancer Cell*, vol. 24, no. 2, pp. 213–228, 2013.
- [21] Y. Liu, T. Murray-Stewart, R. A. Casero Jr. et al., "Targeting hexokinase 2 inhibition promotes radiosensitization in HPV16 E7-induced cervical cancer and suppresses tumor growth," *International Journal of Oncology*, vol. 50, no. 6, pp. 2011–2023, 2017.
- [22] R. Siegel, D. Naishadham, and A. Jemal, "Cancer statistics," *CA: A Cancer Journal for Clinicians*, vol. 63, no. 1, pp. 11–30, 2013.
- [23] M. Ito, K. Migita, S. Matsumoto et al., "Overexpression of E3 ubiquitin ligase tripartite motif 32 correlates with a poor prognosis in patients with gastric cancer," *Oncology Letters*, vol. 13, no. 5, pp. 3131–3138, 2017.
- [24] G. Xu, Y. Guo, D. Xu et al., "TRIM14 regulates cell proliferation and invasion in osteosarcoma via promotion of the AKT signaling pathway," *Scientific Reports*, vol. 7, no. 1, 2017.
- [25] Y. Zhang, Y. Feng, D. Ji et al., "TRIM27 functions as an oncogene by activating epithelial-mesenchymal transition and p-AKT in colorectal cancer," *International Journal of Oncology*, vol. 53, no. 2, pp. 620–632, 2018.
- [26] W. Song, Z. Wang, X. Gu et al., "TRIM11 promotes proliferation and glycolysis of breast cancer cells via targeting AKT/GLUT1 pathway," *OncoTargets and Therapy*, vol. 12, pp. 4975–4984, 2019.
- [27] C. Wang, J. Xu, H. Fu et al., "TRIM32 promotes cell proliferation and invasion by activating beta-catenin signalling in gastric cancer," *Journal of Cellular and Molecular Medicine*, vol. 22, no. 10, pp. 5020–5028, 2018.
- [28] G. Hua, L. Chaojie, L. Zhixia et al., "DcR3 induces proliferation, migration, invasion, and EMT in gastric cancer cells via the PI3K/AKT/GSK-3 $\beta$ / $\beta$ -catenin signaling pathway," *OncoTargets and Therapy*, vol. 11, pp. 4177–4187, 2018.
- [29] Y. X. Lu, Q. N. Wu, D. L. Chen et al., "Pharmacological ascorbate suppresses growth of gastric cancer cells with GLUT1 overexpression and enhances the efficacy of oxaliplatin through redox modulation," *Theranostics*, vol. 8, no. 5, pp. 1312–1326, 2018.
- [30] A. Riskin and Y. Mond, "Prolactin-induced subcellular targeting of GLUT1 glucose transporter in living mammary epithelial cells," *Rambam Maimonides Medical Journal*, vol. 6, no. 4, 2015.
- [31] X. Sun and L. Zhang, "MicroRNA-143 suppresses oral squamous cell carcinoma cell growth, invasion and glucose metabolism through targeting hexokinase 2," *Bioscience Reports*, vol. 37, no. 3, 2017.
- [32] X. Zhao, C. Lu, W. Chu et al., "MicroRNA-124 suppresses proliferation and glycolysis in non-small cell lung cancer cells by targeting AKT-GLUT1/HKII," *Tumour Biology: The Journal of the International Society for Oncodevelopmental Biology and Medicine*, vol. 39, no. 5, 2017.



## Review Article

# Epithelial Mesenchymal and Endothelial Mesenchymal Transitions in Hepatocellular Carcinoma: A Review

Simona Gurzu <sup>1,2,3</sup> Laszlo Kobori,<sup>4</sup> Decebal Fodor,<sup>1,4,5</sup> and Ioan Jung<sup>1</sup>

<sup>1</sup>Department of Pathology, University of Medicine, Pharmacy, Sciences and Technology, Targu Mures, Romania

<sup>2</sup>Advanced Medical and Pharmaceutical Research Center (CCAMF), University of Medicine, Pharmacy, Sciences and Technology, Targu Mures, Romania

<sup>3</sup>Department of Pathology, Clinical County Emergency Hospital, Targu Mures, Romania

<sup>4</sup>Department of Transplantation and Surgery, Semmelweis University, Budapest, Hungary

<sup>5</sup>Department of Anatomy and Embryology, University of Medicine, Pharmacy, Sciences and Technology, Targu Mures, Romania

Correspondence should be addressed to Simona Gurzu; [simonagurzu@yahoo.com](mailto:simonagurzu@yahoo.com)

Received 25 July 2019; Revised 30 August 2019; Accepted 11 September 2019; Published 29 September 2019

Academic Editor: Nadia M. Hamdy

Copyright © 2019 Simona Gurzu et al. This is an open access article distributed under the Creative Commons Attribution License, which permits unrestricted use, distribution, and reproduction in any medium, provided the original work is properly cited.

**Purpose.** To present a comprehensive review of the literature data, published between 2000 and 2019 on the PubMed and Web of Science databases, in the field of the tumor microenvironment in hepatocellular carcinoma (HCC). All the data were combined with the personal experiences of the authors. **Design.** From 1002 representative papers, we selected 86 representative publications which included data on epithelial-to-mesenchymal transition (EMT), angiogenesis, cancer stem-like cells (CSCs), and molecular background of chemoresistance or resistance to radiotherapy. **Results.** Although the central event concerns activation of the Wnt/ $\beta$ -catenin pathway, other signal pathways, such as c-Met/HGF/Snail, Notch-1/NF- $\kappa$ B, TGF- $\beta$ /SMAD, and basic fibroblast growth factor-related signaling, play a role in the EMT of HCC cells. This pathway is targeted by specific miRNAs and long noncoding RNAs, as explored in this paper. A central player in the tumor microenvironment proved to be the CSCs which can be marked by CD133, CD44, CD90, EpCAM, and CD105. CSCs can induce resistance to cytotoxic therapy or, alternatively, can be synthesized, de novo, after chemo- or radiotherapy, especially after transarterial chemoembolization- or radiofrequency ablation-induced hypoxia. The circulating tumor cells proved to have epithelial, intermediate, or mesenchymal features; their properties have a critical prognostic role. **Conclusion.** The metastatic pathway of HCC seems to be related to the Wnt- or, rather, TGF $\beta$ 1-mediated inflammation-angiogenesis-EMT-CSCs crosstalk link. Molecular therapy should target this molecular axis controlling the HCC microenvironment.

## 1. Introduction

Epithelial-mesenchymal transition (EMT) is a process first known to be involved in embryogenesis and tissue repair [1]. In carcinomas, EMT is defined as the transformation of the epithelial cells in cells with a mesenchymal phenotype [1–3]. The EMT of carcinoma cells, also known as epithelial cell plasticity, usually begins with the loss of epithelial cell polarity and the disintegration of the E-cadherin-related cell-cell adhesive [1]. The acquisition of positivity for mesenchymal markers then induces the increased mobility of the tumor cells and a high risk of lymph node or distant metastases.

Although more than 200 papers appear every year in the English-language literature, regarding the EMT of hepatocellular carcinoma (HCC) cells, the exact pathway and interaction of this process with other particular events of the tumor microenvironment, such as angiogenesis, inflammation, and stemness features, are still poorly understood. The main aim of this review is to synthesize the information in the literature regarding the particularities of the HCC microenvironment, taking into account not only the tissue and circulating biomarkers but also the background of peritumor liver parenchyma.

HCC is the fifth most common cancer, the most common malignant primary tumor of the liver, and the third

leading cause of cancer-associated mortality worldwide [2, 4–6]. In some Asiatic regions, such as Taiwan, HCC is the leading cause of cancer-related death [7]. In addition to multifocality (intrahepatic metastases), which is a factor of aggressiveness, it has been proven that HCC is one of the tumors with the highest metastatic capacity and that it has a high risk of recurrence. More than 65% of patients showed metastases at autopsy [2]. As very limited and poorly effective therapeutic options exist for HCC [2], the possible predictive role of EMT for the targeted therapy of HCC is also explored in this paper.

## 2. Methodology

For this review, a systematic search of the literature was undertaken to identify papers reporting data on the particularities of the tumor microenvironment in HCC. The review focused on the molecular biomarkers driving HCC plasticity and the possible prognostic and predictive roles of these markers, which were experimentally proven. One of the purposes was to identify which of the markers, which are assumed to act as potential promoters of aggressiveness, proved to be useful for predicting a patient's prognosis, thus indicating the most appropriate therapeutic regimen. The possible role of the tumor microenvironment in inducing resistance to radiotherapy or sorafenib, classic cytotoxic drugs, or other agents used in clinical trials was also taken into account.

To enrich the abovementioned aim and in turn understand the HCC microenvironment, we have selected, from the PubMed and Web of Science databases, representative publications using the MeSH terms and text words “hepatocellular carcinoma,” “epithelial-mesenchymal transition,” “tumor microenvironment,” “stemness,” and “angiogenesis.” Data assessment was conducted independently by all of the authors using predefined terms.

There were 3497 studies published between January 2000 and August 2019, including 12 papers resulting from personal research or from other databases identified via a manual search.

After elimination of non-English-language papers, duplicates, or letters, along with noninformative articles (Figure 1), 86 articles were considered to elaborate this review. Besides the clinical studies ( $n=22$ ), we have also selected those papers in which the clinical findings were further checked by *in vivo* or *in vitro* experiments ( $n=18$ ). At the same time, HCC cell line-based experiments were included ( $n=21$ ), then, in the same way as the *in vitro* experiments, *in vivo* experiments were validated ( $n=16$ ). As nine review-type articles were considered relevant, they were also selected for in-depth analysis and included in the reference list.

## 3. Molecular Pathways of EMT in HCC

There are several biomarkers that are supposed to be involved in EMT which are independent of the type and localization of carcinomas. The biomarkers expression can be successfully quantified in the tumor cells using immunohistochemical (IHC) methods [1].

EMT is IHC and characterized by a decrease or absence of the transmembrane adhesive of glycoprotein E-cadherin and the E-cadherin-to-N-cadherin (neural cadherin) switch [2, 8–10]. E-cadherin is linked to the actin cytoskeleton via the catenin family ( $\alpha$ -catenin,  $\beta$ -catenin,  $\gamma$ -catenin, and p120) [9] and other proteins, such as claudins (types 3, 4, and 7), occludin, ZO-1, desmoplakin, and plakoglobin [1, 2, 8]. EMT is induced by transcription factors that repress the E-cadherin expression. These include Twist1, Twist2, Snail1/Snail, Snail2/Slug, and zinc finger E-box-binding homeobox 1 (ZEB1) and ZEB2 [1, 2, 11–13]. The membrane-to-nuclear translocation of  $\beta$ -catenin is also an indicator of EMT, similar to Snail nuclear translocation [7, 8, 13]. The other markers that contribute to the orchestration of EMT include tumor growth factor  $\beta$  (TGF- $\beta$ ), epidermal growth factor (EGF), platelet-derived growth factor (PDGF), fibronectin, vimentin, hepatocyte growth factor (HGF), tumor necrosis factor (TNF), and ubiquitin regulator A20 [1, 2, 10–13].

As in other carcinomas, the EMT of HCC cells can be regulated by microRNAs (miRNAs) and long noncoding RNAs (lncRNAs) [3, 8, 14, 15]. The miRNAs are small noncoding RNAs comprising 18–22 nucleotides lengthways, which trigger specific proteins and can act as tumor suppressors or oncogenes [1, 14–16]. The lncRNAs are non-coding RNA transcripts that are longer than 200 nucleotides [4, 14].

**3.1. Wnt/ $\beta$ -Catenin Pathway.** Similar to other carcinomas, the EMT of the HCC cells appears to be driven by the Wnt/ $\beta$ -catenin signaling pathway. In patients with hepatitis-induced HCC,  $\beta$ -catenin mutations were reported to occur in 13–41% of cases [7]. In more than 55% of the cases, the mutations occur at the serine/threonine residues in the GSK-3 $\beta$  region of the  $\beta$ -catenin gene [7]. Codons 32, 33, 34, 41, and 45 of the gene can also be mutational spots [7].

The IHC studies that have taken into consideration this molecular pathway showed a loss of the membrane expression of the adhesive molecule E-cadherin in 17–69% of HCC cases [2, 9, 11, 13]. The membrane expression of  $\alpha$ -,  $\beta$ -, and  $\gamma$ -catenin and p120 is also reduced in 76%, 63%, 71%, and 73%, respectively, of HCC cases [9].

The reduced positivity of E-cadherin or other catenins is considered to be an independent indicator of poor survival [9]. Most of the authors admit that E-cadherin expression does not depend on clinicopathological parameters, such as a patient's age and gender, the tumor diameter, the serum level of alfa-fetoprotein (AFP), and the background development of chronic hepatitis or cirrhosis [13]. In other papers, it was proven that reduced positivity of the E-cadherin/catenin complex was inversely correlated with the histological grade of the tumor and directly correlated with the presence of intrahepatic metastasis and capsular invasion, without correlation with satellite nodules [9]. The membrane expression of  $\alpha$ -,  $\beta$ -, and  $\gamma$ -catenin and p120 was correlated with tumor size and stage [9]. Of the four catenins, only p120 was found to be correlated with the AFP serum level [9].

Catenins are especially expressed in the cell membrane or cytoplasm but can also enter the nucleus [9]. Nuclear

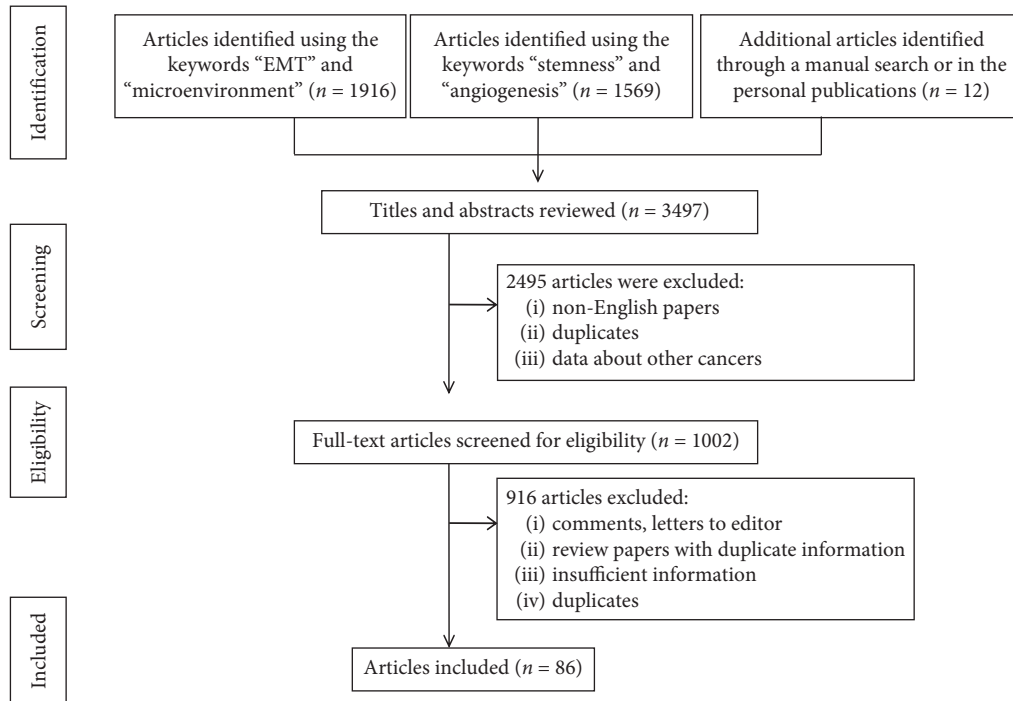


FIGURE 1: Preferred reported items for systematic reviews and meta-analyses (PRISMA) flow diagram, adapted for data on the tumor microenvironment in hepatocellular carcinoma from the PubMed and Web of Science databases between 2000 and 2019.

$\beta$ -catenin immunoeexpression was reported with large variations, with between 5% and 50% of the cases being found to be positive [5, 11, 13]. Most of the HCC cases showing a diffuse membrane expression of E-cadherin also present membrane positivity for  $\beta$ -catenin, but the loss of E-cadherin is usually associated with  $\beta$ -catenin nuclear expression [13].

The IHC membrane-to-nuclear translocation of  $\beta$ -catenin is considered to reflect the presence of mutations in the CTNNB1 gene, which is an indicator of EMT [7, 13].  $\beta$ -Catenin can be translocated from membrane to nucleus by the adhesion of the Tcf-Lef family of DNA-binding proteins [7]. About 80% of the  $\beta$ -catenin mutated cases presented IHC nuclear expression but not all of the cases with nuclear positivity showed  $\beta$ -catenin mutations in exon 3 (GSK-3b phosphorylation sites) using the primer sense 5'-AGCTGATTTGATGGAGTTGG-3' and antisense 5'-ACCAGCTACTTGTCTTGAG-3' [7]. Although  $\beta$ -catenin nonmembranous expression is considered to be a negative prognostic factor of HCC, this is probably the reason why  $\beta$ -catenin mutation has proven, in a few studies, to be an indicator of a favorable prognostic factor related to low-stage (I, II), low-grade, hepatitis B virus-negative (HBV-negative) HCCs that predominately occur in elderly patients with low serum levels of AFP [7]. The rate of  $\beta$ -catenin mutations does not depend on the tumor size, uni- or multifocality, or even the presence or absence of cirrhosis [7]. It was suggested that there are two genetically distinguished groups of HCC: mutant nuclear  $\beta$ -catenin, with a survival rate of more than five years (over 60%), and wild-type nuclear  $\beta$ -catenin HCCs, with a more unfavorable prognosis (a five-year overall survival below 35%)

[7, 13]. This hypothesis should be tested among large cohorts.

Snail, Twist, and Slug positivity was reported in 57%, 43%, and 51%, respectively, of primary HCCs [7, 11, 13]. E-cadherin expression was shown to be inversely correlated with Snail and Twist [2, 11] (but not Slug), which are assumed to be the main mediators in the EMT of HCC cells [11]. Although independently regulated, Snail and Twist have experimentally been shown to have the potential for added aggressiveness, independent of Slug expression.

The E-cadherin negativity/Snail/Twist positivity/ $\beta$ -catenin nuclear expression could be considered to be an independent negative prognostic factor of HCC and an indicator of a high metastatic capacity [2, 11].

N-cadherin marks about 17% of HCC cases and shows membrane IHC expression with/without associated cytoplasmic positivity [13]. The correlation between E-cadherin and N-cadherin is rejected by most of the authors [13], proving that N-cadherin is not a key player for the EMT of HCC cells.

It was recently demonstrated that Wnt signaling can be activated by noncatenin proteins such as MUC13 [17] and collagen triple helix repeat containing 1 (CTHRC1) [18]. MUC13 can be detected in over 40% of HCCs and is correlated with tumor size and stage, encapsulation, venous invasion, and poor outcome [17]. MUC13 seems to induce  $\beta$ -catenin phosphorylation at Ser552 and Ser675 sites and, subsequently,  $\beta$ -catenin nuclear translocation [17].

CTHRC1 inhibits collagen 1 and stimulates the migration of HCC cells and EMT via PI3K/Akt/ERK/CREB/Snail/TGF $\beta$ /MMPs (matrix metalloproteinases 2 and 9) signaling [18]. CTHRC1 mRNA is positively correlated with tumor

size and stage, microvascular invasion, and intrahepatic metastasis [18].

Vimentin positivity is an independent indicator of EMT, early recurrence, and risk of lung metastases and a poor prognosis of HCC [19].

**3.2. *c-Met/HGF/Snail Pathway.*** HGF is encoded by the MET proto-oncogene [3, 8]. Its receptors stimulate the EMT markers, such as c-MET [19] and growth factor receptor tyrosine kinase (RTK) [2, 11], via the c-MET/Snail pathway [3, 8]. The suppressor of cytokine signaling 1 (SOCS1) was recently shown, in HCC lines, to regulate the HGF signal; SOCS1 inhibited the HGF-induced MET-mediated cell growth/proliferation, the invasion of the extracellular matrix, and the dissemination of tumor cells [2]. The HGF/MET axis also interacts with other biomarkers, such as integrins, semaphorins, EGFR, HER2, or the proapoptotic receptor, FAS [12].

Only a few complex studies have taken into account the IHC expression of c-MET in HCC [20, 21]. They revealed that the c-MET overexpression should be considered to be an independent negative prognostic factor, indicating early recurrence and poor survival [20]. The c-MET overexpression appears to be more frequent in poorly differentiated HCCs and correlates with  $\beta$ -catenin nuclear expression [21]. These aspects reveal an interaction between Wnt/ $\beta$ -catenin and c-Met/HGF/Snail pathways. There is no consensus regarding the best method and system for the IHC quantification of c-MET expression [20].

**3.3. *Notch-1/NF- $\kappa$ B Pathway.*** NF- $\kappa$ B is a transcription factor that can be activated during the EMT of several carcinomas, including HCC [22, 23]. It exerts an anti-apoptotic effect via the Notch-1/NF- $\kappa$ B pathway and interacts with the genes involved in apoptosis, such as Bcl-2, cyclin D1, survivin, and cIAPs (cellular inhibitor of apoptosis) [22, 23]. The NF- $\kappa$ B is suppressed by TNF which is encoded with the TNFAIP3 gene [23]. NF- $\kappa$ B is also known as the ubiquitin regulator A20 or alpha-induced protein 3 [23].

**3.4. *TGF- $\beta$ /SMAD Signaling.*** In HCC, TGF- $\beta$  can act as an autocrine or paracrine growth factor or can exert an extrinsic activity which induces a change in the tumor microenvironment [24]. TGF- $\beta$  interacts with the extracellular matrix metalloproteinase, MMP3, and appears to be downregulated by agents such as CR6-interacting factor 1 (CRIF1) [25]. CRIF1 also regulates the genes PTEN, SMAD (2, 3, and 6), and CDK6 and induces EMT via decreased E-cadherin and the upregulation of Twist, N-cadherin, and Snail [10, 24, 25].

**3.5. *Basic Fibroblast Growth Factor- (bFGF-) Related Signaling.*** In vitro, the complex bFGF and its receptors induced EMT and the metastasis of HCC cells via activation of the AKT/GSK-3 $\beta$ /Snail/Twist1 signaling pathway [26].

**3.6. *miRNAs Targeting the EMT-Related Biomarkers.*** Although miRNAs are described as attractive therapeutic targets, the molecular mechanisms of their signals are still unknown [3, 8].

The Met/Snail signal is suppressed by miR-148a [3]. Its expression is decreased in HCC compared with normal liver parenchyma, with a more significant loss in cases with portal vein tumor thrombosis [3]. In human HCC, miR-148a expression has been shown to be directly correlated with the mRNA level of the E-cadherin gene and inhibits the expression of other EMT markers, such as fibronectin, N-cadherin, vimentin, and nuclear Snail [3].

Similar to miR-148a, miR-449a inhibits EMT via the Met/Snail signal, but other targets (e.g., Bcl-2, cyclin D1, E2F3, Notch1, KLF4, and androgen receptor) can also be involved [2, 8]. Its decreased expression was also more frequently found in cases with portal vein tumor thrombosis, with the overexpression of miR-449a supposed to inhibit cell motility, reduce the nuclear accumulation of Snail, and decrease the rate of occurrence of pulmonary metastases [8].

miR-1271 targets the forkhead box Q1 (FOXQ1) protein, which appears to be involved in EMT. This miRNA was recently proven to be downregulated in HCC, compared with normal liver parenchyma [14]. In other carcinomas, FOXQ1 was demonstrated to be a target of TGF- $\beta$ - (e.g., breast cancer) or the Wnt- $\beta$ -catenin signaling pathway (e.g., colorectal cancer) [1, 14]. Although miR-1271 induced apoptosis in HCC lines, its role in the genesis and evolution of this hepatic tumor is still unknown [14].

Other supposed HCC-related miRNAs are miR-26a, miR-26b, miR-101, miR-122, miR-124, miR-150, miR-181 (expressed in  $\alpha$ -fetoprotein-positive HCCs), miR-195, miR-199a, miR-216a/217, and miR-331-3p [6, 10, 27–31]. The downregulation of miR-124 and miR-26b induces the EMT-related aggressive behavior of HCC [10]. miR-124 negatively regulates the oncogenes ROCK2 and EZH2 [10]. miR-150 directly targets ZEB1 and two proteins involved in DNA repair (MMP14 and MMP16) [28, 32]. MMP16 induces E-cadherin loss and directly correlates with the overexpression of the mesenchymal markers, vimentin, and N-cadherin, at both mRNA and protein levels [32]. miR-195 is a member of the miR-15 family [29] which is favored by downregulation in the occurrence of lung metastasis by targeting the FGF2 and vascular endothelial growth factor A (VEGF-A) genes [30]. miR-199a regulates E-cadherin expression via Notch1 direct targeting [31].

In the most recent studies, the signature sets of miRNAs are described as being involved in HCC genesis. In non-alcoholic steatohepatitis-associated HCC cell lines, a panel of 10 miRNAs was experimentally proven to suppress the most frequent carcinogenesis pathways, especially Wnt/ $\beta$ -catenin and TGF- $\beta$ , the signal transducer and activator of transcription 3 (STAT3), extracellular signal-regulated kinase 1 (ERK/MAPK), PPAR $\alpha$ /RXR $\alpha$ , PTEN, RAR, cell cycle regulation, stem cell regulation, c-myc, and the mechanistic target of rapamycin (mTOR) and amphiregulin (AREG), EGF, and NF- $\kappa$ B signaling [15]. These 10 miRNAs were identified as hepatocarcinogenesis suppressors: miR-17-5p, miR-221-3p, miR-93-5p, miR-25-3p, miR-181b-5p, miR-



106b-5p, miR-186-5p, miR-222-3p, miR-15b-5p, and miR-223-3p [15].

In HCC developed in patients with cirrhosis, a panel of 12 miRNAs was proposed to influence carcinogenesis and tumor progression [16]. The upregulation of miR-221 and miR-222 in HCC samples, compared with cirrhosis, was a common event [16]. These miRNAs trigger the CDK inhibitors p27 and p57 and the PI3K-PTEN-AKT-mTOR signaling pathway [16]. miR-106b, miR-21, miR-210, miR-224, miR-34a (target of p53), miR-425, miR-519a, miR-93, and miR-96 were also upregulated, whereas let-7c was downregulated in HCC, compared with normal or cirrhotic liver parenchyma [16].

The five miRNAs, which were common to the two studies involving HCC lines derived from nonalcoholic steatohepatitis and cirrhosis, were miR-34a, miR-93, miR-106b, miR-221, and miR-222 [15, 16]. Independent of the previous aspect of liver parenchyma, miR-21, miR-221, miR-222, and miR-224 appear to be predominately overexpressed in HCC and can serve as therapeutic targets [15, 16]. On the other hand, miR-210, miR-220, miR-224, miR-425, and miR-519a were hypothesized to be more HCC-specific [16]. In the most recent studies, the miRNA signature was hypothesized to influence the speed of HCC cells proliferation. In fast-growing HCC, downregulation of E-cadherin was associated with EMT via upregulation of five miRNAs, namely, miR-15b-5p, miR-421, miR-1303, miR-221-3p, and miR-486-5p [33].

**3.7. lncRNAs and the EMT of HCC Cells.** lncRNAs have been shown to influence the progression of HCC and to promote invasive capacity [28, 34–36], especially in HBV-related tumors [4, 37], but the understanding of their role in EMT is still incomplete. Several lncRNAs are described as being involved in HCC progression: HOTTIP, HOXA13, MALAT1 (metastasis-associated lung adenocarcinoma transcript 1), HOTAIR (HOX transcript antisense RNA), HULC (highly upregulated in liver cancer), MEG3 (also known as GTL2), ZFAS1, ZEB1-AS1, ZEB2-AS1, Linc00974, Linc00261, H19, DANCR, TCF7, Dreh, MVIH, HEIH, LET, ATB, ITGB1, antisense Igf2r (AIR), CCAL, uc002mb, and PVT-1 [28, 34–41].

In HCC tissue, CCAL overexpression is associated with a larger tumor size, an advanced pTNM stage and a low apoptotic rate; it induces EMT via the Wnt/ $\beta$ -catenin pathway activation [40]. HOTAIR is also overexpressed compared with normal parenchyma and induces aggressiveness in tumor cells [41]. HOTAIR inhibits the mismatch repair (MMR) proteins, MSH2 and MSH6 and, as result, enhances the microsatellite instability (MSI) status of HCC cells [41].

Linc00261 is decreased in HCC tissue compared with normal liver parenchyma [39]. Its decreased level might induce EMT via activation of the Notch-1/NF- $\kappa$ B pathway and is correlated with tumor size, TNM stage, and low survival rate [39].

The first lncRNA described as influencing the EMT of HBV-induced HCC was HULC; a single nucleotide

polymorphism, such as rs7763881, may induce EMT [40, 42, 43]. ZEB2-AS1 upregulation induces metastatic ability via the downregulation of E-cadherin and the upregulation of vimentin [37]. Recently, it was experimentally demonstrated that the HCC core of lncRNAs includes the following five lncRNAs: FABP5P3, LOC100996735, LOC100996732, ZEB1-AS1, and ZFAS1 [28]. The most upregulated lncRNA was found to be ZFAS1 [28]. As ZFAS1 contains a site for miR-150, which targets ZEB1 (which regulates E-cadherin), MMP14, and MMP16, we can suppose that ZFAS1 might play an important role in the EMT of HCC cells via matrix metalloproteinases and the Wnt/ $\beta$ -catenin pathway [28].

EMT can also occur via the IL-6/STAT3/lncTCF7 signaling axis [38].

#### 4. Cancer Stem-Like Cell Biomarkers

Similar to other carcinomas, the EMT pathways are commonly driven via the activation of cancer stem-like cells (CSCs) [44–46]. These are also known as progenitor cells or tumor-initiating cells (TICs) and present self-renewable capacities [44–48]. The CSCs may activate the Wnt/ $\beta$ -catenin pathway and induce chemo/radiotherapy resistance, disease relapse, and metastasis [46, 47] and are also responsible for tumor heterogeneity [48].

The markers that have been proven to act as hepatic CSCs are A6, OV6, CD133 (also known as prominin-1), CD44 standard isoform (CD44s), CD90, CD45, CD13, CD24, cytokeratin 19 (CK19), the epithelial cell adhesive molecule (EpCAM, also known as CD326), octamer-binding transcription factors (Oct3/4), aldehyde dehydrogenase-1 (ALDH1), SOX2, nestin, C-KIT, and CD105 (also known as endoglin) [12, 19, 27, 43, 44, 49–53]. The CSC-related genes are Notch,  $\beta$ -catenin, and Oct3/4 [27]. In an experimental study that investigated the mRNA expression of 12 EMT-related/stemness markers (CD133, CD90, CD44, ALDH1, CK19, OCT4, SOX2, vimentin, nestin, CD13, and EpCAM), only CD44 and CD133 proved to be upregulated in HCC cells, compared with normal hepatic parenchyma [49].

The cell surface adhesive, glycoprotein CD44s, is not expressed in the normal mature hepatocytes but marks over 55% of HCC cells [45, 49]. The positivity of CD44 is directly correlated with Twist 1 overexpression [27, 45] and interacts with the HGF/MET or TGF- $\beta$  molecular axes [12, 27, 45]. Although the prognostic value of CD44 is controversial [45], a meta-analysis comprising 14 studies with more than 2200 patients showed that CD44 expression was directly correlated with the pTNM stage but not with the tumor grade or AFP serum level [47]. Its positivity was shown to be an indicator of poor overall survival, but the association with disease-free survival was rejected [47]. The heterogeneity of the reported results is based on the use of several clones/isoforms (CD44, CD44s, and CD44v6) and a lack of consensus regarding the cutoff value (which was reported as at least one positive cell or a value of 10%, 25%, or 50%, respectively) [47].

CD133 has been shown to be a CSC hepatic marker since 2007 [43]. It marks over 25–50% of HCC cells [49, 52]. CD133-positive HCCs are more aggressive, express CSC-



related genes, and present low overall survival [27, 44, 49]. Some studies rejected the independent prognostic role of CD133 [52].

CD90 is especially expressed in poorly differentiated HCCs [27]. Of all of the stemness markers, it appears to be the one that is most involved in inducing lung metastases [52] and can coexist with c-KIT, CD105 (endoglin), and FLT1 positivity [48, 53]. About 40% of HCC showed CD105 positivity in the tumor cells as an indicator of microvascular invasion and poor recurrence-free survival [53].

No standard cutoff value is known for CD133, CD90, or other CSCs markers. We consider that 10% should be the cutoff value for the IHC quantification of all CSC markers and the stromal expression should also be taken into account as a prognostic indicator. We also agree with the use of the three scores utilized by Zhao et al.: score 0 (no stained or < 10% stained cells), score 1 (11–50% stained cells), score 2 (51–80% stained cells), and score 3 (>80% stained cells) [49]. Moreover, CD44 variant isoforms (CD44v8-10) should not be used to study HCC behavior [45], while an HCC stem cell should not be defined based on its IHC positivity for only one of the CSC markers [45]. To define a CSC and establish its prognostic value, double positivity for CD44s/CD133 or CD44s/CD90 is required [27, 45, 49].

Double positivity for CD44s and CD90 was proven to be associated with CD45 negativity and a higher aggressiveness, compared to only CD133-positive HCC cells [27]. Double positivity for CD44/CD133 was found in over 36% of HCC cases and demonstrated to be a strong negative prognostic indicator [49]. Double positivity for CD90/CD105 can be an indicator of EMT associated with endothelial-mesenchymal transition (End-MT); this can confirm the vasculogenic mimicry or the possible role of CD105 as a CSC [10, 53].

The CSC marker, CD13, is overexpressed in one-third of HCCs and considered to be a marker of semiquiescent HCC cells [19, 27]. Although its positivity was proven to be a negative prognostic factor, especially in patients with large tumors, no correlation with E-cadherin or vimentin was emphasized [19]. The cell division rate appears to be influenced by the expression of CSC biomarkers. CD13(+)/CD90(–) cells are mainly in the G0/G1 phase, and CD13(+)/CD90(+) cells are in the S-to-G2/M phase, whereas CD13(–)/CD90(+) cells are more frequent in the G2/M-to-S phase [44].

The epithelial cell adhesive molecule, EpCAM (CD326), is considered to mark epithelial CSCs [41]. EpCAM appears to increase the invasiveness potential of tumor cells as well as the risk of portal vein invasion [27]. The CSCs' proliferation rate is influenced by lncRNAs such as HOTAIR [41].

The exact mechanism of the CK19-inducing aggressiveness of HCC and its relationship with CSCs are unclear [51]. In normal liver parenchyma, CK7 and CK19 are not expressed; they mark the bile duct cells [50]. The normal hepatocytes usually express CK8 and CK18 [50]. Some studies have confirmed that about one-third of HCCs are CK7(+)/CK19(–) [50]. CK19 marks 11–31% of HCCs [50, 52], and the coexpression of CK7 and CK19 was described in 9% of HCCs [50]. CK19 and/or CK7 positivity is an indicator of the high risk of recurrence and low overall

survival [50–52]. CK19 positivity is directly correlated with tumor size and portal vein invasion [51]. The HCC cells marked by biliary markers might occur as the aberrant differentiation of CSCs [50, 51]. This aspect was experimentally proven by the self-renewal capacity of CK19-positive cells, which were capable of transforming into CK19-negative cells and induced EMT via TGF $\beta$ /SMAD signaling [51]. CK19 can be coexpressed with TGF $\beta$  and EpCAM, especially in large tumors [51].

## 5. Circulating Tumor Cells

In the peripheral blood of patients with HCC, the EpCAM-based identification of circulating tumor cells (CTCs) is considered to be an indicator of portal vein thrombosis, early recurrence risk, and high metastatic potential [33, 45, 54–57].

The mechanism for the survival of CTCs is still unclear. They can be epithelial on release but acquire a mesenchymal or an intermediate phenotype (a hybrid cell that expresses both epithelial and mesenchymal markers; also known as the semimesenchymal cell) during hematogenous transit [54, 55, 57]. A mesenchymal phenotype might protect them from apoptosis, anoikis, and immune mechanisms [54, 55, 57]. Smad-induced Wnt signaling activation was proposed to be involved in the EMT of hepatic CTCs [57].

These CTCs are marked by DAPI and the IHC biomarkers pan-CK, CDH1, and hepatocyte-specific antigen (HSA) and negative for the leukocyte markers CD45 and CD16 [56, 57]. More than 80% of CTCs express vimentin, Twist, Smad, and CTNBN1 as indicators of EMT [56, 57]. The positivity rate for Twist and vimentin is correlated with tumor size and TNM stage but not with the number of tumors [56]. The vimentin-positive CTCs were more frequently detected in patients within Milan criteria, compared with those beyond Milan criteria [56]. Other transcription markers, such as ZEB1, ZEB2, and Snail, can be detected in the CTCs without prognostic value [55]. E-cadherin and Slug did not mark the hepatic CTCs [56].

CD44s-positive HCC circulating cells confirmed EMT during the metastatic step; the mesenchymal phenotype is even more expressed in CD44s(+)/CD90(+) cells [44]. Some of the EpCAM-positive CTCs can be negative for CSC markers such as CD90 [44].

bFGF-related EMT was proven by an increase in serum bFGF in patients with HCC compared with healthy volunteers and a decrease compared with patients with chronic hepatitis and/or cirrhosis [26, 58]. Circulating TGF- $\beta$  level was shown to be increased in patients with fast-growing HCC, compared with slow HCC [33].

Due to the spatial heterogeneity of CTCs, it was suggested that they should be counted in the hepatic vein, where they are in clusters; these cells are more isolated in the peripheral veins [57]. In the hepatic vein, the epithelial and intermediate phenotypes predominated compared with the more frequent mesenchymal cells detected in the peripheral veins [57]. As the EpCAM is downregulated during the EMT of CTCs, a low number of CTCs can be detected in the peripheral bloodstream of patients with HCC; they do not

reflect the true number of viable cells in circulation [55]. For this reason, novel biomarkers, such as the major vault protein (MVP) [55] and CTHRC1 [18], are proposed for use as a more proper detection of HCC circulating cells with a mesenchymal or an intermediate phenotype [55]. The number of CTCs is positively correlated with the number of mesenchymal cells detected in the HCC tissue using specific IHC markers; they are not correlated with the amount of epithelial or intermediate HCC tissue cells [54].

## 6. EMT and Inflammation

The interplay between inflammation, hypoxia, and EMT seems to be the critical link that shapes the HCC microenvironment [59]. On the one hand, intratumoral interleukins, such as IL-1 $\beta$  and IL-6, are correlated with the number of proinflammatory tumor-associated macrophages [38, 59]. At the same time, IL-1 $\beta$  mediates the functional maintenance of M2 monocyte-derived macrophages, which play a proinflammatory role and enhance the proliferation and invasion of HCC cells [60]. On the other hand, transactivation of the complexes IL-6/STAT3/lncTCF7 or IL-6/STAT3/Snai1-Smad3/TGF- $\beta$ 1 promotes the invasion of HCCs developed in patients with hepatitis [24, 38, 61], especially the nonalcoholic type [15].

In cell lines with hepatitis virus C-related (HCV-related) HCC, Twist positivity, an independent negative prognostic marker, is more frequent than it is in HCC developed in non-hepatitis-related carcinomas [11, 58]. In human samples with HCV-related HCC, EMT was found to be driven by the Wnt- $\beta$  catenin pathway, which is probably modulated by some viral proteins, such as NS5A [13], or occurs as a result of bFGF activation [58]. Although it was hypothesized that mutations in the CTNNA1/ $\beta$ -catenin gene, exon 3, occur more frequently in patients with non-HBV-related HCC [7], this aspect was not confirmed in all further studies [12]. However, the mutation spectrum appears to be different: codons 33 and 41 were more frequently mutated in patients with HBV-related HCC, whereas in patients with non-HBV-related HCC, codon 45 was the mutational hotspot of exon 3 of the  $\beta$ -catenin gene [7]. The rate of mutations within codons 32 and 34 was not dependent on the viral history of the patient; this was similar in both HCV-related and HBV-related HCCs and should be considered as the mutational hotspot of these carcinomas [7].

The distribution of some stemness markers also appears to be correlated with inflammation. CD90 is more frequently expressed in patients with hepatitis-related, compared with non-hepatitis-related, HCCs, whereas CD133-positive HCCs are more frequently non-hepatitis-related [44]. Other studies showed that the coexpression of CD44 and CD133 is not influenced by HBV but that CD133 is more frequently expressed in HCC developed in patients with cirrhosis [49]. In HBx-infected hepatoma cells, TGF- $\beta$  proved to upregulate CD133 expression and induce cancer stemness and EMT [62].

The CD13-positive CSCs are equally distributed in hepatitis-related and non-hepatitis-related HCC cell lines [44]. CK19 positivity is more frequent in HBV-induced HCCs and a negative prognostic factor [50].

HBV induces the mesenchymal phenotype of HCC cells via the Wnt pathway (E-cadherin loss/upregulated vimentin), which is mediated by lncRNAs such as ZEB2-AS1 [37]. In addition to the Wnt pathway, activated c-Src, STAT3, Akt, and Notch1 were also identified as mediators of EMT induced by HBV [37, 63, 64].

## 7. EMT and Angiogenesis

The HGF/MET axis promotes angiogenesis via interaction with proangiogenic factors such as the vascular endothelial growth factor receptor (VEGFR2) and reverse correlation with thrombospondin-1 [12]. Hypoxia stimulates c-MET overexpression in HCC cells [21].

On the other hand, hypoxia-inducing factor 1 $\alpha$  (HIF-1 $\alpha$ ) proved to enhance the EMT of HCC cells [54, 64]; its expression correlates with IL-1 $\beta$ -related inflammation intensity [44]. Although the hypoxia microenvironment may induce EMT, the hypoxia-related EMT cascade cannot be activated without the simultaneous activation of actin cytoskeleton remodeling via the Wnt/ $\beta$ -catenin pathway [65–69]. This remodeling process is expressed more in large HCCs due to tumor size (over 5 cm), while portal invasion remains the most important prognostic indicator of these tumors [51, 66]. Hypoxia-related EMT is also linked with the aberrant hedgehog pathway which plays an important role in maintaining the stem cell capacity of tumor cells [62, 64, 66].

Hypoxia could also promote the EMT of HCC cells via Twist1 upregulation [64]. In cell cultures, 24 h of hypoxia is sufficient for inducing architectural disorders of the cells, along with the upregulation of HIF-1 $\alpha$  and the downregulation of E-cadherin levels in the tumor cells [67].

VEGFA activation via the downregulation of miR-195 is another supposed mechanism for inducing EMT-related angiogenesis [30]. VEGF positivity can be found in about 70% of HCCs, especially in early stages of HCC developed in cirrhosis [52, 68].

In mouse models, it was demonstrated that proinflammatory IL-1 $\beta$  promoted HCC metastasis and induced poor prognosis [59].

In addition to inducing EMT, TGF $\beta$ 1 also appears to play a role in the End-MT of intratumor endothelial cells, via CD133 upregulation [10]. The endothelial marker, CD105, is a coreceptor of TGF $\beta$ 1 and has stemness properties, being coexpressed with CD90 but not with EpCAM [53]. HIF-1 $\alpha$ -related hypoxia is also involved in the maintenance of CSCs, via CD90 and CD133, although the IHC expression of VEGF is not correlated with the stemness markers CD133, CK19, and EpCAM [54, 69].

Although the metastatic pathway of HCC is not completely understood (Figure 2), it seems to be hypoxia-dependent and is related to the Wnt-mediated or, rather, the TGF $\beta$ 1-mediated inflammation-angiogenesis-EMT-CSCs crosstalk link [10, 59].

## 8. Tumor Microenvironment and Therapy

**8.1. EMT and Chemotherapies.** Reducing mortality in HCC strongly depends on the identification of molecular targets

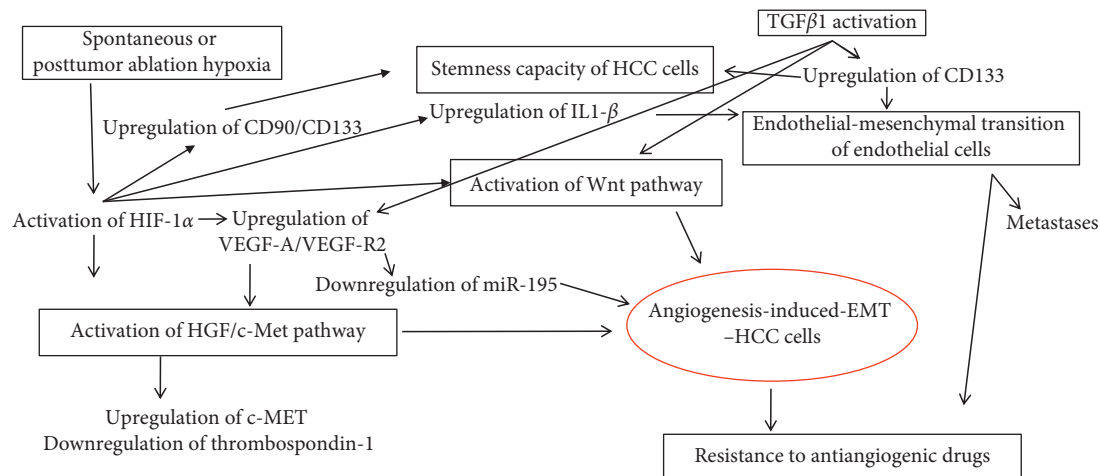


FIGURE 2: Molecular pathway signaling of angiogenesis-induced epithelial-mesenchymal transition in hepatocellular carcinoma.

that might be used for individualized therapy [2]. The targeting drugs include selective or multikinase inhibitors, as well as antibodies targeting HGF or MET (e.g., DN-30) [11, 12].

Sorafenib, the multikinase inhibitor and antiangiogenic, is currently the only molecular-targeted drug approved by the US Food and Drug Administration to be used as first-line therapy for patients diagnosed with advanced stages of HCCs [10, 12, 69, 70]. Although sorafenib targets the Raf/MEK/ERK signaling pathway and several genes such as c-KIT, c-RAF, b-RAF, VEGF-R, c-KIT, and PDGFR $\beta$ , the response rate is low and secondary chemoresistance is frequent [10, 12, 23, 70]. Chemoresistance to sorafenib might be related to the CSCs biomarkers; it is more frequent in those HCCs that express positivity for more than one CSC marker [27, 43, 67, 71]. The CSCs have a quiescent status and can survive after chemotherapy [49]. Experimentally, the CD44(+)/CD133(+) HCC cells proved to be more resistant than CD44(-)/CD133(+) cells [27, 72]. The resistance of CD44(+)/CD133(+) HCC cells might occur as a result of the upregulation of the ATP-binding cassette (ABC) superfamily transporters [73]. Sorafenib proved to decrease the number of CD90(+) cells via c-KIT or TGF- $\beta$  inhibition [48]. As sorafenib upregulates EpCAM expression, PARP inhibitors might be added to target EpCAM + CSCs [48]. For HCCs expressing CD105 in the tumor cells, sorafenib might be combined with the anti-CD105 agent TRC105 (galunisertib), which is currently being tested in a phase II clinical trial [53, 74].

Resistance to cisplatin can be induced by the ABC subfamily member, ABCB1, which forms a complex with STAT3, and also by overactivation of the HOTAIR lncRNA [73]. As HOTAIR enhances the MSI status of HCC cells [41], patients with overexpressed HOTAIR may also be resistant to 5-fluorouracil (5-FU) [74, 75] but may benefit from immunotherapy.

Resistance to classic cytotoxic agents, such as 5-FU and/or adriamycin/doxorubicin/epirubicin, might also be induced by the CSC markers CD13, CD133, CD90, EpCAM, and CK19 [20, 27, 44, 48, 51]. On the other hand, CD13,

CD90, EpCAM, CK19, and CD105 might be generated, de novo, after chemotherapy [44, 53]. 5-FU induces EMT via the activation of Snail1 and Snail2 [53].

The anti-VEGFR2 apatinib is an oral drug tested in clinical trials among sorafenib-resistant patients [70]. The oral selective c-Met receptor tyrosine kinase inhibitor, known as tivantinib, is currently being tested as a second-line therapy in a phase II trial, involving patients with advanced HCC and compensated liver cirrhosis [10, 20, 76]. Due to reverse MET-VEGF interaction, it is supposed that antiangiogenic drugs might enhance MET activity [10, 12]. In mouse models, drugs, such as the oral multikinase inhibitor foretinib (with the dual inhibition of angiogenesis and c-MET signaling), proved to successfully deactivate the VEGFR2/MET signaling pathways and induce tumor cells' apoptosis [77].

As the E-cadherin/catenins complex has been shown to be involved in HCC progression, it was suggested that Wnt/ $\beta$ -catenin signaling inhibition should be used as a target complex for the synthesis of anti-HCC drugs [9, 78]. The antifibrotic molecule pirfenidone, which is used in patients with idiopathic pulmonary fibrosis, has been experimentally proven to inhibit the proliferation of HCC and to promote apoptosis via  $\beta$ -catenin suppression [78].

Inhibition of the other signaling pathways, such as Notch-1/NF- $\kappa$ B, was also proposed for use in EMT-related targeted therapy [23, 24].

The TGF- $\beta$  inhibitor, known as LY2157299, is currently being tested in phase II clinical trials [24, 51, 79]. In experimental studies, LY2157299 has also been demonstrated, in a dose-dependent manner, to induce the dephosphorylation of FAK, b1-integrin, MEK, ERK, AKT, mTOR, and PTEN but not p-38-MAPK-kinase [24, 79]. This drug might be especially useful for the targeted therapy of patients with HCCs that display CK19 positivity [52].

In a phase II clinical trial, a combination of sorafenib with the TGF- $\beta$  inhibitor galunisertib showed acceptable safety and an increased overall survival of over 14 months [80].

In patients with lung metastases, the anti-VEGF drugs should target miR-195 [30]. As miR-195 targets both VEGF-



A and bFGF2 [30], EMT might be suppressed by anti-bFGF drugs, such as the oral anti-hyperglycemic agent metformin [26]. Sorafenib proved to inhibit CD90-positive pulmonary metastatic cells [48].

**8.2. EMT and Radiotherapy.** In patients with HCC, radiotherapy is used for the local control of extrahepatic spread or macrovascular invasion [81]. Resistance to ionizing radiation is a characteristic of HCC cells, although the mechanism of induction is still unknown [23, 78]. The most commonly used techniques are radiofrequency ablation, radio-embolization, transarterial chemoembolization (TACE), and cryoablation [23, 26, 52, 69, 82, 83]. The newest techniques are three-dimensional conformal radiotherapy, immunoradiotherapy, and image-guided radiotherapy [23, 78, 83, 84]. A combination of chemo- and radiotherapy is also used in advanced HCCs [81, 83].

More than 27% of patients show residual viable tumor cells after TACE [52]. CD105-positive tumor cells, in particular, survive at the periphery of the tumor parenchyma [53]. The radioresistance of HCC cells may be induced via the NF- $\kappa$ B signaling axis [23]. In resistant cells, the inhibition of the NF- $\kappa$ B pathway via enhancing the A20 protein was proposed as a novel therapeutic strategy [23].

In addition to resistance to radiotherapy, TACE-induced hypoxia was shown to produce stromal alteration and the upregulation of stemness markers with a further increased risk of relapse [52]. The IHC studies have reveal an increased intensity and percentage of HCC-positive cells after TACE, compared with the biopsy specimens, especially for CD133, CK19, and EpCAM [52]. The tumor stroma becomes more fibrotic after TACE [52].

After radiofrequency ablation, it was proven that the hypoxic medium might induce the proliferation of stem-like cells, through HIF-1 $\alpha$ /VEGF-A signaling [69] (Figure 2). These cells showed chemoresistance capacity and increased proliferative and metastatic potential, especially in patients with residual cells after ablation [69].

After insufficient radiofrequency ablation, sorafenib seems to inhibit the EMT of residual cells, via HIF-1 $\alpha$ /VEGF-A signaling [69, 84, 85]. For this reason, combined radiochemotherapy is recommended to be used [69, 84, 85].

Immunoradiotherapy was recently validated for local HCC. This can be performed using the CD147-targeted agent known as I131-metuximab (I131-mab or CD147-mab) [86]. Although the molecular mechanism is still unknown, the I131-mab appears to inhibit EMT by suppressing the phosphorylation of VEGFR-2 [86].

## 9. Summary and Future Perspectives

Although, in carcinomas, the tumor microenvironment is defined by the old concept of EMT, this has proven to be more challenging for HCC. This comprehensive review of the literature has revealed that similar to other carcinomas, the Wnt pathway is the central event in the EMT of HCC cells, but it does not define the tumor microenvironment. Rather, it is characterized by the interaction between EMT

markers and stemness agents. Understanding the molecular pathway of the EMT-angiogenesis-CSCs crosstalk (Figure 2) is mandatory for a therapy that is properly targeted. The EMT markers that deserve further exploration in HCC are E-cadherin and  $\beta$ -catenin, which should be correlated with the epithelial stemness marker EpCAM and the mesenchymal CSCs markers CD44, CD133, CD90, and CD105. The molecular mechanism of CK7 and CK19 positivity should also be identified.

The targeted therapy should aim at decreasing hypoxia-mediated stromal changes, especially for large tumors. TACE and radiofrequency ablation should be avoided in large tumors which express CD133, CK19, or EpCAM. In selected cases, radiotherapy should be combined with chemotherapeutics. The CD90-positive HCCs with pulmonary metastases should be treated with sorafenib, and patients with CK19-positive HCCs should benefit from TGF- $\beta$  inhibitors. In sorafenib-resistant cases, a detailed immunoprofile of tissue cells and CTCs should be used for proper individualized therapy.

## Conflicts of Interest

The authors have no conflicts of interest to report.

## Authors' Contributions

Simona Gurzu and Decebal Fodor have equally contributed to the paper.

## Acknowledgments

This work was supported by a grant of the Romanian National Authority for Scientific Research, CNCS-UEFISCDI, project no. 20 PCCF/2018, code: PN-III-P4-ID-PCCF-2016-0006.

## References

- [1] S. Gurzu, C. Silveanu, A. Fetyko, V. Butiurca, Z. Kovacs, and I. Jung, "Systematic review of the old and new concepts in the epithelial-mesenchymal transition of colorectal cancer," *World Journal of Gastroenterology*, vol. 22, no. 30, pp. 6764–6775, 2016.
- [2] Y. Gui, M. G. M. Khan, D. Bobbala et al., "Attenuation of MET-mediated migration and invasion in hepatocellular carcinoma cells by SOCS1," *World Journal of Gastroenterology*, vol. 23, no. 36, pp. 6639–6649, 2017.
- [3] J.-P. Zhang, C. Zeng, L. Xu, J. Gong, J.-H. Fang, and S.-M. Zhuang, "MicroRNA-148a suppresses the epithelial-mesenchymal transition and metastasis of hepatoma cells by targeting Met/Snail signaling," *Oncogene*, vol. 33, no. 31, pp. 4069–4076, 2014.
- [4] L. Qiu, T. Wang, X. Xu et al., "Long non-coding RNAs in hepatitis B virus-related hepatocellular carcinoma: regulation, functions, and underlying mechanisms," *International Journal of Molecular Sciences*, vol. 18, no. 12, p. 2505, 2017.
- [5] X. Mao, Y. Zhang, and N. Lin, "Application and perspectives of traditional Chinese medicine in the treatment of liver cancer," *Cancer Translational Medicine*, vol. 1, no. 3, pp. 101–107, 2015.

- [6] S. Turdean, S. Gurzu, M. Turcu, S. Voidazan, and A. Sin, "Current data in clinicopathological characteristics of primary hepatic tumors," *Romanian Journal of Morphology and Embryology*, vol. 53, pp. 719–724, 2012.
- [7] H.-C. Hsu, Y.-M. Jeng, T.-L. Mao, J.-S. Chu, P.-L. Lai, and S.-Y. Peng, " $\beta$ -Catenin mutations are associated with a subset of low-stage hepatocellular carcinoma negative for hepatitis B virus and with favorable prognosis," *The American Journal of Pathology*, vol. 157, no. 3, pp. 763–770, 2000.
- [8] S. P. Chen, B. X. Liu, J. Xu et al., "MiR-449a suppresses the epithelial-mesenchymal transition and metastasis of hepatocellular carcinoma by multiple targets," *BMC Cancer*, vol. 15, p. 706, 2015.
- [9] B. Zhai, H.-X. Yan, S.-Q. Liu, L. Chen, M.-C. Wu, and H.-Y. Wang, "Reduced expression of E-cadherin/catenin complex in hepatocellular carcinomas," *World Journal of Gastroenterology*, vol. 14, no. 37, pp. 5665–5673, 2008.
- [10] S. Gurzu, S. Turdean, A. Contac et al., "Epithelial-mesenchymal, mesenchymal-epithelial, and endothelial-mesenchymal transitions in malignant tumors: an update," *World Journal of Clinical Cases*, vol. 3, no. 5, pp. 393–404, 2015.
- [11] M.-H. Yang, C.-L. Chen, G.-Y. Chau et al., "Comprehensive analysis of the independent effect of twist and snail in promoting metastasis of hepatocellular carcinoma," *Hepatology*, vol. 50, no. 5, pp. 1464–1474, 2009.
- [12] S. Giordano and A. Columbano, "Met as a therapeutic target in HCC: facts and hopes," *Journal of Hepatology*, vol. 60, no. 2, pp. 442–452, 2014.
- [13] A. Kasprzak, K. Rogacki, A. Adamek et al., "Tissue expression of  $\beta$ -catenin and E- and N-cadherins in chronic hepatitis C and hepatocellular carcinoma," *Archives of Medical Science*, vol. 6, pp. 1269–1280, 2017.
- [14] A. Qin, J. Zhu, X. Liu, D. Zeng, M. Gu, and C. Lv, "MicroRNA-1271 inhibits cellular proliferation of hepatocellular carcinoma," *Oncology Letters*, vol. 14, pp. 6783–6788, 2017.
- [15] A. De Conti, J. F. Ortega, V. Tryndyak et al., "MicroRNA deregulation in nonalcoholic steatohepatitis-associated liver carcinogenesis," *Oncotarget*, vol. 8, pp. 88517–88528, 2017.
- [16] P. Pineau, S. Volinia, K. McJunkin et al., "miR-221 overexpression contributes to liver tumorigenesis," *Proceedings of the National Academy of Sciences*, vol. 107, no. 1, pp. 264–269, 2010.
- [17] Y. Dai, L. Liu, T. Zeng et al., "Overexpression of MUC13, a poor prognostic predictor, promotes cell growth by activating Wnt signaling in hepatocellular carcinoma," *The American Journal of Pathology*, vol. 188, no. 2, pp. 378–391, 2018.
- [18] Y. Wang, M. Lee, G. Yu et al., "CTHRC1 activates pro-tumorigenic signaling pathways in hepatocellular carcinoma," *Oncotarget*, vol. 8, pp. 105238–105250, 2017.
- [19] C. Yamanaka, H. Wada, H. Eguchi et al., "Clinical significance of CD13 and epithelial mesenchymal transition (EMT) markers in hepatocellular carcinoma," *Japanese Journal of Clinical Oncology*, vol. 48, no. 1, pp. 52–60, 2017.
- [20] J. H. Kim, H. S. Kim, B. J. Kim et al., "Prognostic value of c-Met overexpression in hepatocellular carcinoma: a meta-analysis and review," *Oncotarget*, vol. 8, pp. 90351–90357, 2017.
- [21] G. Szparecki, T. Ilczuk, N. Gabzdyl, E. Stocka-Labno, and B. Górnicka, "Expression of c-MET protein in various subtypes of hepatocellular adenoma compared to hepatocellular carcinoma and non-neoplastic liver in human tissue," *Folia Biologica*, vol. 63, pp. 146–154, 2017.
- [22] H. Yu, N. Aravindan, J. Xu, and M. Natarajan, "Inter- and intra-cellular mechanism of NF- $\kappa$ B-dependent survival advantage and clonal expansion of radio-resistant cancer cells," *Cellular Signalling*, vol. 31, pp. 105–111, 2017.
- [23] R. Liu, D. Zhao, X. Zhang et al., "A20 enhances the radio-sensitivity of hepatocellular carcinoma cells to  $^{60}\text{Co-}\gamma$  ionizing radiation," *Oncotarget*, vol. 8, pp. 93103–93116, 2017.
- [24] G. Giannelli, E. Villa, and M. Lahn, "Transforming growth factor- as a therapeutic target in hepatocellular carcinoma," *Cancer Research*, vol. 74, no. 7, pp. 1890–1894, 2014.
- [25] R. Zhuang, D. Lu, J. Zhuo et al., "CR6-interacting factor 1 inhibits invasiveness by suppressing TGF- $\beta$ -mediated epithelial-mesenchymal transition in hepatocellular carcinoma," *Oncotarget*, vol. 8, pp. 94759–94768, 2017.
- [26] W. Chengye, T. Yu, S. Ping et al., "Metformin reverses bFGF-induced epithelial-mesenchymal transition in HCC cells," *Oncotarget*, vol. 8, pp. 104247–104257, 2017.
- [27] W. Zhang, D. Mu, and K. Feng, "Hierarchical potential differentiation of liver cancer stem cells," *Advances in Clinical and Experimental Medicine*, vol. 26, no. 7, pp. 1137–1141, 2017.
- [28] T. Li, J. Xie, C. Shen et al., "Amplification of long noncoding RNA ZFAS1 promotes metastasis in hepatocellular carcinoma," *Cancer Research*, vol. 75, no. 15, pp. 3181–3191, 2015.
- [29] S. Yu, L. Jing, X. R. Yin et al., "MiR-195 suppresses the metastasis and epithelial-mesenchymal transition of hepatocellular carcinoma by inhibiting YAP," *Oncotarget*, vol. 8, pp. 99757–99771, 2017.
- [30] M. Wang, J. Zhang, L. Tong, X. Ma, and X. Qiu, "MiR-195 is a key negative regulator of hepatocellular carcinoma metastasis by targeting FGF2 and VEGFA," *International Journal of Clinical and Experimental Pathology*, vol. 8, pp. 14110–14120, 2015.
- [31] C. Giovannini, F. Fornari, R. Dallo et al., "MiR-199-3p replacement affects E-cadherin expression through Notch1 targeting in hepatocellular carcinoma," *Acta Histochemica*, vol. 120, no. 2, pp. 95–102, 2017.
- [32] Z. Shen, X. Wang, X. Yu et al., "MMP16 promotes tumor metastasis and indicates poor prognosis in hepatocellular carcinoma," *Oncotarget*, vol. 8, pp. 72197–72204, 2017.
- [33] R. Critelli, F. Milosa, F. Faillaci et al., "Microenvironment inflammatory infiltrate drives growth speed and outcome of hepatocellular carcinoma: a prospective clinical study," *Cell Death & Disease*, vol. 8, article e3017, 2017.
- [34] W. W. Yu, K. Wang, and G. J. Liao, "Knockdown of long noncoding RNA linc-ITGB1 suppresses migration, invasion of hepatocellular carcinoma via regulating ZEB1," *European Review for Medical and Pharmacological Sciences*, vol. 21, pp. 5089–5095, 2017.
- [35] M.-c. Lai, Z. Yang, L. Zhou et al., "Long non-coding RNA MALAT-1 overexpression predicts tumor recurrence of hepatocellular carcinoma after liver transplantation," *Medical Oncology*, vol. 29, no. 3, pp. 1810–1816, 2012.
- [36] M. Zhang, W. Wang, T. Li et al., "Long noncoding RNA SNHG1 predicts a poor prognosis and promotes hepatocellular carcinoma tumorigenesis," *Biomedicine & Pharmacotherapy*, vol. 80, pp. 73–79, 2016.
- [37] Y. Jin, D. Wu, W. Yang et al., "Hepatitis B virus x protein induces epithelial-mesenchymal transition of hepatocellular carcinoma cells by regulating long non-coding RNA," *Virology Journal*, vol. 14, no. 1, p. 238, 2017.
- [38] J. Wu, J. Wu, J. Zhang et al., "Long noncoding RNA lincTCF7, induced by IL-6/STAT3 transactivation, promotes hepatocellular carcinoma aggressiveness through epithelial-mesenchymal transition," *Journal of Experimental & Clinical Cancer Research*, vol. 34, p. 116, 2015.



- [39] H.-F. Zhang, W. Li, and Y.-D. Han, "LINC00261 suppresses cell proliferation, invasion and Notch signaling pathway in hepatocellular carcinoma," *Cancer Biomarkers*, vol. 21, no. 3, pp. 575–582, 2018.
- [40] Y. Liu, Y. Yang, T. Wang et al., "Long non-coding RNA CCAL promotes hepatocellular carcinoma progression by regulating AP-2 $\alpha$  and Wnt/ $\beta$ -catenin pathway," *International Journal of Biological Macromolecules*, vol. 109, pp. 424–434, 2017.
- [41] H. Li, J. An, M. Wu et al., "LncRNA HOTAIR promotes human liver cancer stem cell malignant growth through downregulation of SETD2," *Oncotarget*, vol. 6, pp. 27847–27864, 2015.
- [42] K. Panzitt, M. M. O. Tschernatsch, C. Guelly et al., "Characterization of HULC, a novel gene with striking up-regulation in hepatocellular carcinoma, as noncoding RNA," *Gastroenterology*, vol. 132, no. 1, pp. 330–342, 2007.
- [43] Y. Liu, S. Pan, L. Liu et al., "A genetic variant in long non-coding RNA HULC contributes to risk of HBV-related hepatocellular carcinoma in a Chinese population," *PLoS One*, vol. 7, Article ID e35145, 2012.
- [44] S. Ma, K. W. Chan, L. Hu et al., "Identification and characterization of tumorigenic liver cancer stem/progenitor cells," *Gastroenterology*, vol. 132, no. 7, pp. 2542–2556, 2007.
- [45] H. Okabe, T. Ishimoto, K. Mima et al., "CD44s signals the acquisition of the mesenchymal phenotype required for anchorage-independent cell survival in hepatocellular carcinoma," *British Journal of Cancer*, vol. 110, no. 4, pp. 958–966, 2014.
- [46] M. M. Kazi, T. I. Trivedi, T. P. Kobawala et al., "The potential of Wnt signaling pathway in cancer: a focus on breast cancer," *Cancer Translational Medicine*, vol. 2, no. 2, pp. 55–60, 2016.
- [47] Y. Luo and Y. Tan, "Prognostic value of CD44 expression in patients with hepatocellular carcinoma: meta-analysis," *Cancer Cell International*, vol. 16, p. 47, 2016.
- [48] M. Yoshida, T. Yamashita, H. Okada et al., "Sorafenib suppresses extrahepatic metastasis de novo in hepatocellular carcinoma through inhibition of mesenchymal cancer stem cells characterized by the expression of CD90," *Scientific Reports*, vol. 7, no. 1, article 11292, 2017.
- [49] Q. Zhao, H. Zhou, Q. Liu et al., "Prognostic value of the expression of cancer stem cell-related markers CD133 and CD44 in hepatocellular carcinoma: from patients to patient-derived tumor xenograft models," *Oncotarget*, vol. 7, pp. 47431–47443, 2016.
- [50] T. Uenishi, S. Kubo, T. Yamamoto et al., "Cytokeratin 19 expression in hepatocellular carcinoma predicts early post-operative recurrence," *Cancer Science*, vol. 94, no. 10, pp. 851–857, 2003.
- [51] T. Kawai, K. Yasuchika, T. Ishii et al., "Keratin 19, a cancer stem cell marker in human hepatocellular carcinoma," *Clinical Cancer Research*, vol. 21, no. 13, pp. 3081–3091, 2015.
- [52] J. H. Nahm, H. Rhee, H. Kim et al., "Increased expression of stemness markers and altered tumor stroma in hepatocellular carcinoma under TACE-induced hypoxia: a biopsy and resection matched study," *Oncotarget*, vol. 8, pp. 99359–99371, 2017.
- [53] Y. Nomura, T. Yamashita, N. Oishi et al., "De novo emergence of mesenchymal stem-like CD105<sup>+</sup> cancer cells by cytotoxic agents in human hepatocellular carcinoma," *Translational Oncology*, vol. 10, no. 2, pp. 184–189, 2017.
- [54] N. Haraguchi, H. Ishii, K. Mimori et al., "CD13 is a therapeutic target in human liver cancer stem cells," *Journal of Clinical Investigation*, vol. 120, no. 9, pp. 3326–3339, 2010.
- [55] H. M. Lee, J. W. Joh, S. R. Seo et al., "Cell-surface major vault protein promotes cancer progression through harboring mesenchymal and intermediate circulating tumor cells in hepatocellular carcinomas," *Scientific Reports*, vol. 7, no. 1, p. 13201, 2017.
- [56] Y.-M. Li, S.-C. Xu, J. Li et al., "Epithelial-mesenchymal transition markers expressed in circulating tumor cells in hepatocellular carcinoma patients with different stages of disease," *Cell Death & Disease*, vol. 4, no. 10, p. e831, 2013.
- [57] Y. Sun, W. Guo, Y. Xu et al., "Circulating tumor cells from different vascular sites exhibit spatial heterogeneity in epithelial and mesenchymal composition and distinct clinical significance in hepatocellular carcinoma," *Clinical Cancer Research*, vol. 24, no. 3, pp. 547–559, 2017.
- [58] H. Tsunematsu, T. Tatsumi, K. Kohga et al., "Fibroblast growth factor-2 enhances NK sensitivity of hepatocellular carcinoma cells," *International Journal of Cancer*, vol. 130, no. 2, pp. 356–364, 2012.
- [59] Z. Wang, L. Luo, Y. Cheng et al., "Correlation between postoperative early recurrence of hepatocellular carcinoma and mesenchymal circulating tumor cells in peripheral blood," *Journal of Gastrointestinal Surgery*, vol. 22, no. 4, pp. 633–639, 2018.
- [60] Q. Zhang, H. Wang, C. Mao et al., "Fatty acid oxidation contributes to IL-1 $\beta$  secretion in M2 macrophages and promotes macrophage-mediated tumor cell migration," *Molecular Immunology*, vol. 94, pp. 27–35, 2018.
- [61] B. Wang, T. Liu, J. C. Wu et al., "STAT3 aggravates TGF- $\beta$ 1-induced hepatic epithelial-to-mesenchymal transition and migration," *Biomedicine & Pharmacotherapy*, vol. 98, pp. 214–221, 2017.
- [62] P. Rawal, H. Siddiqui, M. Hassan et al., "Endothelial cell-derived TGF- $\beta$  promotes epithelial-mesenchymal transition via CD133 in HBx-infected hepatoma cells," *Frontiers in Oncology*, vol. 9, p. 308, 2019.
- [63] S. Z. Yang, L. D. Zhang, Y. Zhang et al., "HBx protein induces EMT through c-Src activation in SMMC-7721 hepatoma cell line," *Biochemical and Biophysical Research Communications*, vol. 382, no. 3, pp. 555–560, 2009.
- [64] J. Teng, X. Wang, Z. Xu, and N. Tang, "HBx-dependent activation of twist mediates STAT3 control of epithelium-mesenchymal transition of liver cells," *Journal of Cellular Biochemistry*, vol. 114, no. 5, pp. 1097–1104, 2013.
- [65] J. Zhang, Q. Zhang, Y. Lou et al., "Hypoxia-inducible factor-1 $\alpha$ /interleukin-1 $\beta$  signaling enhances hepatoma epithelial-mesenchymal transition through macrophages in a hypoxic-inflammatory microenvironment," *Hepatology*, vol. 67, no. 5, pp. 1872–1889, 2018.
- [66] Z. Liu, K. Tu, Y. Wang et al., "Hypoxia accelerates aggressiveness of hepatocellular carcinoma cells involving oxidative stress, epithelial-mesenchymal transition and non-canonical Hedgehog signaling," *Cellular Physiology and Biochemistry*, vol. 44, no. 5, pp. 1856–1868, 2017.
- [67] J.-M. Peng, R. Bera, C.-Y. Chiou et al., "Actin cytoskeleton remodeling drives epithelial-mesenchymal transition for hepatoma invasion and metastasis in mice," *Hepatology*, vol. 67, no. 6, pp. 2226–2243, 2018.
- [68] D. Fodor, I. Jung, S. Turdean, C. Satala, and S. Gurzu, "Angiogenesis of hepatocellular carcinoma: an immunohistochemistry study," *World Journal of Hepatology*, vol. 11, no. 3, pp. 294–304, 2019.
- [69] Y. Tong, H. Yang, X. Xu et al., "Effect of a hypoxic microenvironment after radiofrequency ablation on residual hepatocellular cell migration and invasion," *Cancer Science*, vol. 108, no. 4, pp. 753–762, 2017.

- [70] Y. Kong, L. Sun, Z. Hou et al., "Apatinib is effective for treatment of advanced hepatocellular carcinoma," *Oncotarget*, vol. 8, pp. 105596–105605, 2017.
- [71] X. D. Zhang, X. Q. Dong, J. L. Xu, S. C. Chen, and Z. Sun, "Hypoxia promotes epithelial-mesenchymal transition of hepatocellular carcinoma cells via inducing Twist1 expression," *European Review for Medical and Pharmacological Sciences*, vol. 21, pp. 3061–3068, 2017.
- [72] Z. Zhu, X. Hao, M. Yan et al., "Cancer stem/progenitor cells are highly enriched in CD133<sup>+</sup>CD44<sup>+</sup> population in hepatocellular carcinoma," *International Journal of Cancer*, vol. 126, pp. 2067–2078, 2010.
- [73] J. J. Zhou, D. Cheng, X. Y. He, Z. Meng, H. L. Ye, and R. F. Chen, "Knockdown of long non-coding RNA HOTAIR sensitizes hepatocellular carcinoma cell to cisplatin by suppressing the STAT3/ABCB1 signaling pathway," *Oncology Letters*, vol. 14, pp. 7986–7992, 2017.
- [74] A. G. Duffy, C. Ma, S. V. Ulahannan et al., "Phase I and preliminary phase II study of TRC105 in combination with sorafenib in hepatocellular carcinoma," *Clinical Cancer Research*, vol. 23, no. 16, pp. 4633–4641, 2017.
- [75] S. Gurzu, Z. Szentirmay, and I. Jung, "Molecular classification of colorectal cancer: a dream that can become a reality," *Romanian Journal of Morphology and Embryology*, vol. 54, pp. 241–245, 2013.
- [76] A. Santoro, L. Rimassa, I. Borbath et al., "Tivantinib for second-line treatment of advanced hepatocellular carcinoma: a randomised, placebo-controlled phase 2 study," *The Lancet Oncology*, vol. 14, no. 1, pp. 55–63, 2013.
- [77] H. Huynh, R. Ong, and K. C. Soo, "Foretinib demonstrates anti-tumor activity and improves overall survival in pre-clinical models of hepatocellular carcinoma," *Angiogenesis*, vol. 15, no. 1, pp. 59–70, 2012.
- [78] W. J. Zhou, Z. Huang, T. P. Jiang et al., "Pirfenidone inhibits proliferation and promotes apoptosis of hepatocellular carcinoma cells by inhibiting the Wnt/ $\beta$ -catenin signaling pathway," *Medical Science Monitor*, vol. 23, pp. 6107–6113, 2017.
- [79] E. Fransvea, A. Mazzocca, A. Santamato, A. Azzariti, S. Antonaci, and G. Giannelli, "Kinase activation profile associated with TGF- $\beta$ -dependent migration of HCC cells: a preclinical study," *Cancer Chemotherapy and Pharmacology*, vol. 68, no. 1, pp. 79–86, 2011.
- [80] R. K. Kelley, E. Gane, E. Assenat et al., "A phase 2 study of galunisertib (TGF- $\beta$ 1 receptor type I inhibitor) and sorafenib in patients with advanced hepatocellular carcinoma," *Clinical and Translational Gastroenterology*, vol. 10, no. 7, article e00056, 2019.
- [81] Y. Wada, Y. Takami, H. Matsushima et al., "The safety and efficacy of combination therapy of sorafenib and radiotherapy for advanced hepatocellular carcinoma: a retrospective study," *Internal Medicine*, vol. 57, no. 10, pp. 1345–1353, 2018.
- [82] B. A. Suci, S. Gurzu, L. Marginean et al., "Significant shrinkage of multifocal liver metastases and long-term survival in a patient with rectal cancer, after trans-arterial chemoembolization (TACE)," *Medicine*, vol. 94, no. 42, article e1848, 2015.
- [83] D. Fodor, B. A. Suci, I. Jung et al., "Transarterial chemoembolization (TACE) with Lipiodol® in HCC patients. Technical, clinical and imagistic aspects," *Materiale Plastice*, vol. 56, no. 1, pp. 195–198, 2019.
- [84] S. Dong, J. Kong, F. Kong et al., "Sorafenib suppresses the epithelial-mesenchymal transition of hepatocellular carcinoma cells after insufficient radiofrequency ablation," *BMC Cancer*, vol. 15, p. 939, 2015.
- [85] M. Xu, X.-h. Xie, X.-y. Xie et al., "Sorafenib suppresses the rapid progress of hepatocellular carcinoma after insufficient radiofrequency ablation therapy: an experiment in vivo," *Acta Radiologica*, vol. 54, no. 2, pp. 199–204, 2013.
- [86] L. Wu, B. Sun, X. Lin et al., "I131 reinforces antitumor activity of metuximab by reversing epithelial-mesenchymal transition via VEGFR-2 signaling in hepatocellular carcinoma," *Genes to Cells*, vol. 23, no. 1, pp. 35–45, 2018.